Mechanistic studies of bioadhesion: The role of water in interfacial interactions

By

Nimit Worakul

A dissertation submitted in partial fulfillment

of the requirements for the degree

Doctor of Philosophy

(Pharmaceutical Sciences)

at the

UNIVERSITY OF WISCONSIN-MADISON

2001

Mechanistic studies of bioadhesion: The role of water in interfacial interactions

Submitted to the Graduate School of the
University of Wisconsin-Madison
in partial fulfillment of the requirements for the
Degree of Doctor of Philosophy

by

Nimit Worakul

Date of Final Oral Examination: ***November 16, 2001***

Month & Year Degree to be awarded: ***December 2001***

****

Approval Signatures of Dissertation Committee

Joseph R. Robinson

George Zografi

Ralph Allcruft

Signature, Dean of Graduate School

Mechanistic studies of bioadhesion: The role of water in interfacial interactions

Nimit Worakul

Under the supervision of Professor Joseph R. Robinson

at the University of Wisconsin-Madison

There were two main purposes in these studies. The first purpose was to give a greater understanding of bioadhesion of polymeric gels used in drug delivery, and in particular to better understand the role of water in interfacial interactions taking place during bioadhesion and the effect of mucin in the medium on the change of this behavior. The second purpose was to provide a theoretical approach, using surface free energy parameters and solubility parameters as tools, to explain the bioadhesive property and solubilizing capacity of a bioadhesive system. The polymers used were hydroxypropyl cellulose (HPC) and hydroxypropylmethyl cellulose (HPMC), both water soluble and widely used in pharmaceutical products. The substrates used as model surfaces, to which adhesion of the polymers occurred were glass, Plexiglass (polymethylmethacrylate) and Teflon (polytetrafluoroethylene). The order of hydrophobicity is Teflon > Plexiglass > glass. Hydration of polymer gels was measured gravimetrically. Surface free energies associated with films of polymer

gels, spread on glass slides and immersed in water were determined from contact angles measured using air and n-octane droplets. Bioadhesion was determined by measuring the force of detachment of the polymer gel from the various solid substrates. The state of water in the polymer gel (freezable or non-freezable water) was determined by differential scanning calorimetry. Computer simulations were carried out to help predict adhesive behavior based on surface free energies and polarity of the substrates and the environment.

It was demonstrated that the hydrophilicity of polymer gel surfaces increased as the water content of the polymer increased, resulting in a change in bioadhesive behavior. The calculated work of adhesion, obtained from contact angle measurements, between the polymer gels and substrate surfaces in water exhibited parabolic changes in adhesion as a function of water content. Comparisons between different substrate surfaces showed that the work of adhesion is higher when the hydrophobicity of the substrate surface is higher. This appears to be due to a higher polar interfacial free energy contribution, γ_{SL}^{p}, between the substrate surface and water.

Differential scanning calorimetry data indicate that there is no effect of polymer molecular weight on the amount of non-freezable water in the polymer gels. It is concluded that non-freezable water, that water directly bound to the polymer, is essential for the initiation of the

adhesion process, while the presence of freezable water at the interface of polymer gels, tends to reduce adhesion. The results show some dependency of adhesion on the molecular weight of HPC and HPMC, but there is no clear correlation between the maximum work of adhesion and molecular weight. The water present at maximum adhesion is a combination of both freezable and non-freezable water. Since the amount of non-freezable water is constant for a particular polymer, the amount of freezable water required for optimum arrangement of polymer chains depends on the polymer molecular weight; a higher molecular weight polymer requires more freezable water to be present. Mucin has been shown to exhibit surface activity in an aqueous environment, and therefore, it reduces the work of adhesion between the polymer gel and the substrate surface by reducing the interfacial free energy between a medium and a substrate surface. Simulations involving the use of surface free energy parameters and solubility parameters have proved some insights into the role of polarity in bioadhesion and solubilizing capacity of a bioadhesive system.

Date: 12/05/01

Nimit Worakul

Approved:

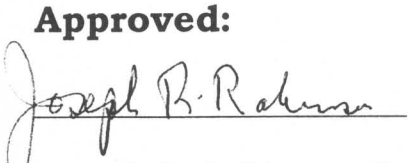

Joseph R. Robinson, Professor

Acknowledgements

I wish to express my deep appreciation to Professor Joseph R. Robinson for his suggestions and guidance throughout the course of this exciting journey and for his other interesting vision not only on scientific research but also the philosophy of life. I feel honored to be one of his graduate students and hope that this experience will be with me forever and will be very helpful for my future career.

I would also like to express my special thanks to Professor George Zografi who gave me valuable discussions and allowed me to use his facilities for my research. I should note that he introduced me to the field of interfacial phenomena. In addition, I would like to thank my other committees including Professor Ralph Albrecht, Associate Professor Glen Kwon and Assistant Professor Weiyuan John Kao for their kindness and valuable suggestions, and Professor Kenneth Connors who provided me the information about solubility study.

I also attribute much of my development as a pharmaceutical scientist to faculties and graduate students in pharmaceutics department during my time in Madison (1995-2001). I am grateful to Mr. Surawut Watana, Mr. Jae Han Park and Mr. Jeremy Bartlett for their friendship, which made the years seem more interesting. In addition, I wish to express my sincere appreciation to my colleagues at Prince of

Songkla University, Thailand who work hard and be patient waiting for my graduation.

I gratefully acknowledge the financial support by The Royal Thai Government and School of Pharmacy, University of Wisconsin-Madison.

Finally, I am deeply indebted to my parents, my family in Thailand for their mentally support; and my wife, Sasithorn Worakul, who is with me in Madison for her companionship and encouragement.

Table of Contents

Pages

Pages

List of tables

Tables **Pages**

List of figures

Figures **Pages**

Figures **Pages**

Figures **Pages**

Figures **Pages**

Chapter I : Introduction

A. Background:

❖ Definition and applications of bioadhesion

A bioadhesive substance is defined as a material that is capable of adhering to a biological surface, and being retained on that surface for an extended period of time. Accordingly, bioadhesion is described as the interfacial interaction between a bioadhesive substance and a biological surface. If the biological surface is covered by mucus, the term mucoadhesion is used [1-4]. Bioadhesion can be achieved by either nonspecific or specific interactions. Nonspecific interactions are driven by the physicochemical properties of the bioadhesive system, surface and environment, while specific interactions are driven by recognition of the ligand at the mucosal surface. This work will emphasize nonspecific interactions.

The concept of bioadhesion has received considerable interest in the pharmaceutical sciences as a platform for controlled drug delivery systems [3-26]. Attention has been focused on the potential to prolong residence time within a specified region of the body and create an intimate contact with the absorbing membrane. In recent years, other

novel concepts associated with bioadhesion have been proposed [19-26], these include permeability modification, inhibition of proteolytic enzymes and creating of specificity for targeting.

Currently, bioadhesive systems are successfully used to increase the residence time at several sites, such as the mouth, nose, eyes, and vagina (Table 1). However, human gastrointestinal bioadhesive drug delivery systems have not yet been established.

❖ Fundamentals of bioadhesion

The establishment of a nonspecific bioadhesive bond may be regarded as a series of steps. Initially, wetting and swelling of the bioadhesive polymer to permit intimate surface contact between the bioadhesive and the adherent surface has to be established. Subsequently, both phases may interdiffuse or interpenetrate to a certain extent. These steps establish the area of contact between the bioadhesive and substrate surface. Following these processes, interfacial bond formation is established through secondary chemical bonds, i.e., London forces, hydrogen bonding, or a hydrophobic effect [1-2]. The bioadhesion phenomenon is a complex process. Several theories have been proposed to explain the detailed mechanism involved in bioadhesion; however, no single theory sufficiently explains this mechanism. The most cited

Table 1 The effect of a bioadhesive system on the approximate clearance time of applied solutions for selected areas of the human body [13, 27]

Route	Residence time without bioadhesive	Residence time with bioadhesive polycarbophil
Ocular	1-2 minutes	12-15 hours
Nasal	2-60 minutes	6-12 hours
Buccal	2-30 minutes	6-12 hours
Vaginal	30-90 minutes	3-4 days
Stomach	5-100 minutes[A]	5-100 minutes[A]
Small intestine	85-250 minutes[A]	95-285 minutes[A]

A = $t_{90\%}$ of powder in capsule dosage form

mechanism that is used to explain bioadhesion involves wetting, adsorption and diffusion, and usually some combination of two or three of these theories.

The wetting and adsorption theories

The adsorption theory states that the adhesion of a bioadhesive polymer on a mucus layer is the result of surface forces acting between atoms in the two surfaces. This interaction is achieved based on a sufficiently intimate intermolecular contact. These forces include van der Waals forces and hydrogen bonding, and are referred to as secondary bonds. The term secondary is in a sense a measure of the relative strength of the bonds (Table 2). Although individually these forces are weak, strong adhesion can be produced through numerous interaction sites. Since the prerequisite for the adsorption process involves intimate contact between two materials, this theory can be linked to a wetting theory. The wetting theory uses surface free energy parameters, i. e., interfacial free energy, spreading coefficient and work of adhesion, to predict spreading or the wetting ability of an adhesive on a substrate [29-31]. Good wettability means good adhesion. These parameters will be clarified in more detail later.

Table 2 Types of physical attractive forces and typical bond energies [28]

Types	Bond energy (kJ/mol)
Ionic	590-1,050
Covalent	63-710
Metallic	113-347
Permanent dipole-dipole interactions:	
-Hydrogen bonds involving fluorine	Up to 42
-Hydrogen bonds excluding fluorine	10-26
-Other dipole-dipole(excluding hydrogen) bonds	4-21
Dipole-induced dipole	Less than 2
Dispersion(London) forces	0.08-42

Lehr et.al. [32-34] proposed that the formation of a mucoadhesive bond is primarily governed by the aforementioned surface energy effects and spreading processes. By using electron microscopic examination, they found that there was no evidence for interpenetration between mucus and the mucoadhesive hydrogel in the micron-range. However, in the nanometer-range this possibility still exists [32]. They used surface free energy analysis theory, which considers interfacial phenomena in terms of polar and dispersive components, and calculated these components using contact angle data. By comparing the fractional polarity of a mucus surface and polymer surface, they explained the adhesion of a polymer to a mucus surface [33]. They also proposed a new parameter, a combined spreading coefficient, which provided a good correlation between predicted and measured mucoadhesive performance in different aqueous media [34]. Note that this approach does not consider possible binding forces in bioadhesion due to interdiffusion and ionic interactions. Similar work was done by considering interfacial phenomena in terms of the Lifshitz-van der Waals and acid-base components. Rillosi and Buckton [35] applied this theory to explain the mucoadhesive property of Carbopol to mucin. They found that the surface energy of Carbopol changed when hydrated, therefore Carbopol, but not mucin, was changed in surface energy as a function of pH. In addition, the surface energy of a dry polymer gave a better correlation

with mucoadhesive strength after a short contact time, while the surface energy of the hydrated polymer was found to give the best correlation with mucoadhesion after a longer contact time. They also concluded that the interpenetrating stage of mucoadhesion has a driving force, which is related to interfacial phenomena.

The diffusion theory

The diffusion theory states that intrinsic bioadhesion is due to diffusion of adhesive molecules across an interface. This theory supports the concept that interpenetration and entanglement of bioadhesive polymer chains and mucus produce semipermanent adhesive bonds. It is believed that bond strength increases with the degree of penetration of the polymer chains into the mucus layer [28, 36-37]. This requires that the chain segments of the bioadhesive and mucus possess sufficient mobility and are mutually soluble, i.e., they have similar values of the solubility parameter [28, 38-39]. However, where the solubility parameter of the materials are not similar, or where one material is highly crosslinked, is crystalline or is below its glass transition temperature, then interdiffusion is an unlikely mechanism [28-29]. In a previous study [40], it was proposed that one of the factors that controls the strength of mucoadhesion is the expanded nature of both the interacting mucus and

polymer network. By using ATR-FTIR spectroscopy, Jabbari et al. [41] showed that entanglements and secondary chemical bonds can be formed through the occurrence of interpenetration. A similar conclusion was made using viscoelastic measurements. It was concluded that gel strengthening at the mucoadhesive-mucus interface is the main reason for increased mucoadhesion. Interpenetration and hydrogen bond formation of mucus/mucoadhesive molecules are the likely mechanisms to change rheology at the interface [42-44]. In the case of dry and partially hydrated dosage forms, however, water movement from mucus to the dosage forms, rather than polymer interpenetration, could be important because dehydration of the mucus layer could increase its adhesive and cohesive properties, and this would be expected to strengthen the mucoadhesive joint [45]. It must be noted that excess hydration could lead to a weakening of the mucoadhesive joint, and eventual formation of a slippery mucilage [46]. Therefore, the relative importance of each factor will vary, depending on contact time, the nature of the mucosal surface, presence and thickness of the mucus layer, and the nature and degree of hydration of the mucoadhesive [42].

❖ Theory of interfacial phenomena

It has been recognized for many years that the establishment of intimate molecular contact is a necessary requirement for developing strong adhesive joints. This means that an adhesive needs to spread over the surface of a substrate. An adhesive that conforms ideally to these conditions must exhibit [28]:

- A zero or near zero contact angle when it is a liquid;
- Have a viscosity that should be relatively low at some time during the bonding process;
- Be brought together with the substrate at a rate and manner that assists in the displacement of any trapped air.

In order to assess the ability of a given adhesive/substrate combination to meet these criteria, it is necessary to consider the following parameters:

- wetting equilibrium;
- values of the surface free energies of the adhesive and substrate;
- free energy of the adhesive/substrate interface;
- kinetics of the wetting process;
- details of the bonding operation.

Surface tension is a direct measure of intermolecular forces. Tension in the surface layer is the result of attraction of the bulk material for the surface layers, and this attraction tends to reduce the number of molecules in the surface region resulting in an increase in intermolecular distance. The increase in distance requires work to be done and returns work to the system upon a return to a normal configuration. This explains why tension exists and why there is a surface free energy [28, 47-48].

The most common type of physical attractive forces is van der Waals force, which can be attributed to [49-50]:

- Dispersion (or London) force arising from internal electronic motion which is independent of dipole moments;
- Orientation (or Keesom) force arising from the orientation of permanent electric dipoles;
- Induction (or Debye) force arising from random orientation of dipole-induced dipole.

Dispersion force is universal, and all materials exhibit it. Another type of force that may operate is hydrogen bonding. The various types of physical attractive forces are listed in Table 2.

The ability of a liquid to wet or adhere to a substrate surface is determined essentially by surface tensions of the two materials. The surface tension of a liquid can be measured directly; however, the

The work of adhesion (W_a) between two phases is the work required to reversibly separate them. This can be calculated by the Young-Dupre equation:

$$W_a = \gamma_{SV} + \gamma_{LV} - \gamma_{SL} = \gamma_{LV}(1+ \cos \theta) \quad \text{Eq. 3}$$

The interfacial free energy between two phases, in terms of polar and dispersive components [51-53], can be calculated using the geometric mean equation:

$$\gamma_{ij} = \gamma_i + \gamma_j - 2(\gamma_i^d \gamma_j^d)^{0.5} - 2(\gamma_i^p \gamma_j^p)^{0.5} \quad \text{Eq. 4}$$

Wu [53-55] used the harmonic-mean equation to express the optimum wettability condition for adhesion in terms of polarity and surface free energy as follow:

$$\gamma_{ij} = \gamma_i + \gamma_j - 4(\gamma_i^d \gamma_j^d)/(\gamma_i^d+\gamma_j^d) - 4(\gamma_i^p \gamma_j^p)/(\gamma_i^p+\gamma_j^p) \quad \text{Eq. 5}$$

This equation is normally regarded as the preferred method for calculating the interfacial free energy between polymers. In order to calculate work of adhesion between two surfaces in a third medium, a three-phase system equation (Eq. 6) can be used [49, 56-60]:

$$W_a^T = W_a^{PS} + W_c^L - W_a^{PL} - W_a^{SL} = \gamma_{SL} + \gamma_{PL} - \gamma_{PS} = -\Delta G_a^T \quad \text{Eq. 6}$$

Where T, P, L and S represent total, polymer, liquid medium and substrate surface, respectively. W_c^L is the work of cohesion of the liquid medium, which is equal to $2\gamma_{LV}$. ΔG_a^T is the free energy of interaction between two surfaces in a medium. A positive value for W_a^T will result in a net attraction between polymer and substrate surface in the liquid medium. Therefore, it is advantageous to minimize the interfacial free energy between polymer and surface (γ_{PS}), while maximizing the interfacial free energy between the other two interfaces (γ_{SL}, γ_{PL}). This approach has been used to explain several bioadhesion processes, i.e., the adhesion of bacteria to solid substrates in a specific medium [60-65], and binding of a polymer to mucus in the presence of buffer [34, 66].

According to wetting theory, the spreading coefficient has been suggested as a driving force for the wetting process, which is a prerequisite for good adhesion. In principle, the spreading coefficient of each situation can be calculated by using the following equations [34, 67]:

$$S_L = \gamma_{PS} - \gamma_{PL} - \gamma_{SL} \quad \text{Eq. 7}$$

$$S_P = \gamma_{SL} - \gamma_{PL} - \gamma_{PS} \quad \text{Eq. 8}$$

$$S_S = \gamma_{PL} - \gamma_{PS} - \gamma_{SL} \qquad \text{Eq. 9}$$

Where S_L, S_P and S_S represent the spreading coefficients for liquid, polymer and substrate, respectively.

Kaelble and Moacanin [67] described the strength of adhesion by using the spreading coefficient of a liquid phase on a substrate. The adhesive bond is favored when this spreading coefficient is negative. It is important to note that this idea is exactly the same as using the three-phase system work of adhesion, since the negative value of the spreading coefficient will give a positive value of the work of adhesion (Eq. 6). Later, Lehr et al. [34] proposed that a negative value for S_L is only a necessary, but not a sufficient condition, for spontaneous bonding in this system. To provide spontaneous and stable bonding, either the polymer speading coefficient (Eq. 8) or substrate spreading coefficient (Eq. 9) must be positive values. Therefore, they unified two spreading coefficients (S_L and S_P) into a single parameter, a combined spreading coefficient (Eq. 10). This new parameter can be used to predict bioadhesive performance in a wide variety of situations.

$$S_C = (-S_L/2)^{0.5} (S_P/2)^{0.5} \qquad \text{Eq. 10}$$

❖ Surface free energy measurement of polymer gels

Previous studies have concluded that a hydrogel surface is capable of changing its surface free energy through reorientation of the polymer side chains and chain segments depending on the nature of the environment [68-72]. Therefore, the contact angle of a liquid on a dry polymer is not appropriate to calculate surface free energy of a hydrogel in an aqueous environment. An alternative technique, which was originated by Hamilton [73], has been used to determine the dispersive and polar components of hydrogels [33, 69-72] and consists of measuring the contact angle of a captive air bubble and drop of n-octane on the swollen hydrogel surface in a fixed environment, i.e., water, buffer, saline (Figure 1A). As shown in Figure 1B, Young's equation can be applied as follow:

For a drop of n-octane at the gel-liquid interface:

$$\gamma_{SO} = \gamma_{SL} + \gamma_{LO} \cos \theta_O \qquad \text{Eq. 11}$$

For a captive air bubble at the gel-liquid interface:

$$\gamma_{SV} = \gamma_{SL} + \gamma_{LV} \cos \theta_V \qquad \text{Eq. 12}$$

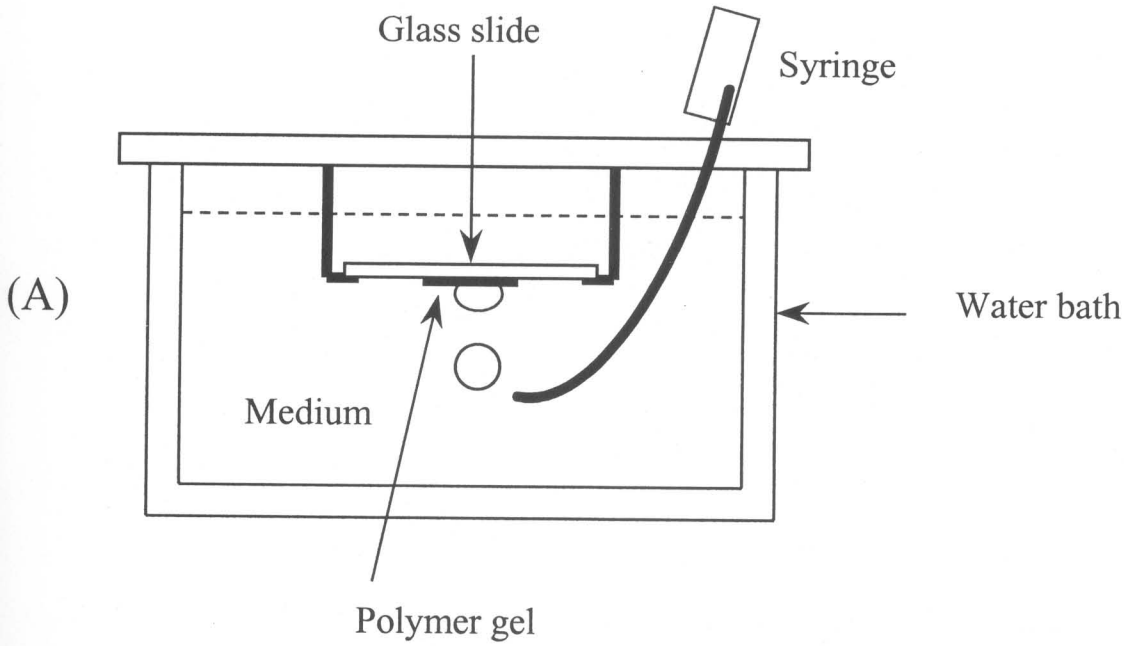

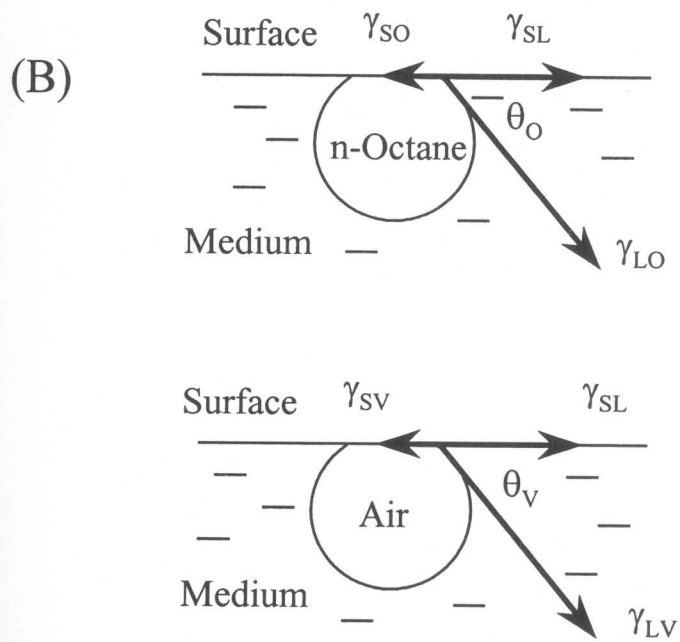

Figure 1 Schematic drawing of contact angle measurement

(A) Apparatus for measuring contact angle

(B) Surface free energy balance; the explanation is in the context

Where S, L, V, and O are gel or solid, liquid, vapor, and n-octane, respectively.

By using the harmonic-mean concept (Eq. 5), the dispersive component can be calculated by modifying Eq. 11 as shown in the series of equations:

$$\gamma_{SV} + \gamma_{OV} - 4(\gamma_{SV}^{d}\gamma_{OV}^{d})/(\gamma_{SV}^{d}+\gamma_{OV}^{d}) = \gamma_{SV} - \gamma_{LV}\cos\theta_V + \gamma_{LO}\cos\theta_O$$

$$4(\gamma_{SV}^{d}\gamma_{OV}^{d})/(\gamma_{SV}^{d}+\gamma_{OV}^{d}) = \gamma_{OV} + \gamma_{LV}\cos\theta_V - (\gamma_{LV}+\gamma_{OV}-4(\gamma_{LV}^{d}\gamma_{OV}^{d})/(\gamma_{LV}^{d}+\gamma_{OV}^{d}))\cos\theta_O$$

let $K_O = \gamma_{OV} + \gamma_{LV}\cos\theta_V - (\gamma_{LV} + \gamma_{OV} - 4(\gamma_{LV}^{d}\gamma_{OV}^{d})/(\gamma_{LV}^{d}+\gamma_{OV}^{d}))\cos\theta_O$

$$\therefore \quad \gamma_{SV}^{d} = (K_O\gamma_{OV}^{d})/(4\gamma_{OV}^{d} - K_O) \qquad \text{Eq. 13}$$

Then, the equation for calculating the polar component can be derived from Eq. 12 as follow:

$$\gamma_{SV} = \gamma_{SV} + \gamma_{LV} + \gamma_{LV}\cos\theta_V - 4(\gamma_{SV}^{d}\gamma_{LV}^{d})/(\gamma_{SV}^{d}+\gamma_{LV}^{d}) - 4(\gamma_{SV}^{p}\gamma_{LV}^{p})/(\gamma_{SV}^{p}+\gamma_{LV}^{p})$$

$$4(\gamma_{SV}^{p}\gamma_{LV}^{p})/(\gamma_{SV}^{p}+\gamma_{LV}^{p}) = \gamma_{LV}(1+\cos\theta_V) - 4(\gamma_{SV}^{d}\gamma_{LV}^{d})/(\gamma_{SV}^{d}+\gamma_{LV}^{d}) = K_V$$

$$\therefore \quad \gamma_{SV}^{p} = (K_V\gamma_{LV}^{p})/(4\gamma_{LV}^{p} - K_V) \qquad \text{Eq. 14}$$

The same approach can be used for geometric-mean computation resulting in the following equations:

$$\gamma_{SV}^{d} = K_O^2 \gamma_{OV}^{d}/4 \qquad \text{Eq. 15}$$

$$\gamma_{SV}^{p} = K_V^2 \gamma_{LV}^{p}/4 \qquad \text{Eq. 16}$$

Where $K_O = \gamma_{OV} + \gamma_{LV} \cos\theta_V - (\gamma_{LV} + \gamma_{OV} - 2(\gamma_{LV}^{d}\gamma_{OV}^{d})^{0.5})\cos\theta_O$

$$K_V = \gamma_{LV}(1+\cos\theta_V) - 2(\gamma_{SV}^{d}\gamma_{LV}^{d})^{0.5}$$

❖ Solubility, solubility parameters and surface free energy parameters

Most of the theoretical approaches to solubility are based on the work of Hildebrand and Scott [74-76], through the use of regular solution theory. The solubility of a solute in this theory is obtained by:

$$-\ln X_2 = -\ln {}^{i}X_2 + \ln \alpha_2 \qquad \text{Eq. 17}$$

Where X_2 is the solute mole fraction solubility, ${}^{i}X_2$ is the ideal solubility of the solid solute, and α_2 is the solute activity coefficient.

In an ideal solution, there is no change in enthalpy or volume on mixing. Therefore, the ideal solubility of a solid solute in an ideal solution can be calculated using the following equation [75, 77-80]:

$$-\ln {}^{i}X_2 = (\Delta^{f}H_m/R)((1/T)-(1/T_m)) \qquad \text{Eq. 18}$$

Where $\Delta^{f}H_m$ is the heat of fusion of the solute at the melting point (T_m), T is the temperature of the study, and R is the gas constant.

Since the activity coefficient depends on the nature of both the solute and the solvent as well as the temperature of solution, the ln α_2 term of Eq. 17 needs to be determined. This term is obtained by considering the work that must be done to remove a molecule from the solute phase and deposit it in the solvent. Therefore, the equation for the solute activity coefficient of one liquid in another, according to regular solution theory, is expressed as [75, 77-80]:

$$\ln \alpha_2 = = \ln({}^{i}X_2/X_2) = A(C_{11} + C_{22} - 2C_{12}) \qquad \text{Eq. 19}$$

Where C_{ij} characterizes the intermolecular forces acting between molecules i and j. Therefore, for pure components, C_{11} and C_{22} are the cohesive energy densities (CED) of components 1 and 2. A is a term from regular solution theory:

$$A = (V_2\Phi_1^2)/(RT) \qquad \text{Eq. 20}$$

Where V_2 is the corresponding molar volume of solute which can be calculated from the known values of molecular weight and density, or by using the additive atomic and group contribution for the molar volume as shown in Table 3. Φ_1 is volume fraction of solvent in solution, which is defined as:

$$\Phi_1 = [(1 - X_2)\, V_1]/\, [(1 - X_2)\, V_1 + X_2V_2\,] \qquad \text{Eq. 21}$$

Since solubility parameter (δ_i) is defined as a square root of the cohesive energy density [83-88], the Scatchard-Hildebrand equation simplified by using geometric mean assumption was developed as:

$$\ln \alpha_2 = A(\delta_1 - \delta_2)^2 \qquad \text{Eq. 22}$$

The cohesive energy is a quantity of energy needed to separate the atoms/molecules of a solid or liquid to a distance where they possess no potential energy, and the CED is equal to the cohesive energy per unit volume. Therefore, solubility parameter can be used to predict the solubility of one material in another. If two materials have similar

Table 3 Group contributions for calculating molar volume and partial solubility parameter [81-83]

Groups	V_i (cm^3/mol)	F_{di} ($J^{1/2}cm^{3/2}/mol$)	F_{pi} ($J^{1/2}cm^2/mol$)	F_{hi} (J/mol)
$-CH_3$	33.5	420	0	0
$-CH_2-$	16.1	270	0	0
$-CH<$	-1.0	80	0	0
$-C<$	-19.2	-70	0	0
$=CH_2$	28.5	400	0	0
$-CH=$	13.5	200	0	0
$=C<$	-5.5	70	0	0
-OH	10.0	210	500	20,000
-O-	3.8	100	400	3,000
-CO-	10.8	290	770	2,000
-COO-	18.0	390	490	7,000
-COOH	36.3	530	420	10,000
Phenyl	71.4	1,430	110	0
Phenylene	52.4	1,270	110	0
Ring closure with 5 or more atoms	16.0	190	0	0
Conjugation in ring (each double bond)	-2.2	0	0	0

solubility parameter values, they are likely to be soluble in each other [84, 88-93].

The three-dimensional solubility parameter concept was proposed by Hansen [88], who divided the total interaction energy into three components, i.e., dispersive, polar and hydrogen bonding interactions. In this study; however, the hydrogen bonding and polar interactions will be combined into a specific component (δ_s). Therefore, we can obtain CED from the following simplest equation:

$$CED = \delta^2 = \delta_d^2 + \delta_p^2 + \delta_h^2 = \delta_d^2 + \delta_s^2 \qquad \text{Eq. 23}$$

The degree of interaction and solubility for the solvent and polymer can be predicted by using the distance in space between two sets of parameters. Hanson [88] called this parameter the radius of interaction (R_{12}). In his study, Hanson used 10% w/v of polymer in different solvents to show that higher solubility is expected as the radius of the interaction between polymer and solvent is decreased.

The solubility parameter components of materials can be calculated from group contributions (Table 3) using the following equations:

$$\delta_d = (\Sigma F_{di}) / V_m \qquad \text{Eq. 24}$$

$$\delta_p = (\Sigma F_{pi}^2)^{0.5} / V_m \quad \text{Eq. 25}$$

$$\delta_h = [(\Sigma F_{hi}) / V_m]^{0.5} \quad \text{Eq. 26}$$

$$V_m = \Sigma V_i \quad \text{Eq. 27}$$

It is important to note that the solubility parameter unit is $(cal/cm^3)^{0.5}$, which equals 2.0455 (MPa or $J/cm^3)^{0.5}$.

A two-dimensional approach for utilizing solubility parameter was also successfully used to explain polymer solubility [89-92]. In these studies, the solubility parameter can be expressed as the dispersion and polar components, where the interaction between molecules are:

$$C_{ii} = \delta_{id}^2 + \delta_{is}^2 \quad \text{Eq. 28}$$

$$C_{ij} = \delta_{id}\delta_{jd} + \delta_{is}\delta_{js} \quad \text{Eq. 29}$$

Therefore, Eq. 22 can be modified to add the contribution of polar interactions as:

$$\ln \alpha_2 = A(\delta_{1d}^2 + \delta_{1s}^2 + \delta_{2d}^2 + \delta_{2s}^2 - 2\delta_{1d}\delta_{2d} - 2\delta_{1s}\delta_{2s})$$
$$= A[(\delta_{1d} - \delta_{2d})^2 + (\delta_{1s} - \delta_{2s})^2] = A[(R_{12}^d)^2 + (R_{12}^s)^2] \quad \text{Eq. 30}$$

The expanded parameter approach has been used to predict the solubility of solutes in different solvents [80, 94-99]. Therefore, Eq. 30 can be modified if it is assumed that the solubility parameter of a given solute is constant, and hence, the term $(\ln \alpha_2)/A$ values are regressed on the radius of interaction. Therefore, the solubility of a given solute can be simply estimated by a multiple regression method using the following equation as a model:

$$(\ln \alpha_2)/A = a_0 + a_1(R_{12}^d)^2 + a_2(R_{12}^s)^2 \qquad \text{Eq. 31}$$

Where a_0, a_1, and a_2 are coefficients of the multiple regression.

The solubility parameter was shown to have a good correlation with surface free energy in the following relation [100-110]:

$$\delta^2 (V_m)^{1/3} = 13.8\,\gamma \qquad \text{Eq. 32}$$

$$x^d = \gamma^d/\gamma = (\delta_d/\delta)^2 \text{ or } x^p = \gamma^p/\gamma = 1-(\delta_d/\delta)^2 = (\delta_s/\delta)^2 \qquad \text{Eq. 33}$$

Where x^p and x^d are fractional polarity and non-polarity, respectively.

In a binary system, it is possible to use these parameters to predict solubility and to define the type and strength of the forces, which control compatibility between two substances. In addition, spreading, adhesive and cohesive interactions can be also predicted [106-111]. Therefore, it is interesting to use these parameters to explain adhesion in a three-phase system and to predict solubilizing capacity of the system at the same time.

❖ Classification of water in polymer gels

Hydrogels are water-swollen polymer networks, of either natural or synthetic origin. There is evidence to suggest that water in polymers can exist in more than one state and these states of water in the hydrogel will also affect its properties [112]. In this thesis, we will classify water into two states, freezable water and non-freezable water. Freezable water exhibits all the properties of bulk water because no polymer-water interactions can be detected. It is water with a much greater degree of mobility which is unaffected by the polymeric environment. The melting/ crystallization temperature and enthalpy of melting/crystallization of this water are not significantly different from normal bulk water. Non-freezable water is water, which is directly associated with the polymer network through hydrogen bonding. Therefore, a phase transition leading

to freezing upon cooling to 0 ^{0}C is not observed calorimetrically [113-118]. The properties of a hydrogel are strongly influenced both by its equilibrium water content and the ratio of freezable to non-freezable water. Therefore, the characterization of water is important in classifying the role of water in hydrogels with respect to functionality and structure. The states of water in various polymers have been studied using thermal [115-118], dielectric [112], and spectroscopic analysis [117, 119].

The presentation of these types of water in polymer gels can also be used to explain drug release behavior from sustained release formulations [120]. By using the mixture of hydroxypropyl cellulose and ethylcellulose as a matrix, Aoki et.al. [120] found that the water penetrating into the matrix acted as non-freezable water during the initial stage of dissolution. As the water content of the matrix increased, freezable water was detected. The presence of freezable water within the barrier gel layer plays an important role in drug release from the matrix. It is assumed that drug diffuses through the freezable water in the matrix; therefore, increasing the amount of freezable water will lead to an increase in drug diffusion through the gel layer.

B. Statement of the problem:

Molecules making up the first generation of bioadhesive polymers were generally hydrophilic containing numerous hydrogen bond forming groups, having sufficient flexibility to penetrate the mucus network, and possessing the ability to swell rapidly. These bioadhesive polymers may show strong *in vitro* adhesive bonds, but they may not necessarily allow prolonged *in vivo* adhesion, especially in the gastrointestinal tract [27]. There are several aspects of bioadhesion, which remain critical for this purpose. These are gastrointestinal mobility, turnover of the adherent mucus layer, interaction of the formulation with soluble mucin prior to adhesion, surface hydrophobicity of the stomach, and presence of excess water at the interface.

It is known that a dry hydrophilic polymer needs to absorb water to increase its strength of adhesion and reach maximum adhesion at an optimum degree of hydration, while excess water can cause a weakening of the adhesive joint [46]. The first objective of this work, therefore, is to examine the role of water in the interfacial interactions of a bioadhesive polymer and substrate surface in different environments, especially the effect of water content and states of water on the change in surface free energy parameters for the bioadhesive gel. Moreover, the effect of mucin in the medium on these parameters will be considered.

Another problem related to hydrophilic polymers is a low solubilizing capacity for hydrophobic drugs. In order to create a new generation of bioadhesive polymers, which can be used to solubilize hydrophobic drugs and still have bioadhesive properties, a hydrophobic component must be added to a polymer system. This addition may change the bioadhesive property; therefore, limitations of the hydrophobic part of the system must be defined. Previous studies by others have indicated that the bioadhesive behavior can be explained by using surface free energy parameters [33-34, 66-67]. However, there has been no attempt to explain the relationship between solubilizing capacity and the bioadhesive property of a polymer system. Our second objective is to provide a theoretical approach using surface free energy parameters and solubility parameters as tools, to explain this relationship.

The information obtained from the above studies will lead to a clear picture for further development of bioadhesive drug delivery systems to deliver drugs into an aqueous environment, i.e, the gastrointestinal tract.

Chapter 2: Experimental

A. Materials

Hydroxypropyl cellulose (HPC), mucin (Type II), Glycerol, Ethanol, Propylene glycol, Methyl 4-hydroxybenzoate (Methyl paraben) and n-octane (purity 99+%) were purchased from Aldrich Chemical Company. HPC has average molecular weights of about 300,000 and 1,000,000 g/mol. Crude mucin is extracted from porcine stomach. Hydroxypropyl methylcellulose (HPMC) was a gift from The Dow Chemical Company. Two grades of HPMC were used Methocel® K15M Prem and K100M Prem. An initial letter "K" represents HPMC 2208 (USP XXII). The number that follows identifies the viscosity in millipascal-seconds of that product measured at 2 % concentration in water at 20 ^{0}C. In designation viscosity, the letter "M" is used to represent 1000.

The water was double distilled. Three different solid surfaces used in this study were Glass, Plexiglass® (polymethyl methacrylate), and Teflon® (polytetrafluoroethylene). The glass was micro slide purchased from Corning, Inc., New York.

B. Methods

❖ Preparation of polymer gels

Polymer gels with different water content were prepared by dispersing the polymer in hot water (about 80 ^{0}C), and storing in the refrigerator for at least 48 hours prior to use. The water contents were selected so that the viscosity of polymer gels was in the appropriate range. The water content per gram of dry polymer (W_t) was calculated from the following equation:

$$W_t\,(g/g) = \text{Added water (g)}/\text{Dry polymer (g)} \qquad \text{Eq. 34}$$

❖ Preparation of mucin solution

Mucin powder was dispersed in water at different concentrations ranging from 0 to 2 %w/w, and stored in the refrigerator for 48 hours. The samples were then centrifuged at 4,000 rpm for 2 hours. The supernatant was used for measuring surface tension and contact angle. Only the supernatant of a 2 %w/w solution was used as a medium for measuring the surface free energy of polymer gels.

❖ Hydration of polymer gels

Since the water content in a polymer gel can change during experimentation, a correction to the water content has to be made. The corrected water content was measured by weight difference as follows. Polymer gels with different water content, as used to measure contact angle and force of detachment, were hydrated in water for 1 minute. Samples were collected from the hydrated gels. Any surface water was removed with filter paper before the samples were transferred to bottles. The samples were weighed and dehydrated at 60 ^{0}C until the weight of samples were constant. The corrected water content was calculated using Eq. 34.

❖ Surface free energy measurements

Contact angles were measured directly using a goniometer-telescope (Gaertner Scientific Corporation, Chicago, IL., USA.) by viewing the profile of air bubbles and n-octane drops through the chamber window with the aid of a diffuse backlighting of the drop. The specified surfaces were cleaned using a detergent (Alconox®), and then rinsed with distilled water. The polymer gel was spread uniformly on a glass slide and suspended in the test medium at a controlled temperature of

25 ± 1 ^{0}C (Figure 1A). Air bubbles and n-octane drops of about 10-15 μL were applied to the surface using a microsyringe to obtain the contact angles. Two sides of the drop and air bubble were measured and the average was used as an advancing contact angle. Small air bubbles and n-octane were used in order to minimize any buoyancy correction. The surface free energy of polymer gels and all of the surfaces used were calculated by using Eq. 13 and 14, and interfacial surface free energy and work of adhesion were calculated by using Eq. 5 and 6, respectively. Note that the roughness and heterogeneous of the surfaces were not taken in consideration.

In order to measure the surface tension of the test medium, the Wilhelmy plate method was used, while the contact angle of the medium on Teflon® was used to determine the dispersive component. This contact angle measurement was carried out directly on sessile drops in an environmental chamber. The temperature inside the chamber was controlled at 25 ± 1 ^{0}C. The surface tension and dispersive component of the medium were calculated by the use of Eq. 35 and 36, respectively.

$$\gamma_{LV} = (\Delta W)\, 980/L \qquad \text{Eq. 35}$$

$$\gamma_{LV}^{d} = (\gamma_{SV}^{d})(\gamma_{LV}\,(1+\cos\theta)/[(4\gamma_{SV}^{d}) - (\gamma_{LV}\,(1+\cos\theta)], \qquad \text{Eq. 36}$$

where ΔW is the weight in gram unit used to pull the platimun plate from a liquid medium. L is the length of the platinum plate, which equals 5.16 cm. θ is the contact angle of the medium on Teflon®. The unit of surface tension and its components is dyne/cm, which is equivalent to mN/m or mJ/m^2.

Then the polar component was obtained as the difference between total surface tension and the dispersive component. For all experiments, the results are given as the means of at least three replicate measurements.

❖ Force of detachment measurements

The force of detachment per unit area of surface was measured by using a precision balance in a temperature-controlled chamber, as shown in Figure 2. The specified surfaces were cleaned using a detergent (Alconox®) and attached to the weighted-vial. The polymer gel was spread uniformly on a stopper with a diameter of 6.25 mm. To investigate the force of detachment in water, 30 μL of water was dropped on the specified surface. The stopper was suspended from the scale and set at zero. Then, the surface was slowly raised until it came into contact with the polymer gel on the stopper. Contact was initiated by the weight of the stopper (5 g). The weight on the another side of the balance was

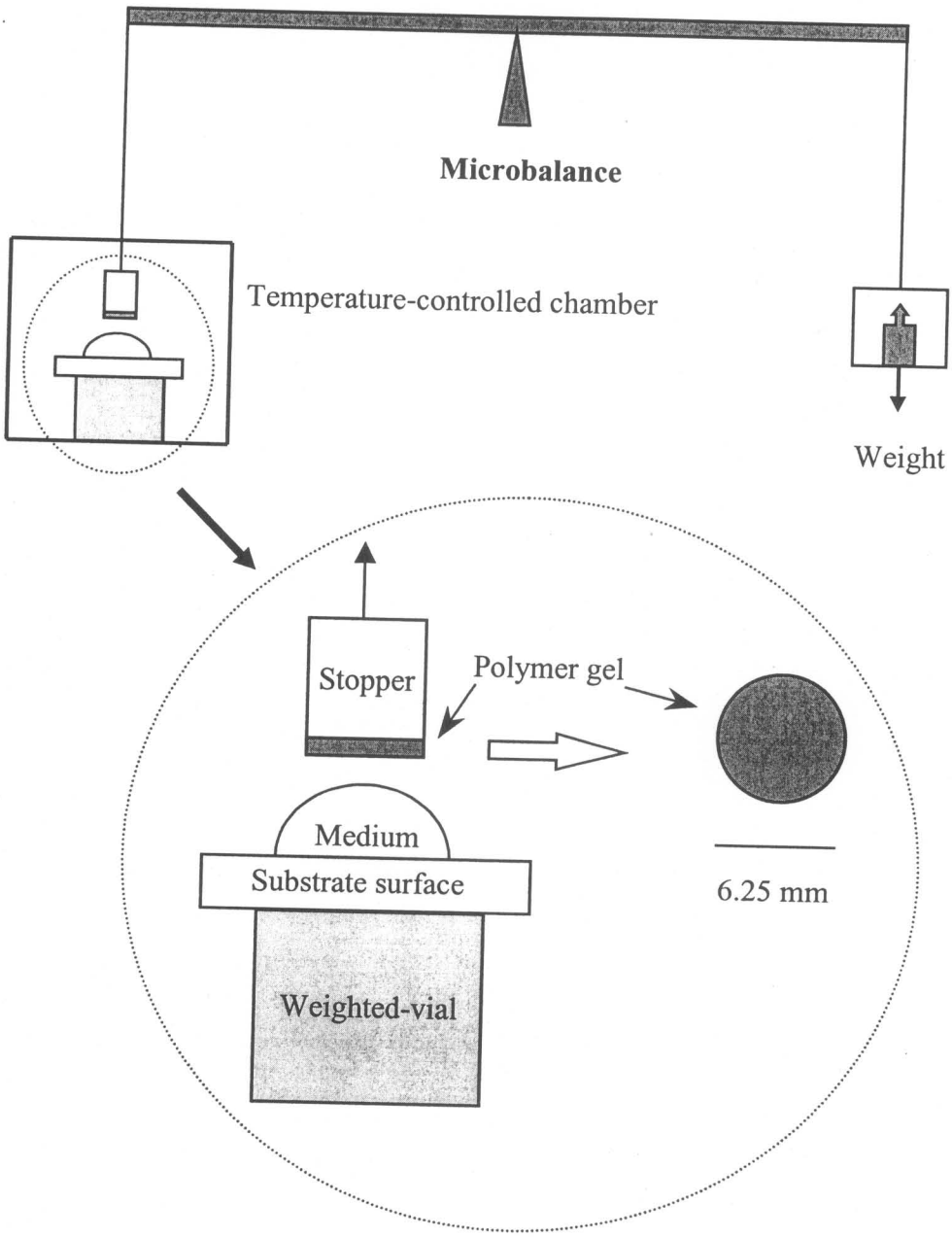

Figure 2 Schematic drawing of the force of detachment measurement

increased at a constant rate of 10 mg/s until the polymer became detached from the surface (W_1). The stopper without initial weight was used as a control (W_2). The force of detachment per unit area (F) was calculated using the following equation:

$$F = [(W_1 - W_2)\ g]/A \qquad \text{Eq. 37}$$

Where g is the gravity constant and A is the surface area of the stopper taken as a circle, which equals $\pi\ (6.25/2)^2\ mm^2$.

For all experiments, the results are given as the means of at least five replicate measurements.

❖ Characterization of the state of water in polymer gels

A Seiko instrument DSC (SSC/5,200) with an attached liquid nitrogen-based cooling apparatus was used for this measurement. Indium and zinc were used as calibrants. Gel samples of 10-20 mg were accurately weighed and analyzed in an aluminium sample pan. The samples were cooled at 10 ^{0}C /min from 20 ^{0}C to -40 ^{0}C. Then the samples were reheated to 40 ^{o}C at the same rate. Each sample was measured twice and the average value was used. The DSC heating curves

show transitions for freezable water at about 0 ^{0}C (Figure 3). Assuming the endotherm enthalpy was due to only water melting, thus the melting enthalpy of water in the polymer gel (ΔH_S) was determined from the area represented by the endothermic transitions. In order to determine the freezable water content per gram of dry polymer in the polymer gel (W_f), the following procedure was used. The amount of freezable water content in the polymer gel (g water/ g gel) was calculated by dividing ΔH_S by the experimental value of the melting enthalpy of pure water (ΔH_W). While the amount of dry polymer in the polymer gel (g polymer/g gel) is equal to $1/(1+ W_t)$. Therefore, the amount of freezable and non-freezable water per gram of dry polymer can be calculated by using the following equations:

$$W_f = (\Delta H_S/\Delta H_W)/(1/(1+ W_t)) \qquad \text{Eq. 38}$$

$$W_f = W_t - W_{nf} \qquad \text{Eq. 39}$$

Where W_f and W_{nf} are the freezable and non-freezable water contents per gram of dry polymer, respectively. The W_{nf} value is calculated from the different between W_t and W_f. ΔH_W is the melting enthalpy of pure water, which is equal to 336.2 mJ/mg).

A plot of W_f and W_t is a straight line with a slope equal or close to unity, and the X-intercept is equal to maximum W_{nf}. This maximum W_{nf}

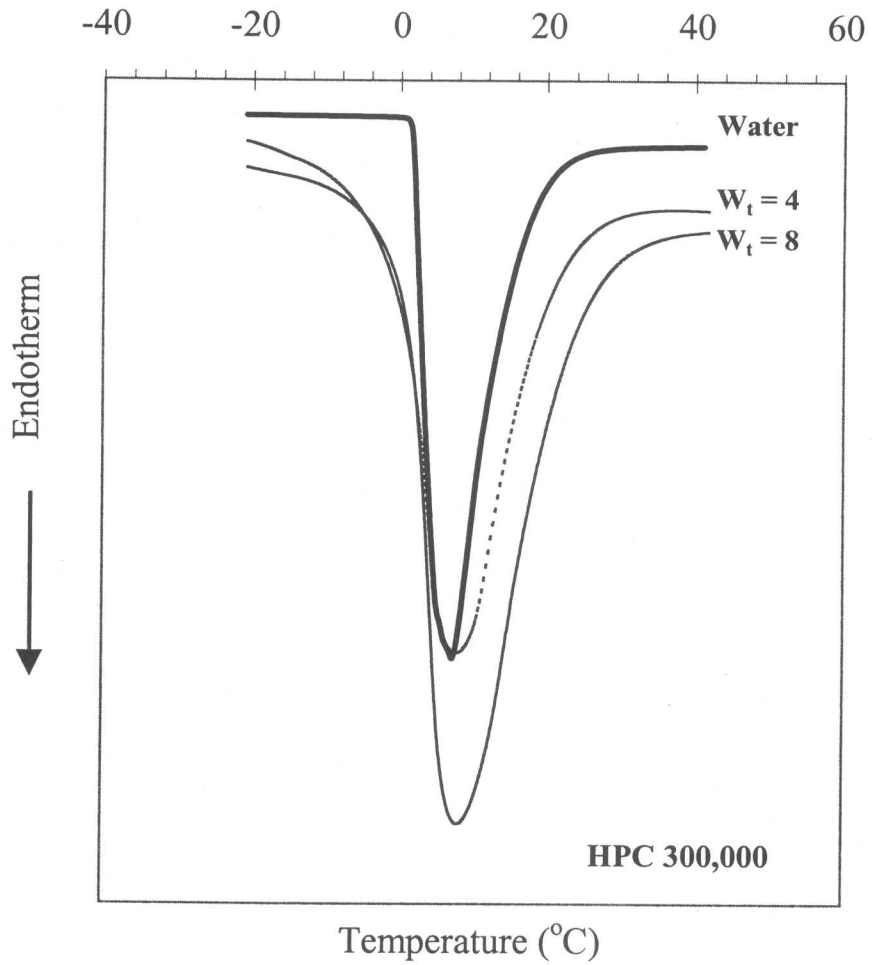

Figure 3 Typical differential scanning calorimetry endotherm of pure water and HPC gels at different water contents

was used to calculate the W_f / W_{nf} ratio in this study.

❖ Solubility determination

The solubility of methyl paraben was determined in different solvents at 25 ^{0}C. A suitable amount of solvent was introduced into vials containing an excess amount of the solute. The vials were shaken in a constant-temperature bath (25 ± 1 ^{0}C) for 48 hours to assure saturation. After equilibrium had been attained, the suspensions were centrifuged at 4,000 rpm for at least 2 hours and the supernatant filtered. The filtrate was then diluted and analyzed. The suitably diluted solutions were assayed using a spectrophotometer set at the maximum wavelength of the solute (256 nm). The solubility of a solute in each solvent was calculated in mole fraction.

The heat of fusion and melting point of methyl paraben was determined using a Seiko instrument DSC. The samples of 10-20 mg were accurately weighed and analyzed in an aluminum pan by heating at 10 ^{0}C/min from 20 ^{0}C to 150 ^{0}C. The sample was measured twice and the average value was used.

❖ Computer simulation

A three-phase equation representing the contributions of polar and dispersive components (Eq. 40) can be used to predict adhesive behavior in the systems of interest.

$$W_a^T = K + 4(\gamma_{PV}^d\gamma_{SV}^d)/(\gamma_{PV}^d+\gamma_{SV}^d) - 4(\gamma_{PV}^d\gamma_{LV}^d)/(\gamma_{PV}^d+\gamma_{LV}^d)$$
$$+ 4(\gamma_{PV}^p\gamma_{SV}^p)/(\gamma_{PV}^p+\gamma_{SV}^p) - 4(\gamma_{PV}^p\gamma_{LV}^p)/(\gamma_{PV}^p+\gamma_{LV}^p) \qquad \text{Eq. 40}$$

Where $K = 2\gamma_{LV} - 4(\gamma_{SV}^d\gamma_{LV}^d)/(\gamma_{SV}^d+\gamma_{LV}^d) - 4(\gamma_{SV}^p\gamma_{LV}^p)/(\gamma_{SV}^p+\gamma_{LV}^p)$

In this study, we have used this equation to simulate the adhesive behavior in a number of different situations. The surface free energies and polarity of a substrate and the environment were assumed to exist for the different conditions including $\gamma_S = \gamma_L$ and $x^p_L > x^p_S$ or $x^p_L < x^p_S$ or $x^p_L = x^p_S$; $\gamma_S > \gamma_L$ and $x^p_L > x^p_S$ or $x^p_L < x^p_S$ or $x^p_L = x^p_S$, and $\gamma_S < \gamma_L$ and $x^p_L > x^p_S$ or $x^p_L < x^p_S$ or $x^p_L = x^p_S$. Then the work of adhesion of an adhesive polymer with different surface properties was calculated and compared. From this simulation, different approaches that could be used to achieve good adhesion can be developed.

Chapter 3: Results and Discussion

A. The effect of water content and states of water in polymer gels on the change of surface free energy parameters and force of detachment

❖ Surface free energy parameters

Since an air bubble and n-octane are hydrophobic, a lower contact angle means the surface is more hydrophilic. Figure 4 illustrates this as the contact angle decreases with the order of surface hydrophobicity of the substrates : Teflon > Plexiglass > Glass. The results for polymer gels surfaces are shown in Figures 5 and 6. It demonstrates that increasing water contents in the polymer gels result in a decrease in both air bubble and n-octane contact angles. Therefore, HPC and HPMC gels in water increase their surface hydrophilic character as water content increases. From these data, surface free energies of substrate surfaces and polymer gels can be calculated for dispersive and polar component using Eqs. 13 and 14, respectively. The results for the substrate surfaces are summarized in table 4, while figure 7 illustrates the surface free energies of polymer gels. Note that the lines in this figure are not the fitting of the

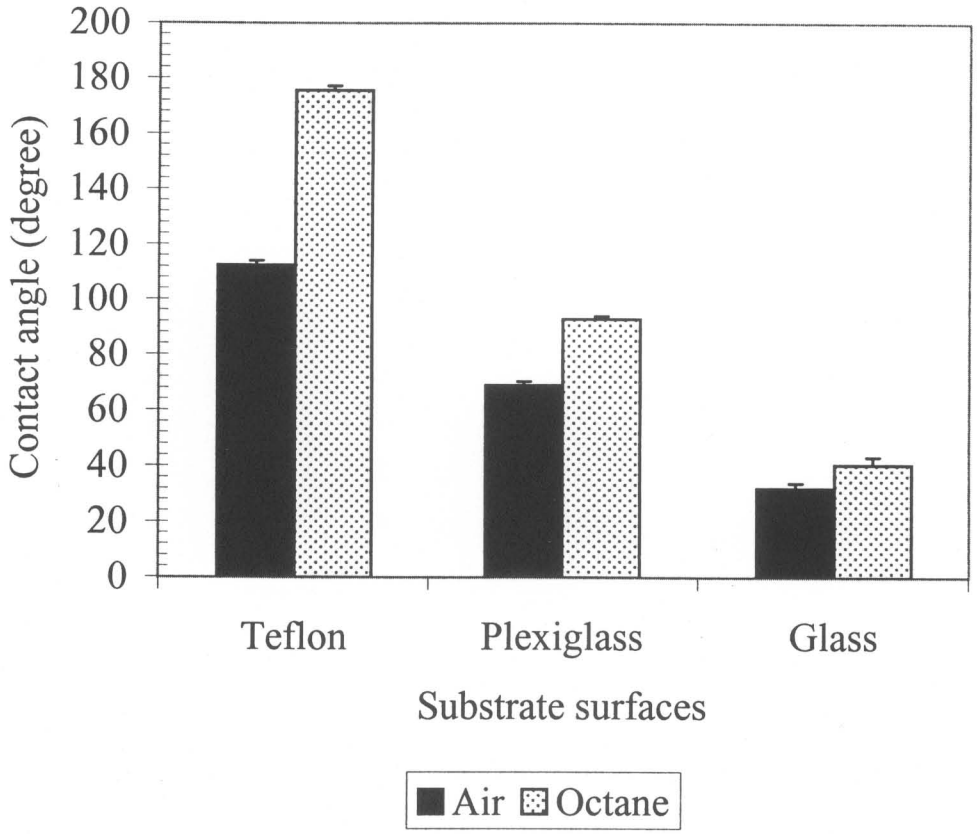

Figure 4 Air bubble and n-octane contact angles on different substrate surfaces under water at 25 ^{0}C

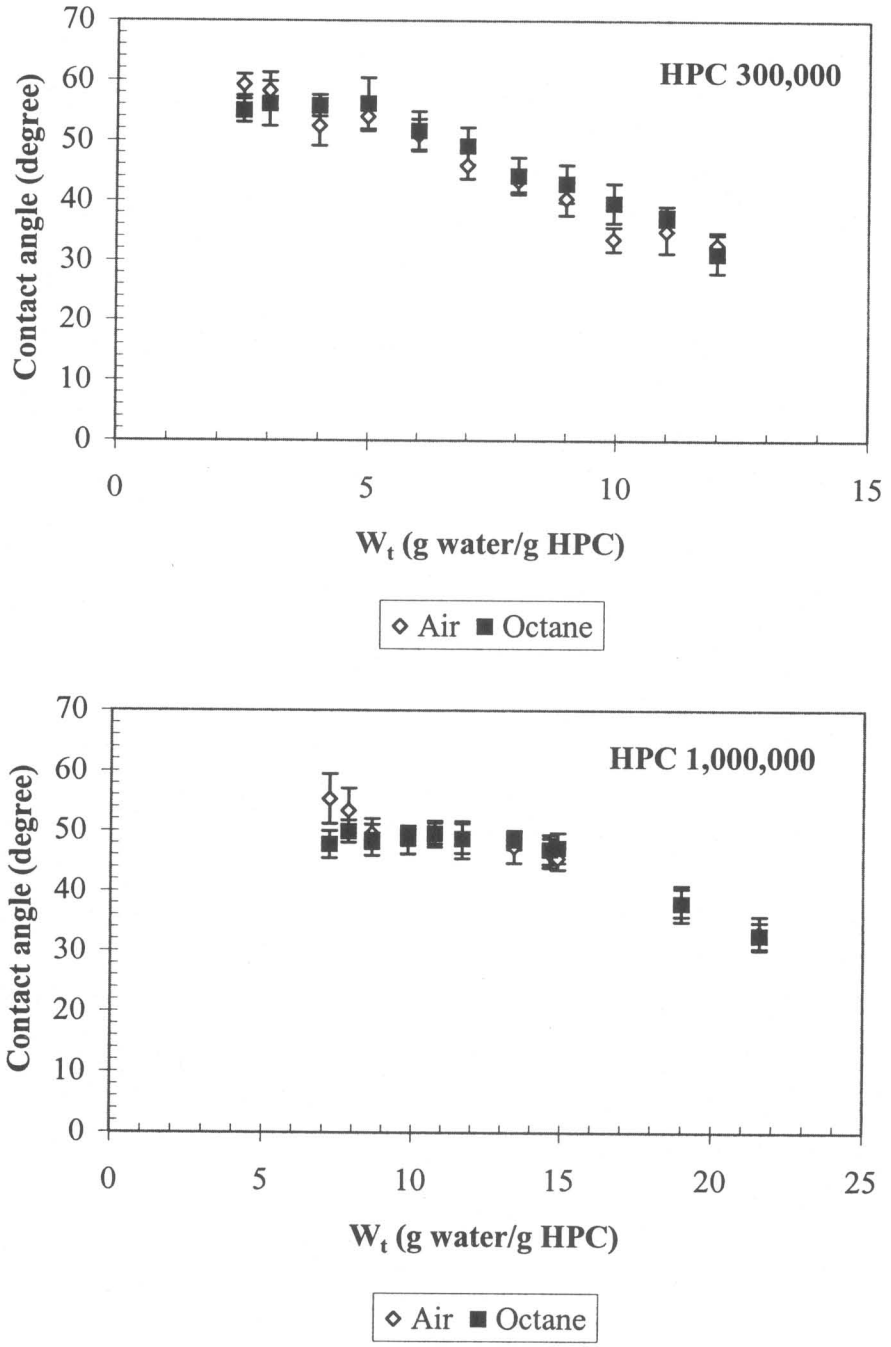

Figure 5 Effect of water content on contact angle of air bubble and n-octane on HPC gels in water at 25 ^{0}C

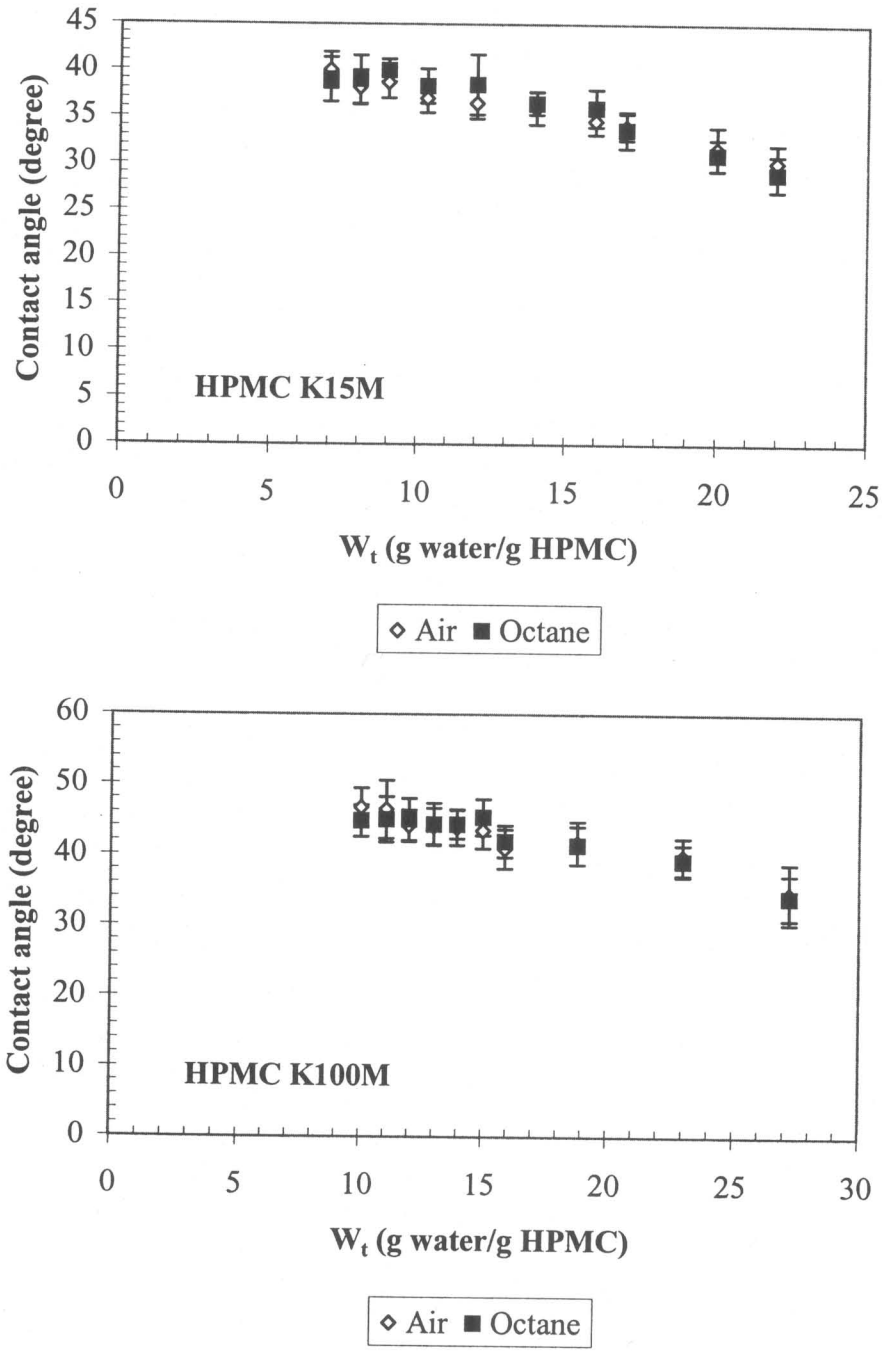

Figure 6 Effect of water content on contact angle of air bubble and n-Octane on HPMC gels in water at 25 ^{0}C

Table 4 Surface free energies of different materials at 25 ^{0}C

Materials	Surface free energy (mJ/m^2)		
	Total	Dispersive	Polar
PTFE	20.9 (0.6)[A]	20.9 (0.6)	-
Water	72.0 (0.6)	21.8 (1.9)	50.2 (1.9)
n-Octane	21.8 (0.1)	21.8 (0.1)	-
PTFE[B]	22.6 (0.8)	22.6 (0.8)	-
PMMA[B]	45.2 (0.7)	29.6 (1.2)	15.6 (0.7)
Glass[B]	62.3 (1.0)	22.9 (1.7)	39.4 (1.0)
PTFE[C]	22.6 (0.7)	22.6 (0.7)	-
PMMA[C]	46.3 (1.4)	27.5 (1.4)	18.8 (0.5)
Glass[C]	51.2 (0.5)	24.2 (0.3)	27.0 (0.5)

A = standard deviation

B = surface free energy under water

C = surface free energy under 2% w/w mucin solution

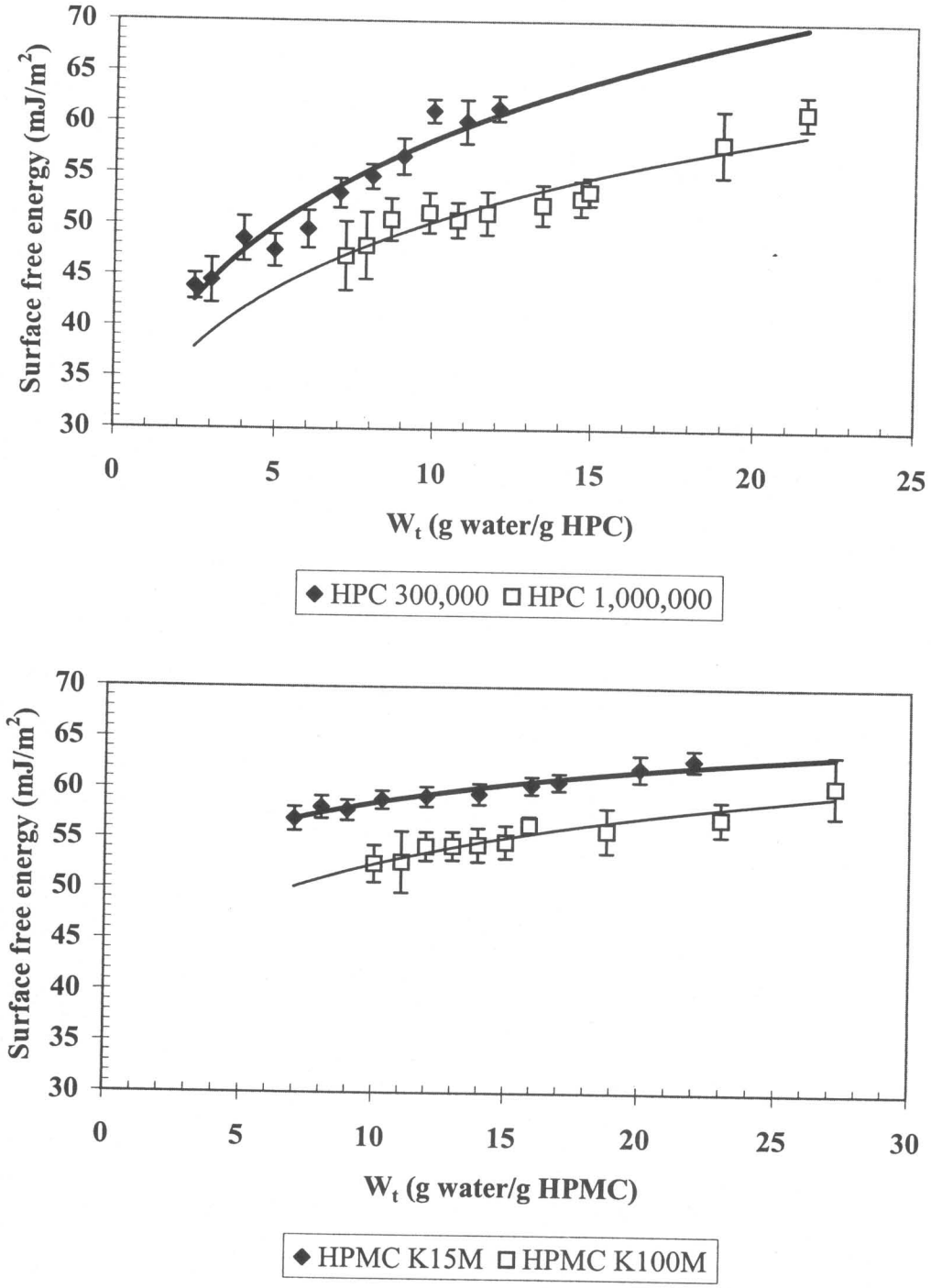

Figure 7 Effect of water content on surface free energies of polymer gels in water at 25 ^{0}C

equations, but they are drawn to show the trend of these data only. Tables 5 and 6 give details for this data. From these calculations, we can see that the surface free energies increase with an increase in water content, which results in a decrease in interfacial free energies between polymer gel surfaces and water.

This phenomenon can be explained by using a reorientation of polymer segments at the interface. When polymer gels are immersed in water, it is energetically more favorable for the polymer segments to reorient in such a way as to expose the hydrophilic parts of the polymer segments toward the water phase [68-72]. Since water can act as a plasticizer, the surfaces of polymer gels with a higher water content are relatively more flexible and easier to rearrange at the interface.

Combining these data with the surface free energies for the substrate surfaces and surface tension of water (Table 4), the work of adhesion between polymer gels and different substrate surfaces in water were calculated using the three-phase system equation (Eq. 6). These are shown in Figures 8 and 9. A maximum work of adhesion can be observed. These results agree well with the explanation provided by Chen and Cyr [46[, in which they concluded that bioadhesive polymers develop their wet adhesive property at various degrees of hydration and reach a maximum at an optimum degree of hydration, whereas excessive water causes a weakening of adhesion.

Table 5 Effect of water content on surface free energies of HPC gels in water at 25 ^{0}C

Polymers	Water content (g water/g polymer)	Surface free energy (mJ/m^2)		
		Total	Dispersive	Polar
HPC 300,000 g/mol	2.49	43.9 (1.3)[A]	11.3 (0.8)	32.5 (1.3)
	3.00	44.4 (2.2)	12.5 (1.7)	32.0 (2.2)
	4.00	48.6 (2.2)	16.4 (1.0)	32.1 (2.2)
	4.97	47.4 (1.6)	15.5 (2.3)	32.0 1.6)
	6.00	49.5 (1.8)	15.4 (1.6)	34.2 (1.8)
	7.00	53.1 (1.4)	17.7 (1.7)	35.4 (1.4)
	8.02	54.7 (1.2)	17.0 (1.5)	37.7 (1.2)
	9.00	56.7 (1.7)	18.4 (1.6)	38.4 (1.7)
	9.94	61.2 (1.1)	21.3 (1.8)	39.8 (1.1)
	11.00	60.2 (2.2)	19.1 (1.0)	41.0 (2.2)
	12.00	61.5 (1.2)	18.0 (1.2)	43.5 (1.2)
HPC 1,000,000 g/mol	7.20	46.9 (3.4)	10.9 (1.0)	36.1 (3.4)
	7.84	47.9 (3.3)	12.9 (0.8)	35.0 (3.3)
	8.63	50.5 (2.1)	14.8 (1.3)	35.7 (2.1)
	9.84	51.2 (2.0)	15.7 (0.6)	35.5 (2.0)
	10.74	50.5 (1.7)	15.3 (0.8)	35.2 (1.7)
	11.68	51.2 (2.1)	15.6 (1.2)	35.6 (2.1)
	13.43	52.0 (2.0)	16.3 (0.7)	35.7 (2.0)
	14.63	52.7 (1.7)	16.2 (1.2)	36.5 (1.7)
	14.90	53.3 (1.4)	17.0 (1.2)	36.3 (1.4)
	19.00	58.1 (3.3)	17.5 (1.0)	40.6 (3.3)
	21.57	61.2 (1.7)	18.4 (1.4)	42.9 (1.7)

A = standard deviation

Table 6 Effect of water content on surface free energies of HPMC gels in water at 25 ^{0}C

Polymers	Water content (g water/g polymer)	Surface free energy (mJ/m^2)		
		Total	Dispersive	Polar
HPMC 15M	7.00	56.9 (1.2)[A]	15.0 (1.1)	37.5 (1.2)
	8.01	58.1 (1.1)	15.3 (1.3)	37.4 (1.1)
	8.99	57.8 (1.0)	16.9 (0.6)	37.4 (1.0)
	10.30	58.8 (0.9)	16.6 (0.9)	37.7 (0.9)
	12.00	59.2 (1.0)	16.7 (1.5)	37.7 (1.0)
	14.00	59.4 (1.0)	17.5 (0.6)	37.2 (1.0)
	15.98	60.3 (0.9)	17.6 (0.9)	38.8 (0.9)
	17.00	60.7 (0.8)	16.7 (0.8)	39.1 (0.8)
	20.00	62.0 (1.3)	17.0 (0.7)	40.1 (1.3)
	21.99	62.8 (1.1)	18.1 (0.8)	42.3 (1.1)
HPMC 100M	10.02	52.5 (1.8)	16.8 (1.7)	40.1 (1.8)
	11.06	52.6 (3.0)	18.0 (1.5)	40.1 (3.0)
	11.98	54.2 (1.4)	18.1 (1.4)	39.7 (1.4)
	13.00	54.3 (1.4)	18.4 (1.5)	40.4 (1.4)
	13.95	54.4 (1.7)	18.8 (1.0)	40.3 (1.7)
	15.00	54.7 (1.6)	18.2 (1.3)	41.2 (1.6)
	15.89	56.4 (0.8)	18.9 (1.1)	41.4 (0.8)
	18.80	55.8 (2.2)	18.2 (1.2)	42.4 (2.2)
	23.00	57.1 (1.7)	18.5 (1.0)	43.5 (1.7)
	27.20	60.4 (3.1)	18.6 (1.4)	44.3 (3.1)

A = standard deviation

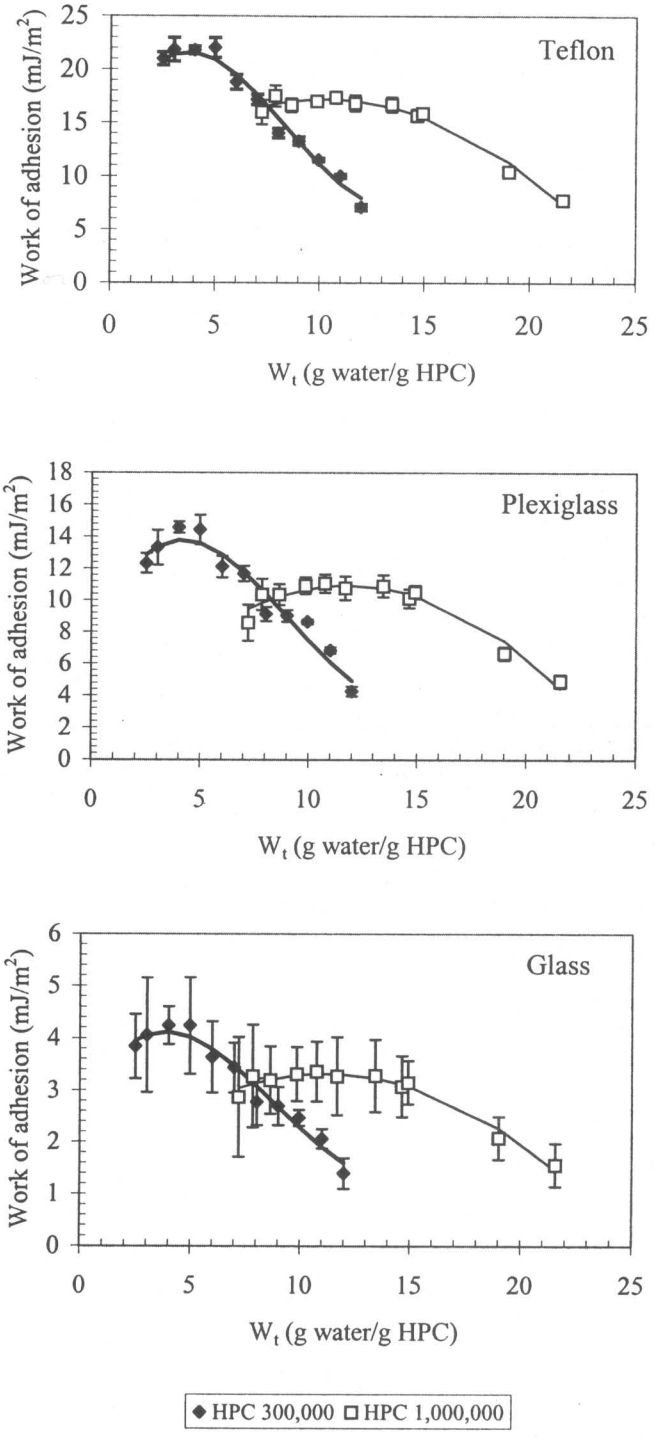

Figure 8 Effect of water content on work of adhesion between HPC gels and substrate surfaces in water at 25 ^{0}C

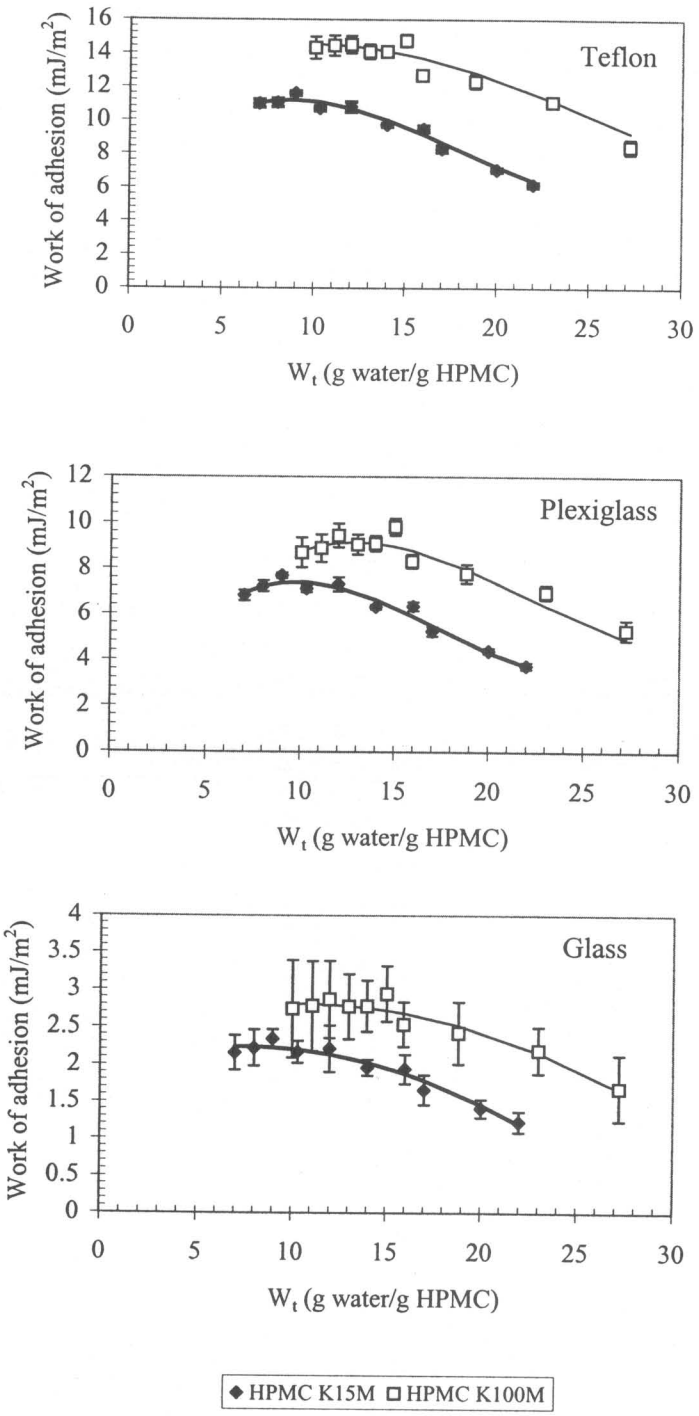

Figure 9 Effect of water content on work of adhesion between HPMC gels and substrate surfaces in water at 25 ^{0}C

Figures 10-13 present the work of adhesion in terms of the contribution of dispersive and polar components. It can be concluded that the total work of adhesion for all polymers and substrate surfaces are mainly from the polar contribution, while a dispersive contribution actually shows a repulsive effect. This repulsive effect can be expected to occur when the surface tension of the medium has a value intermediate to the values of the surface free energy of the two materials ($\gamma_P > \gamma_L > \gamma_S$ or $\gamma_S > \gamma_L > \gamma_P$) [49, 118-119, 121-122]. In other words the dispersive interactions of the bioadhesive polymer and the substrate surface with water (medium) are larger than the interaction between the bioadhesive polymer and the substrate surface. The polar contribution is more significant when the substrate surface is more hydrophobic, i.e., Teflon. However, this contribution does not necessarily result from a better polar interaction between the bioadhesive polymer and the substrate surface. In fact the polar interfacial free energies between bioadhesive polymers and substrate surfaces increase as the hydrophobicity of the surfaces increase (Figures 14 and 15). In other words, the polar interaction between bioadhesive polymers and substrate surfaces is more significant for the hydrophilic substrate. To explain this polar contribution, the interfacial free energy (γ_{SL}) between a substrate surface and water needs to be considered. Figure 16 illustrates the interfacial free energies between substrate surfaces and water. It is shown that a higher

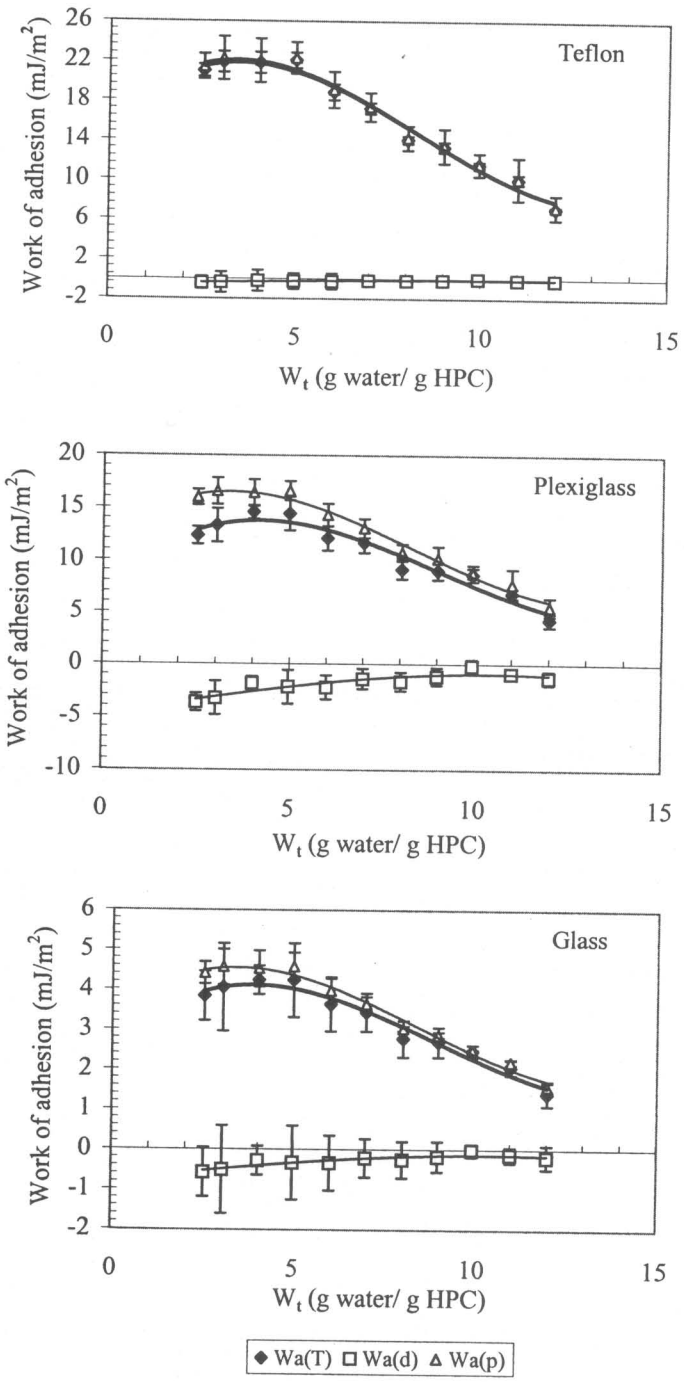

Figure 10 Effect of water content on dispersive and polar contribution to work of adhesion between HPC (300,000 g/mol) gels and substrate surfaces in water at 25 ^{0}C

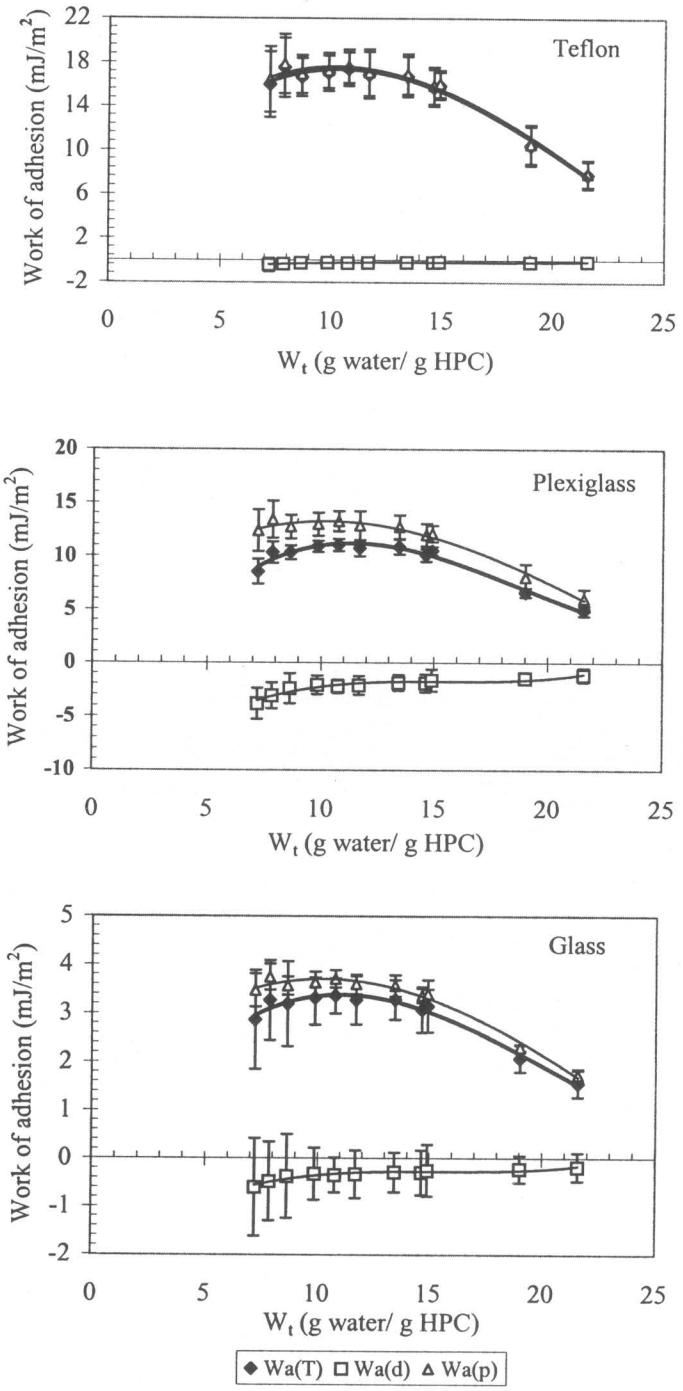

Figure 11 Effect of water content on dispersive and polar contribution to work of adhesion between HPC (1,000,000 g/mol) gels and substrate surfaces in water at 25 ^{0}C

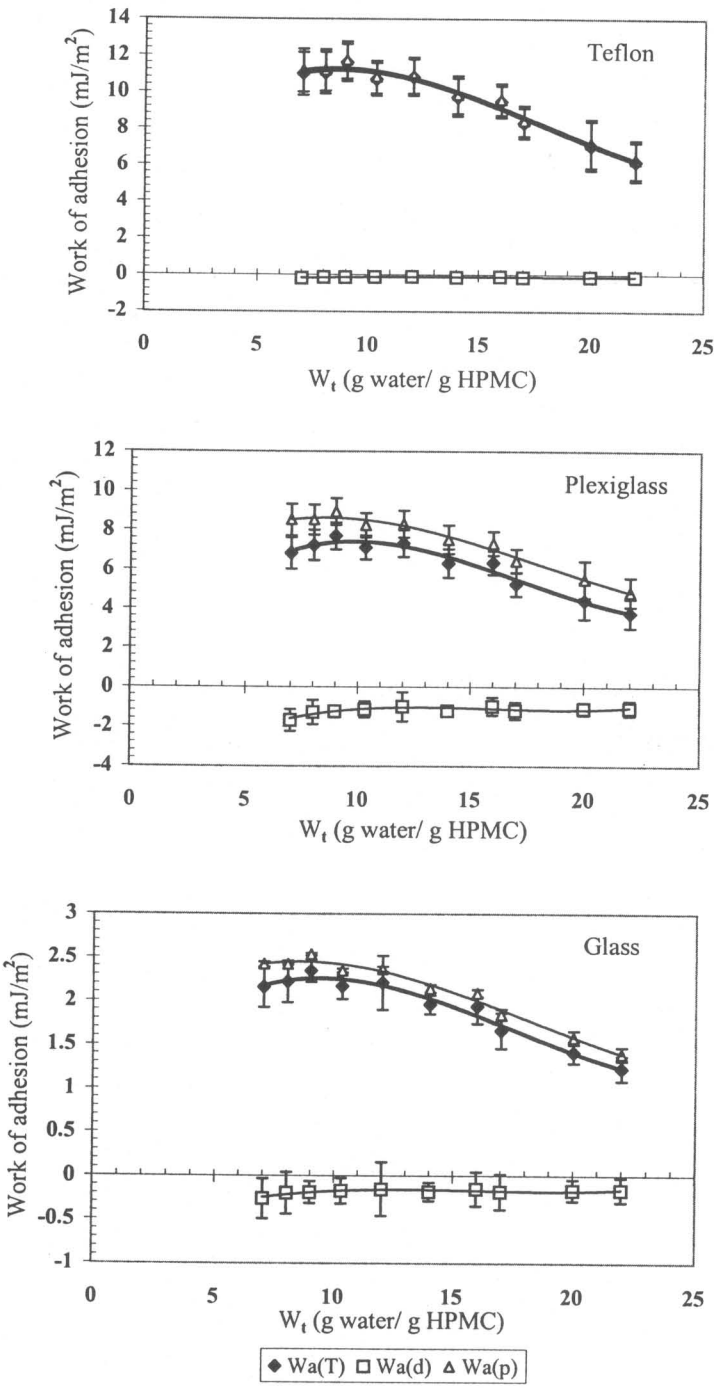

Figure 12 Effect of water content on dispersive and polar contribution to work of adhesion between HPMC K15M gels and substrate surfaces in water at 25 ^{o}C

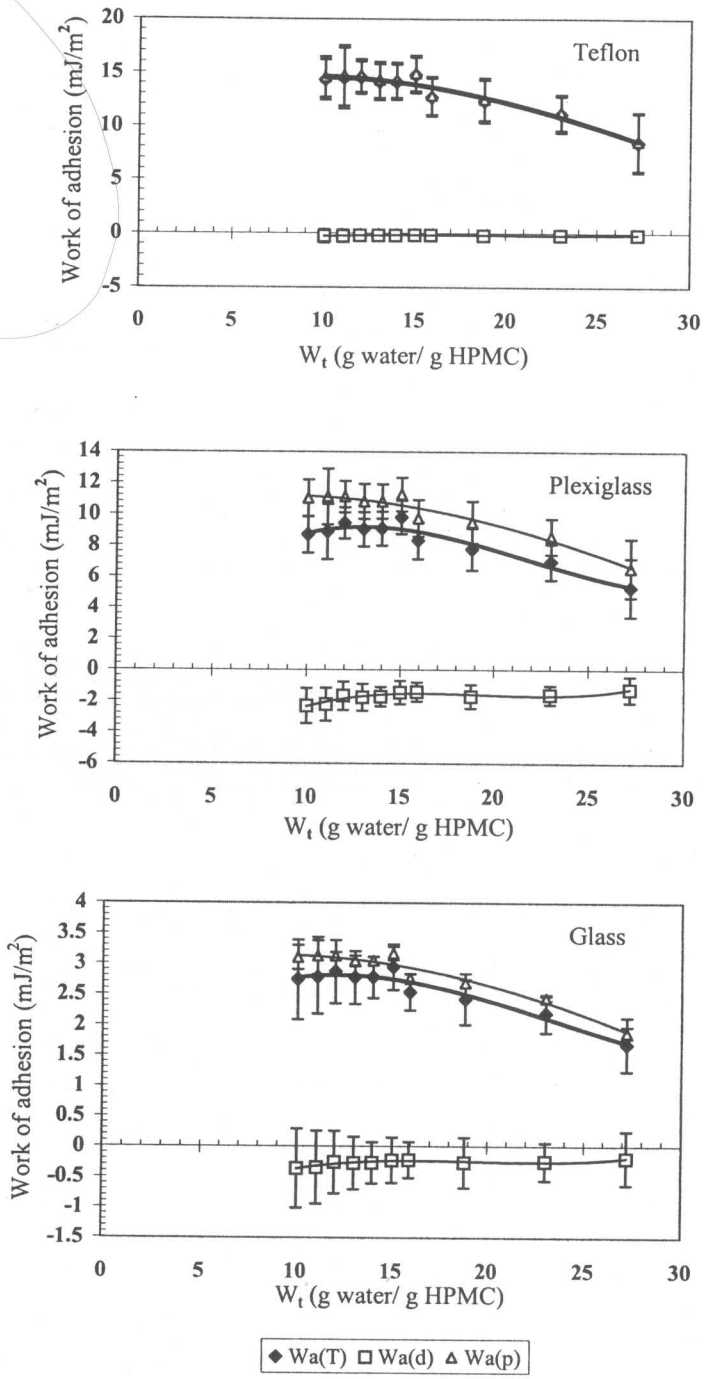

Figure 13 Effect of water content on dispersive and polar contribution to work of adhesion between HPMC K100M gels and substrate surfaces in water at 25 ^{0}C

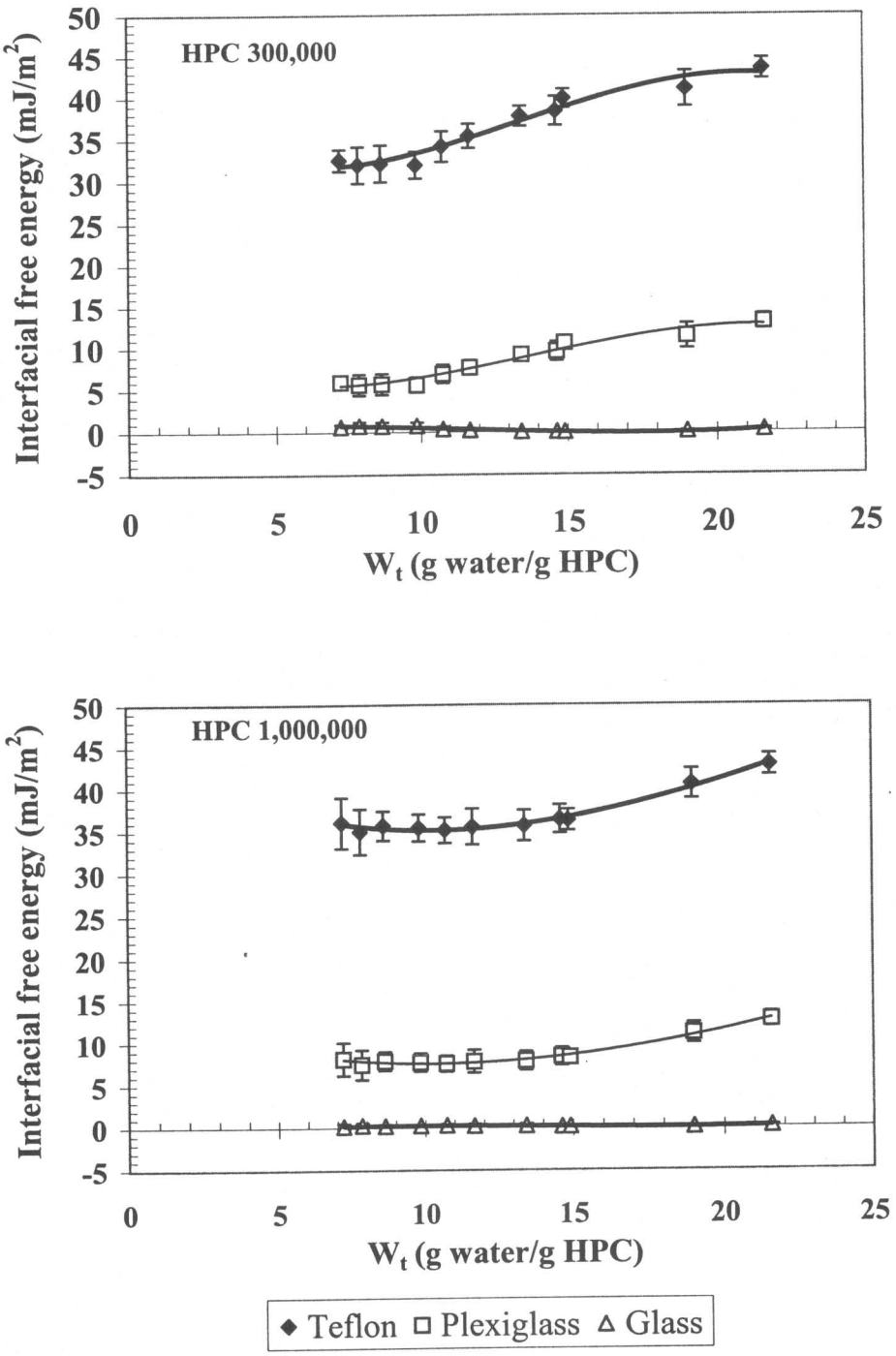

Figure 14 Effect of water content on polar interfacial free energy between HPC gels and substrate surfaces in water at 25 ^{0}C

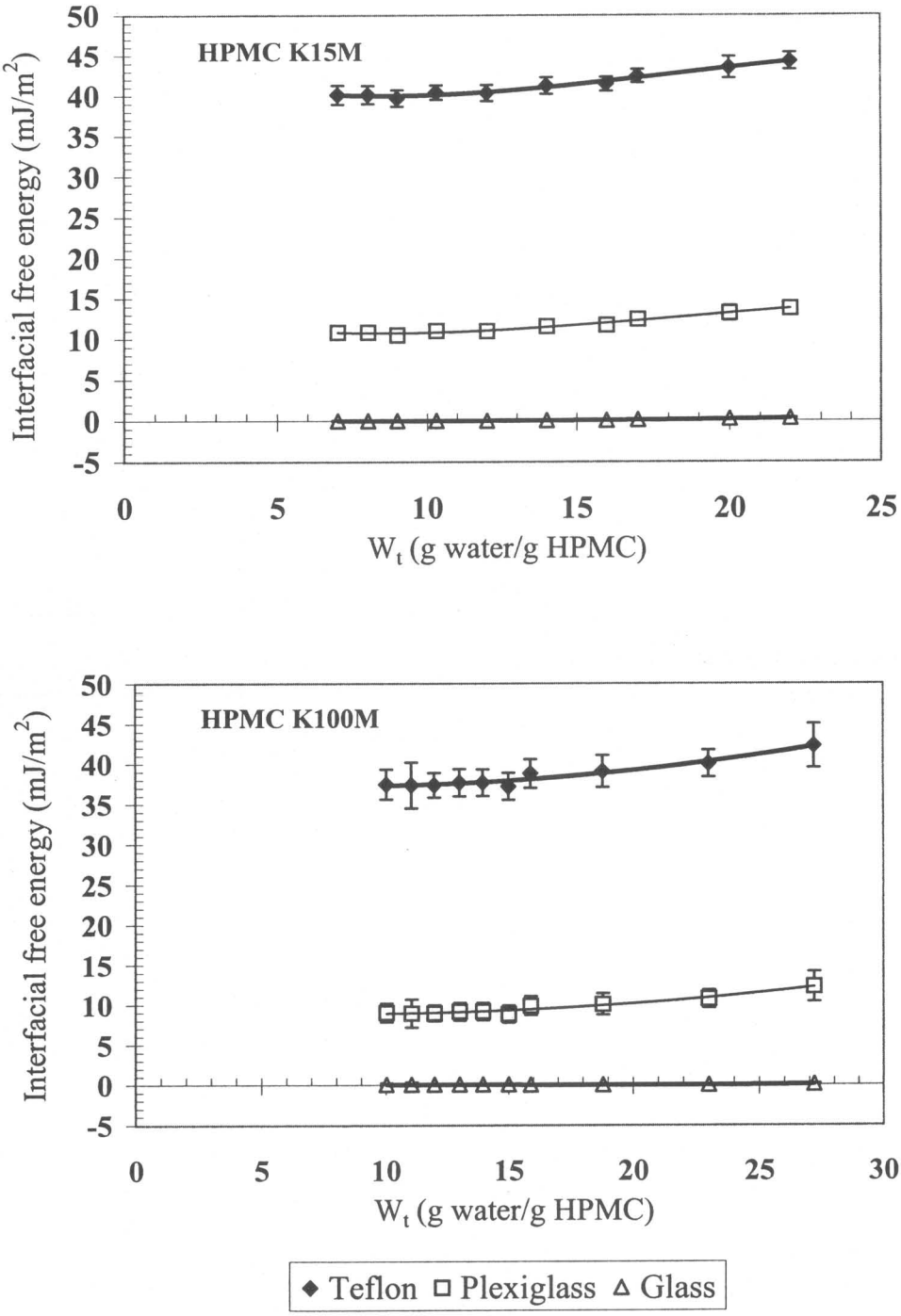

Figure 15 Effect of water content on polar interfacial free energy between HPMC gels and substrate surfaces in water at 25 ^{0}C

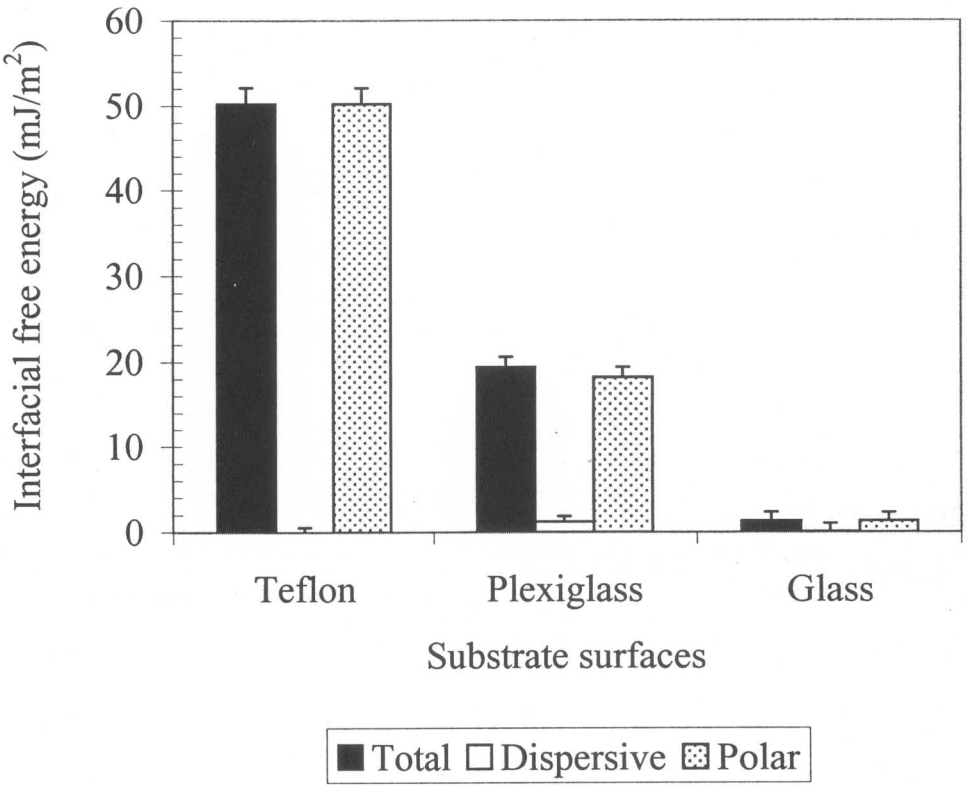

Figure 16 Interfacial free energy between substrate surfaces and water at 25 ^{0}C

interfacial free energy was observed as the hydrophobicity of the substrate surface increases. This result is mainly from the polar contribution. Therefore, it is important to note that the mismatch of polarity between a substrate surface and a medium will result in a better adhesion between the substrate surface and the bioadhesive polymer. These results can also confirm that a better understanding of the effect of environment on adhesion behavior is necessary.

❖ Force of detachment

If only two phases are considered, adhesion between two surfaces increases as the interfacial free energy decreases. HPC and HPMC can be considered as hydrophilic polymers; therefore, a better adhesion to a hydrophilic surface is expected. However, a higher force of detachment is observed as the substrate surface hydrophobicity increases (Figures 17 and 18). This means that the inclusion of a surrounding medium is necessary. By doing that, a good correlation between the maximum force of detachment per unit area of polymer gels on different substrates in water and the calculated work of adhesion is observed (Figure 19). Motazavi and Smart [123] showed that the work of adhesion and maximum detachment force provide the same information on bond strength. Hence, these results confirm that the calculated work of

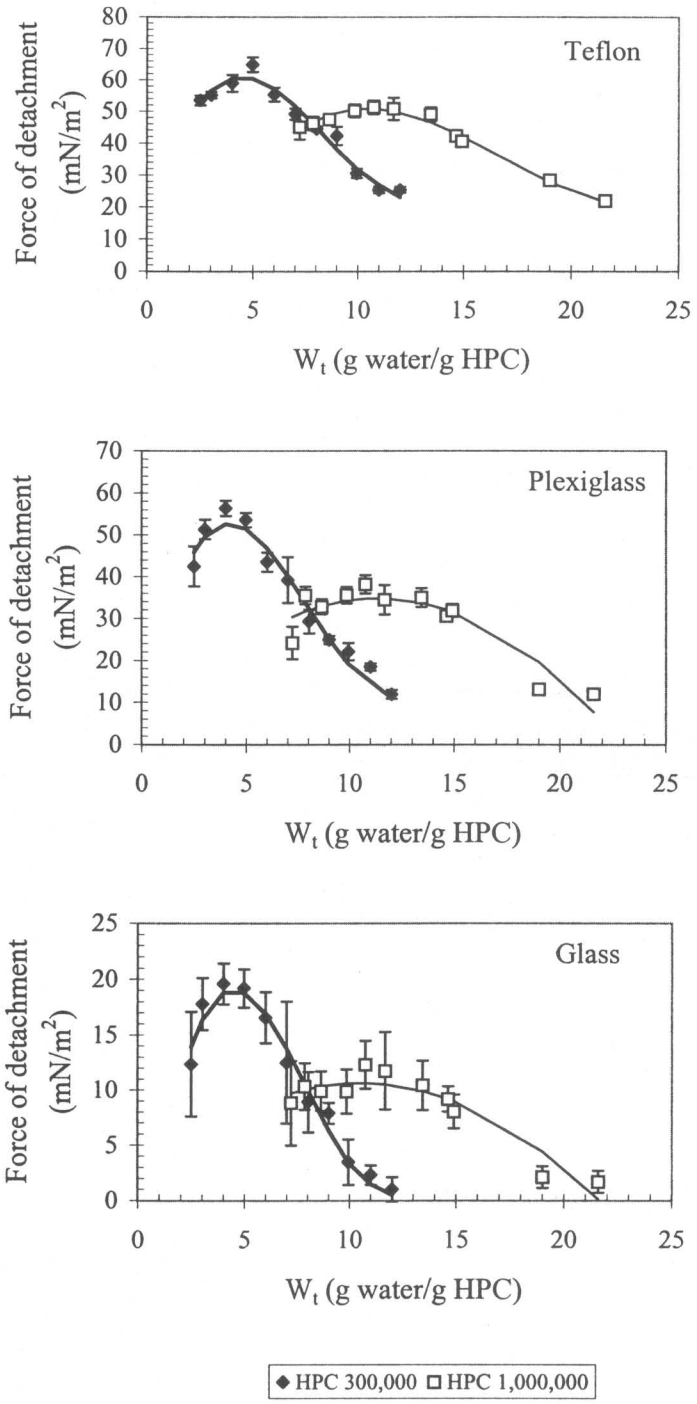

Figure 17 Effect of water content on force of detachment between HPC gels and substrate surfaces in water at 25 ^{0}C

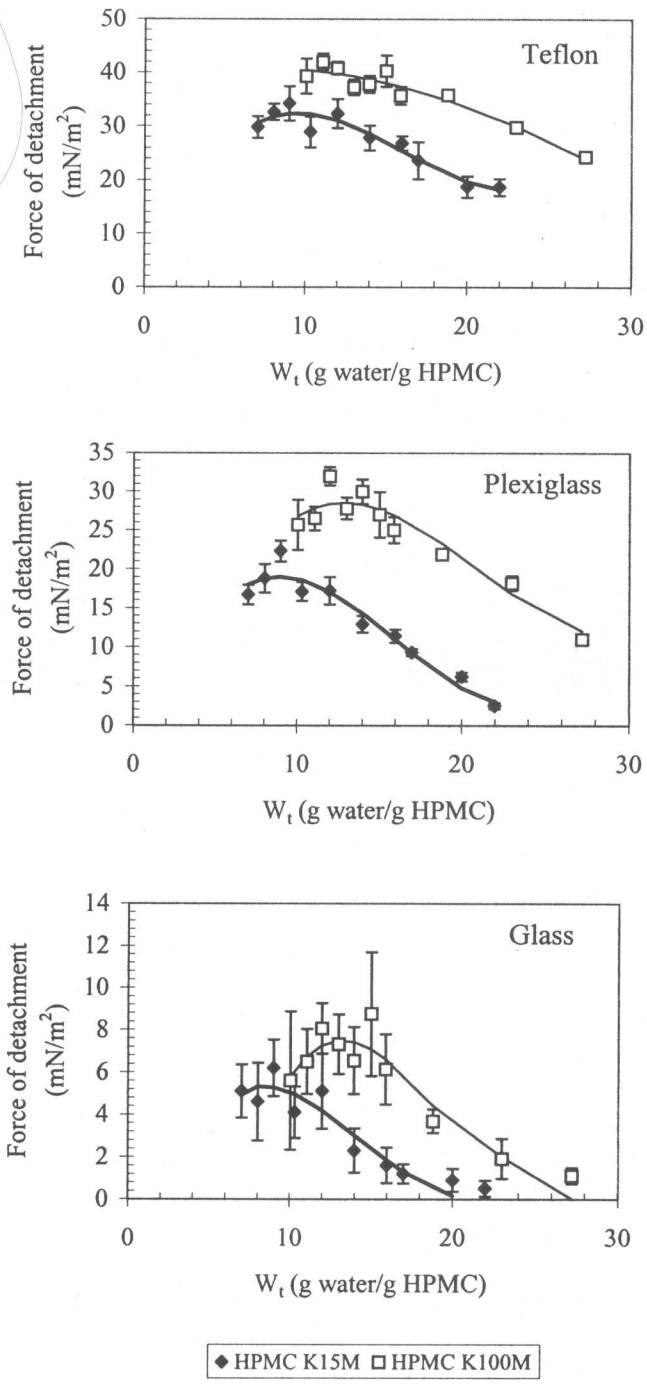

Figure 18 Effect of water content on force of detachment between HPMC gels and substrate surfaces in water at 25 ^{0}C

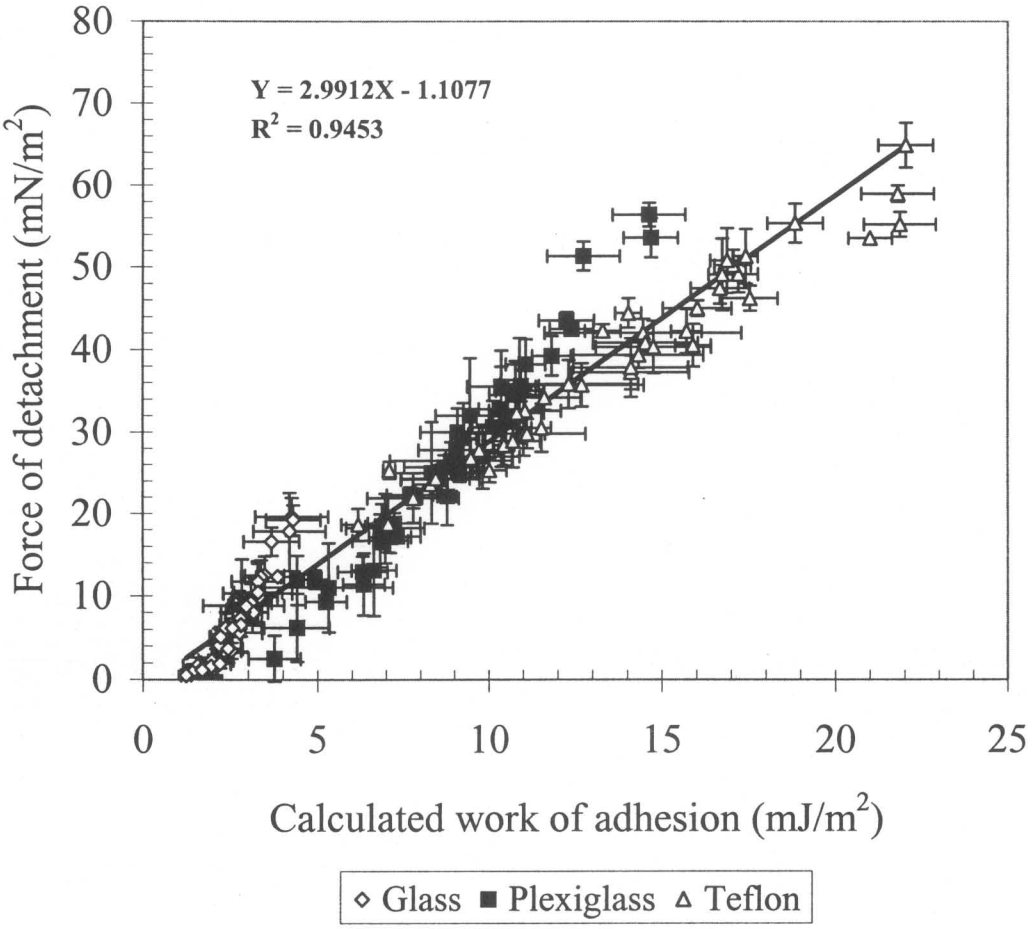

Figure 19 Correlation between calculated work of adhesion and force of detachment between polymer gels and substrate surfaces in water at 25 ^{o}C

adhesion from a three-phase system equation can be used to explain the adhesion behavior especially in the presence of a third medium as is present in the GI-tract. Therefore, we will use the three-phase system approach in this work to explain adhesion behavior.

❖ States of water in polymer gels

The endothermic enthalpy from a DSC heating scan seen with polymer gels is the energy that is required to melt freezable water in the polymer gels. Therefore, as expected, increasing the water content in polymer gels results in an increase in enthalpy (Table 7). By assuming that the enthalpy can be attributed mainly to the melting of the freezable water, it is apparent that there is an increase in the amount of such water as the water content increases. Therefore, there is a limitation required of water to hydrate the polymer as non-freezable water, while extra water will be present as freezable water. The enthalpy data from DSC measurements (Table 7) can be used to calculate the amount of freezable water in polymer gels using Eq. 29, where the melting enthalpy value of pure water is equal to 336.2 mJ/mg. By plotting these data in Figures 20 and 21, a good linear correlation between total water content (W_t) and the amount of freezable water content (W_f) with a slope very close to unity is observed. From Eq. 30, the maximum non-freezable

Table 7 Effect of water content on melting enthalpy of water in polymer gels

Polymers	Water content (g water/g polymer)	Enthalpy[A] (mJ/mg)	Nonfreezable Water content (g water/g polymer)
HPC 300,000 g/mol	3.00	181.1	0.83
	4.00	209.3	
	4.97	235.8	
	6.00	251.1	
	7.00	258.9	
	8.02	268.6	
	9.00	280.5	
	9.94	281.0	
	11.00	284.5	
	12.00	287.7	
HPC 1,000,000 g/mol	6.08	248.1	0.80
	9.02	275.3	
	10.13	283.5	
	10.94	286.7	
	12.04	289.5	
	14.05	296.1	
	19.99	306.8	
HPMC 15M	8.01	273.3	0.69
	10.30	285.3	
	12.00	291.6	
	14.00	297.4	
	15.98	300.7	
	17.00	303.2	
	20.00	309.2	
HPMC 100M	10.05	284.8	0.72
	12.92	296.2	
	13.80	297.2	
	15.02	301.1	
	16.01	302.3	
	17.01	304.9	
	17.90	306.9	

A = Melting enthalpy of water is 336.2 mJ/mg

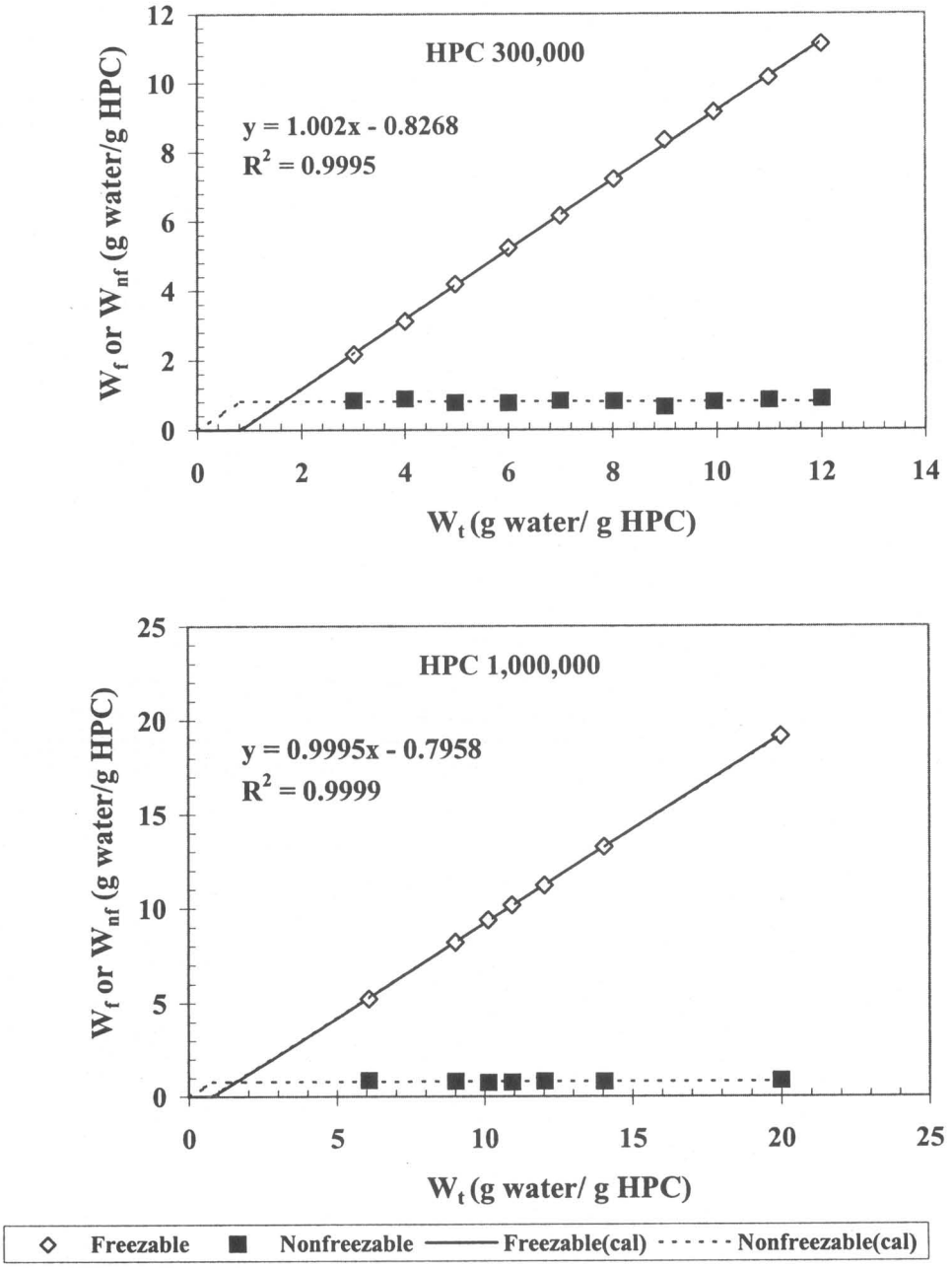

Figure 20 Freezable and non-freezable water as a function of water content in HPC gels

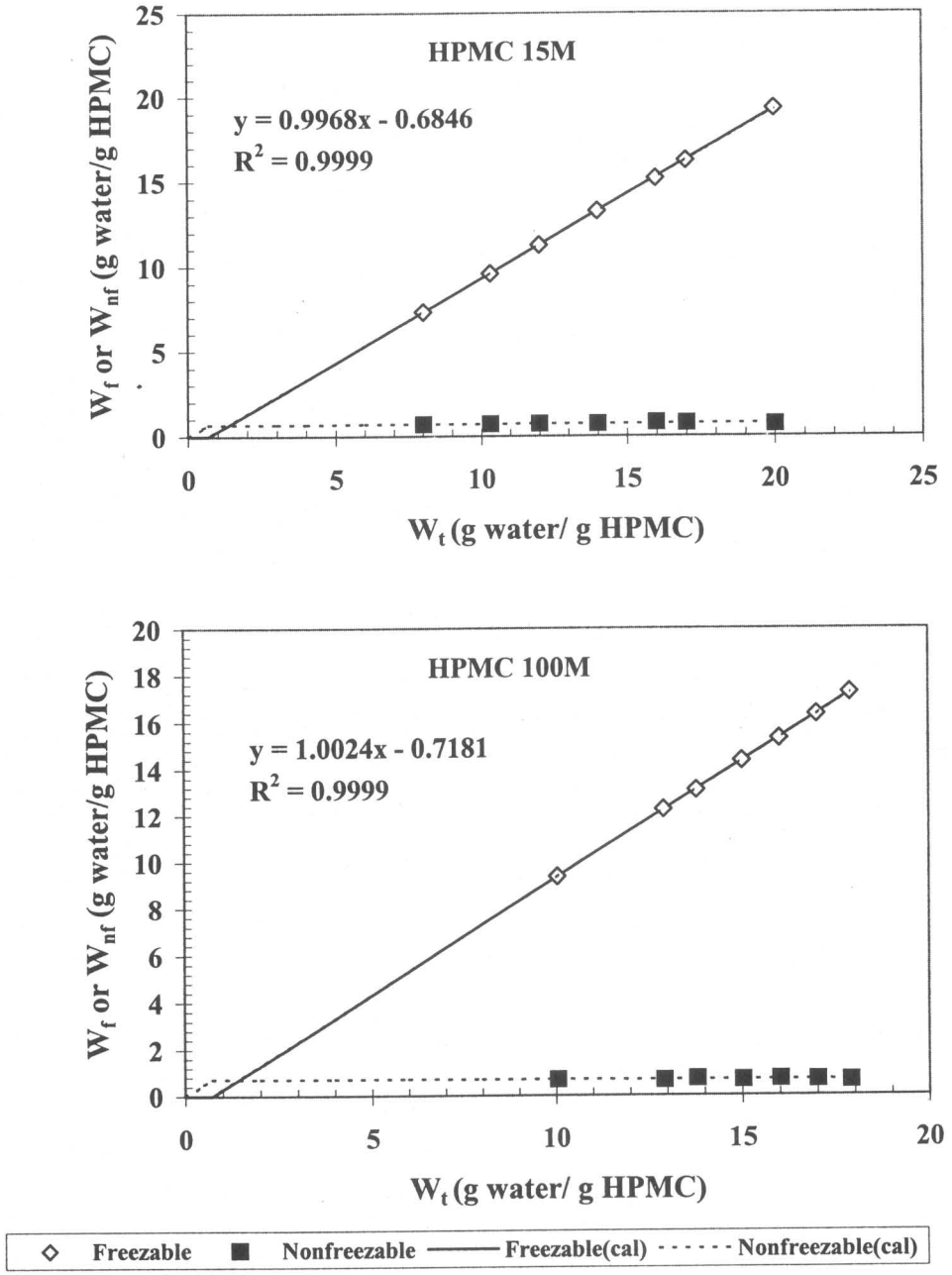

Figure 21 Freezable and non-freezable water as a function of water content in HPMC gels

water content of polymers can be calculated as the x-intercept value as shown in Table 7. The data show that there is no significant effect of polymer molecular weight on the freezable water content. This result agrees well with the work done by Nokhodchi et al. [124-125] who studied the interaction between water and HPMC and concluded that viscosity grade (molecular weight) and particle size had no significant effect on the amount of water bound to HPMC polymers. Whereas, McCrystal et al. [126] found that the bound water content apparently increased with an increase in polymer viscosity within the HPMC K-series after 96 hours equilibration. Note that these papers reported the amount of non-freezable water as moles of water per polymer repeating units. The data also show that HPC has higher freezable water content than HPMC. McCrystal et al. [127] explained this behavior as the result of a higher percentage of hydrophilic hydroxypropoxyl groups in HPC. HPC also has no methoxyl substitution, which is believed to be the major factor in causing a decrease in cellulose ether solubility [128].

To explore the effect of states of water on the adhesion behavior of polymer gels, the ratio between freezable and non-freezable water was calculated and plotted with work of adhesion data as shown in Figures 22 and 23. If non-freezable water is the only contribution to the change of adhesion behavior, the work of adhesion pattern is supposed to be the same for the same polymer with different molecular weights. However, we

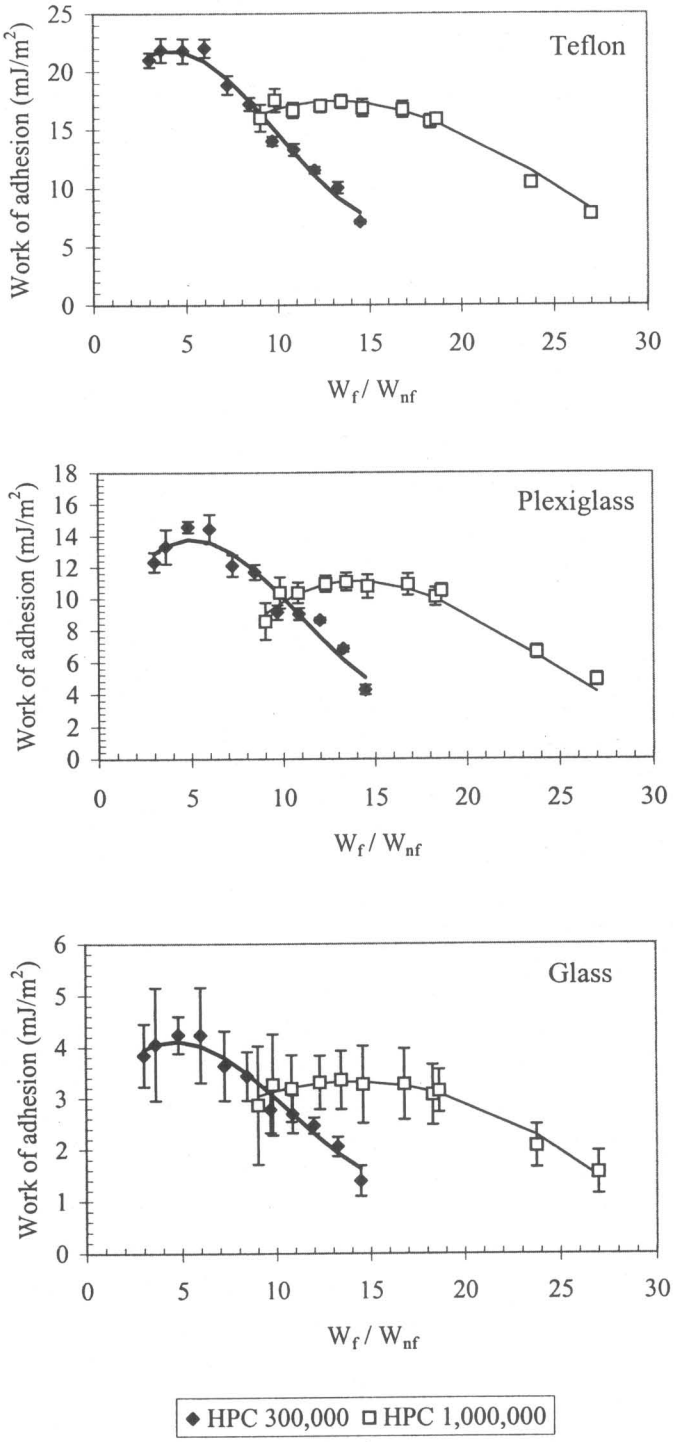

Figure 22 Effect of freezable water content on work of adhesion between HPC gels and substrate surfaces in water at 25 ^{0}C

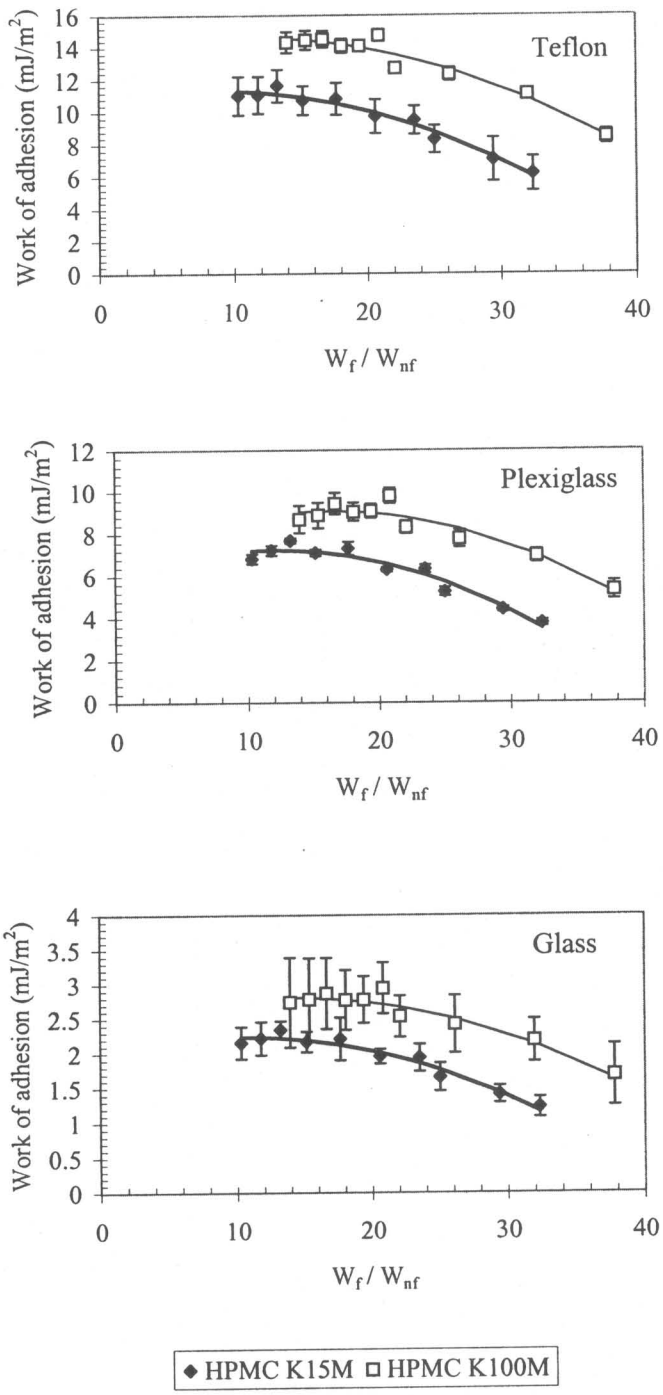

Figure 23 Effect of freezable water content on work of adhesion between HPMC gels and substrate surfaces in water at 25 ^{0}C

can clearly see the dependency of the adhesive pattern on molecular weight for both HPC and HPMC. The results show that a higher molecular weight polymer has maximum adhesion at a higher W_f/W_{nf} ratio and can extend the adhesion to a higher water content. Based upon the data obtained in this study the following model is proposed for an explanation of the adhesion behavior (Figure 24). Polymer in a dry state is a system of macromolecular chains held together by strong intermolecular interactions, i.e., H-bonding. Therefore, polymer in the dry form has a very low adhesion force (stage 1). At this stage, we cannot perform the experiment using our method because the viscosity of the polymer gel is too high. As the polymer absorbs water, strong H-bonding occurs between water molecules and active surface sites of the polymer chains and acts as a plasticizer to increase mobility of the polymer chain [129]. The initially absorbed water molecules are all non-freezable water at this stage. The polymer chain can partially expose its hydrophilic fragment to the surface, which modifies the conformation of the hydrophobic fragment (stage 2). Therefore, the adhesive bond between polymer chains and a substrate surface starts to occur. Successive absorption of water will now allow an easier penetration into the polymer structure with less interaction and increases the flexibility of the polymer chain so it can rearrange itself to a certain level that allows an optimum possible adhesion (stage 3). As water enters the polymer structure, the

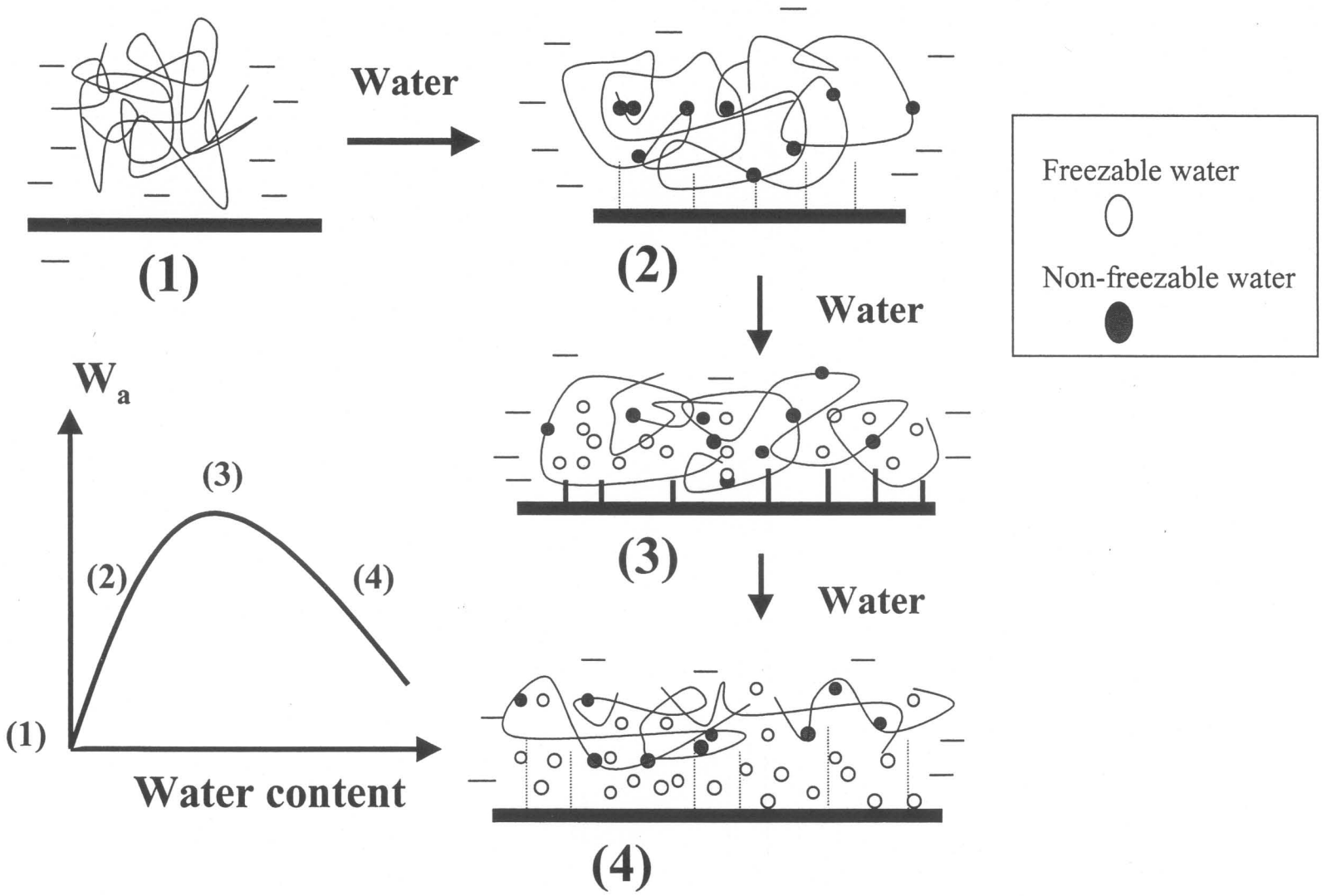

Figure 24 Schematic model for explaining the effect of types of water in polymer gel on adhesion kinetics

polymer begins to swell markedly and creates void spaces for the formation of multilayers of water at the interface. These layers of water will interfere with the interaction between the polymer gel and the substrate surface resulting in a reduction of the adhesion force (stage 4). At this moment excess water is present. Therefore, the excess water can be defined as the water absorbed and present at the interface between polymer and substrate. This water can decrease the adhesion force by lowering the interfacial tension between the polymer surface and the water (medium) and/or interfering with the interaction between the polymer chain and the substrate surface by lengthening the interaction bond (stage 4). This process will continue until the polymer chain cannot hold more water, which results in the erosion of the polymer gel. At this point, we cannot perform the experiment using our method because the viscosity of the polymer gel is too low. Since higher molecular weight polymers have longer polymer chains, the molecular weight of the polymer can play a role in all stages. For example, the polymer needs more water to break up the intermolecular forces between its chains, so that the maximum adhesion can be found at higher water content. The higher molecular weight can also better hold water in the polymer chain. Therefore, it will lose adhesion at higher water content because it will decrease the amount of water at the interface when compared to lower molecular weight polymer at the same water content. Note that this

comparison is best made when comparing the same polymer with different molecular weights.

B. The effect of mucin in the medium on the change of surface free energy parameters

❖ Surface tension of mucin solutions

The dependence of surface tension on mucin concentration is shown in Figure 25. It is clear that the surface tension decreases with an increase in mucin concentration. Beyond a certain concentration (1%w/w), no further significant decrease was observed. This reduction is the result of a decrease in the polar component and is a direct indication of high surface activity of the mucin. Mikos and Peppas [130] measured the surface tension of mucin solutions from different sources, i.e., porcine stomach mucin, bovine submaxillary glands at 37 °C, and found that the porcine stomach mucin solution had a surface tension about 45 mN/m. Finholt and Solvang [131] reported surface tension values between 35-50 mN/m for gastric juice collected from patients with gastrointestinal diseases. The low surface tension of gastric juice has also been recognized by other researchers [132-133]. This finding

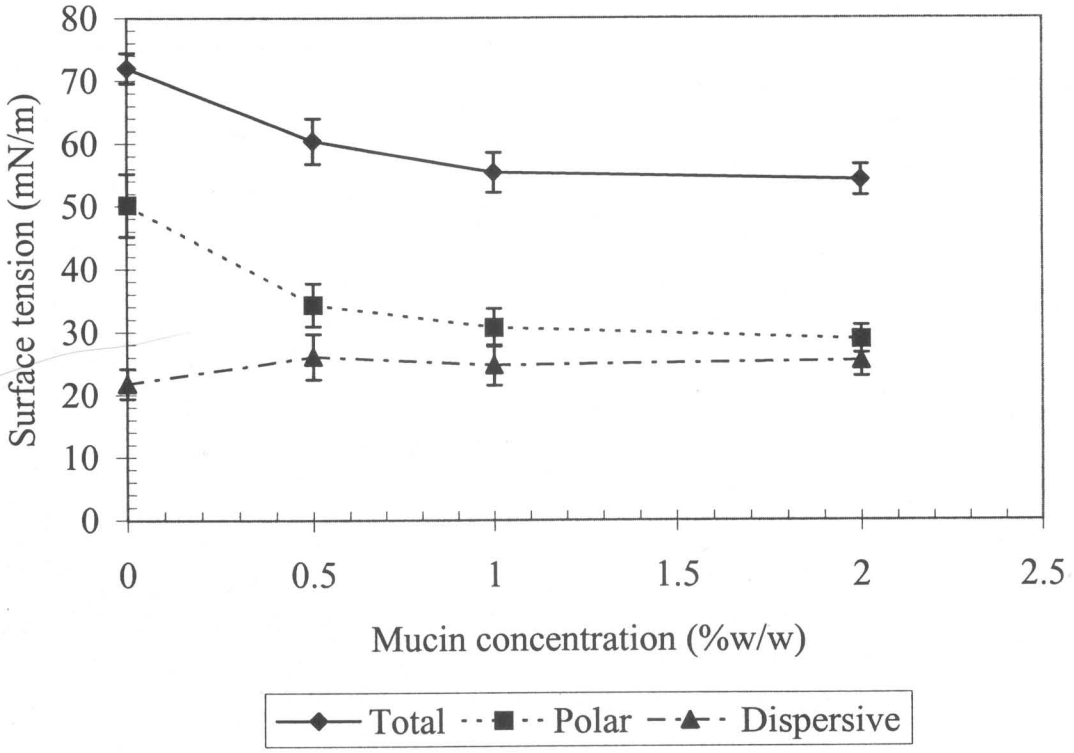

Figure 25 Effect of mucin concentration on surface tension of water at 25 ^{0}C

suggests that mucin in gastric juice is one of the importance sources of its low surface tension.

The stomach mucosal surface has been demonstrated to be quite hydrophobic with a low surface free energy [129-139]. According to their animal studies, Hill et al. [135] proposed that the hydrophobic nature of gastric mucosa is due to a monolayer of surface-active phospholipids oriented with their hydrophobic tails pointed toward the luminal surface. A liquid with less than or equal surface tension to that of the mucosa will have a negative or zero interfacial tension. As a result, gastric juice can wet the mucosa. Note that this issue needs to be clarified because the phospholipid may be present as a bilayer system in the presence of an aqueous environment [138]. However, it is not our goal to explore this matter in this study.

❖ Surface free energy parameters

The surface free energies of HPC and HPMC gels in mucin solution (2%w/w) are shown in Figures 26 and 27, respectively. The lines in these figures represent only the trend of the data. These results show that the surface free energies of these polymer gels decrease significantly compared with the results in water. It is shown that the polymer gel reorients its structure at the surface according to the change of

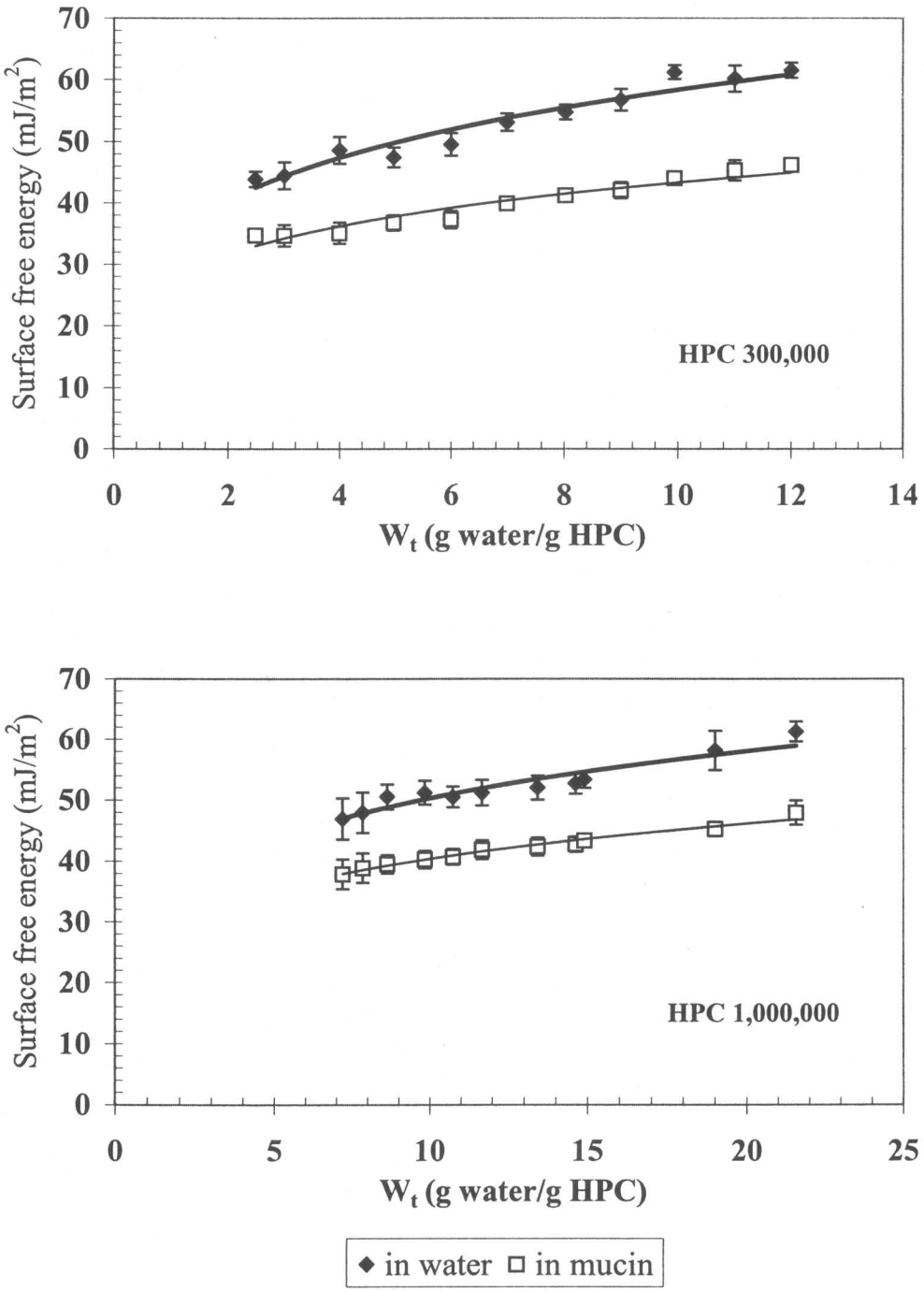

Figure 26 Effect of water content on surface free energies of HPC gels in water or 2% w/w mucin solution at 25 ^{0}C

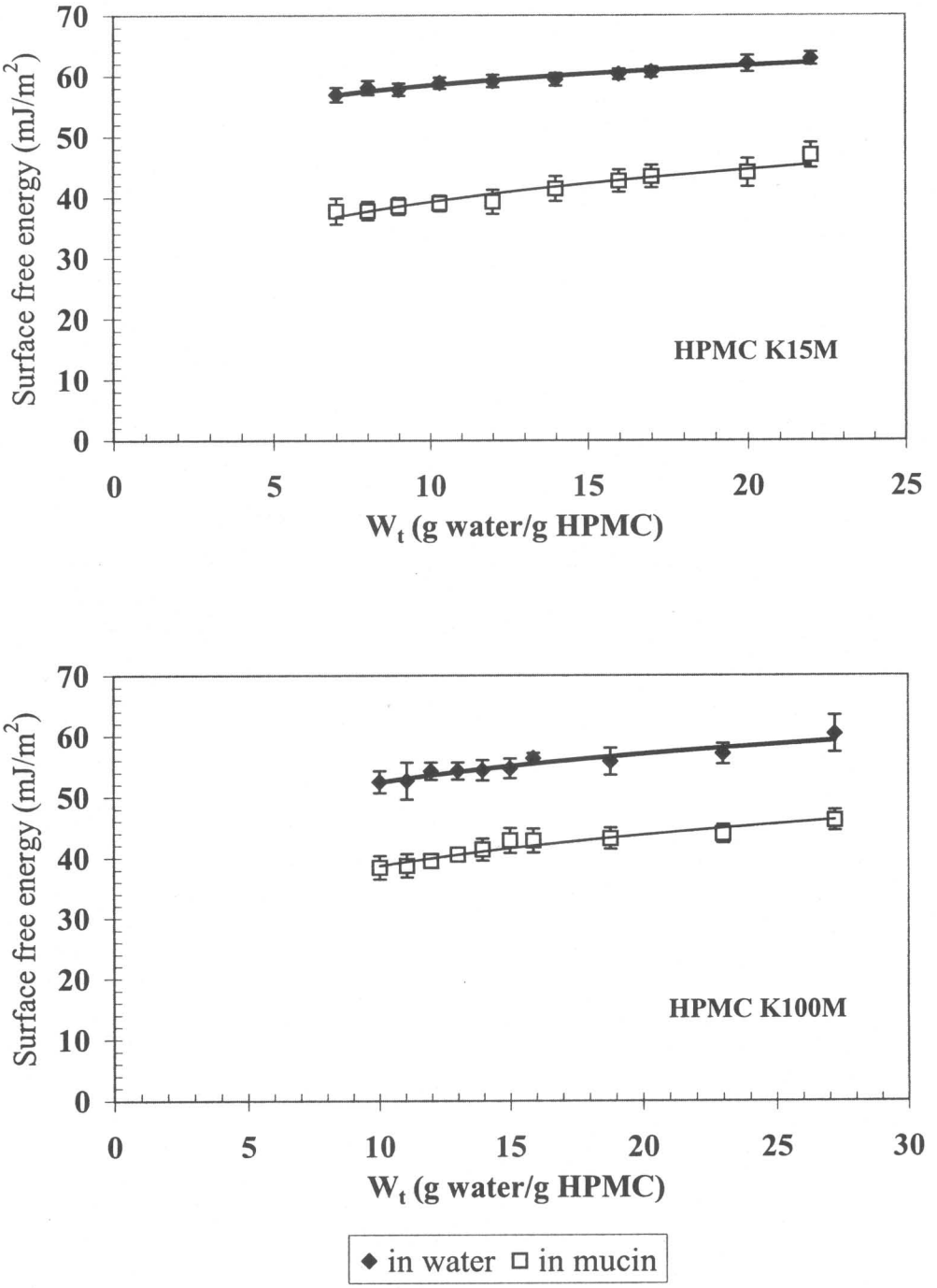

Figure 27 Effect of water content on surface free energies of HPMC gels in water or 2% w/w mucin solution at 25 ^{0}C

environment from water to a mucin solution. This change is less for solid substrate surfaces (Table 4). In the case of the work of adhesion between polymer gels and substrate surfaces in mucin, it is clearly shown that the work of adhesion decreases in the presence of mucin (Figures 28-31). The main reason for this reduction is the decrease of interfacial free energy between the mucin solution and substrate surfaces as shown in Figure 32. These results suggest that mucin in gastric juice affects the adhesion process between the bioadhesive system and mucosa. Possible explanations are the change of surface free energy of the bioadhesive system and the low interfacial free energy between the mucin solution and the mucosal surface. The first explanation can be affected by the adsorption of mucin on the surface or by reorientation of molecules in the polymer surface. The latter explanation is possibly a difficult task to overcome because there is the possibility that gastric juice and the gastric mucosa have very similar polarities and surface free energies. Therefore, gastric juice can act as a lubricant protecting the adhesion of foreign substance to the mucosa. Figure 33 indicates a good correlation between the calculated work of adhesion and force of detachment using HPC (300,000 g/mol) as an example of a polymer system. Therefore, the three-phase system approach can also be used to explain adhesion behavior in the presence of mucin.

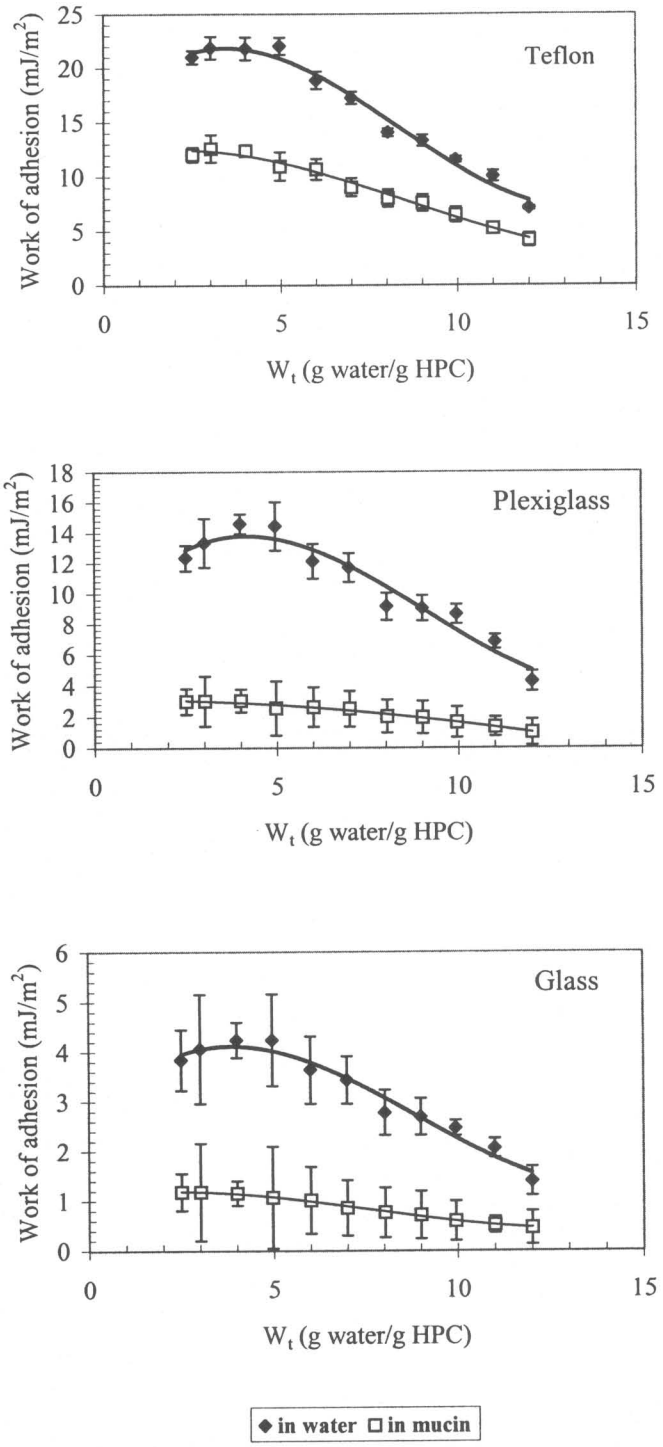

Figure 28 Effect of water content on work of adhesion between HPC (300,000 g/mol) gels and substrate surfaces in 2% w/w mucin solution at 25 ^{o}C

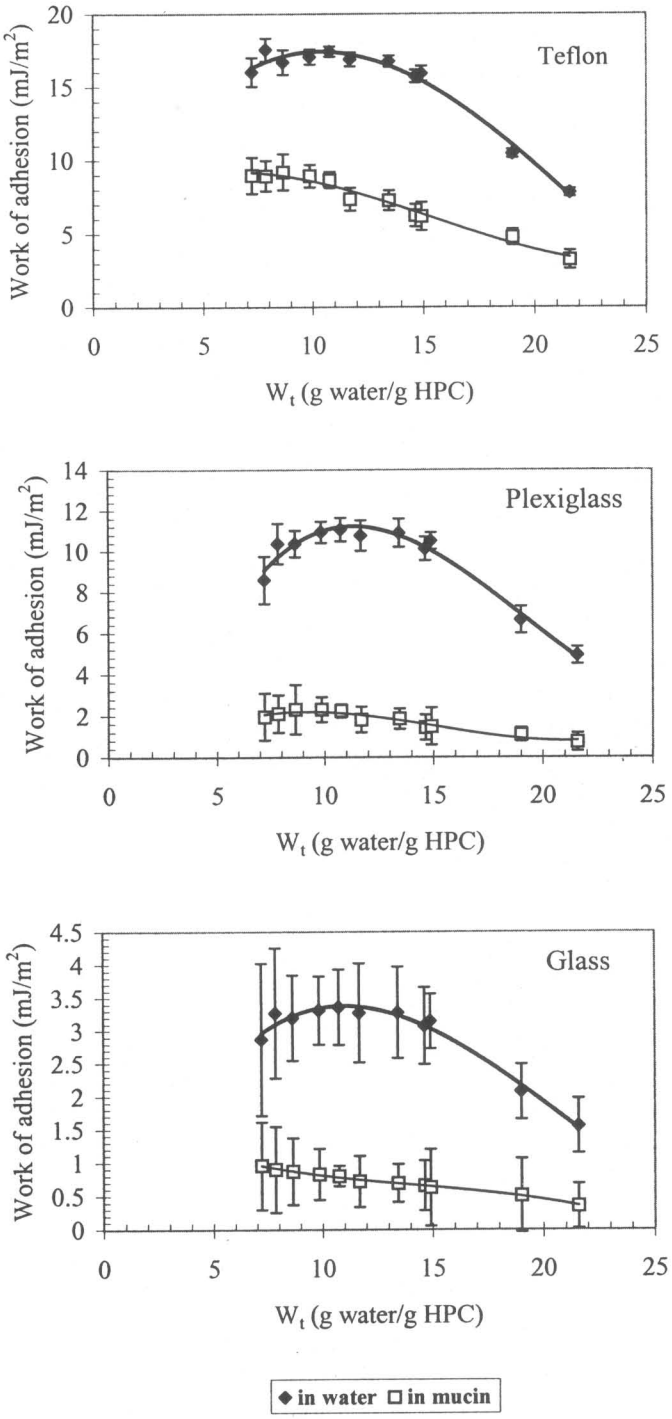

Figure 29 Effect of water content on work of adhesion between HPC (1,000,000 g/mol) gels and substrate surfaces in 2%w/w mucin solution at 25ºC

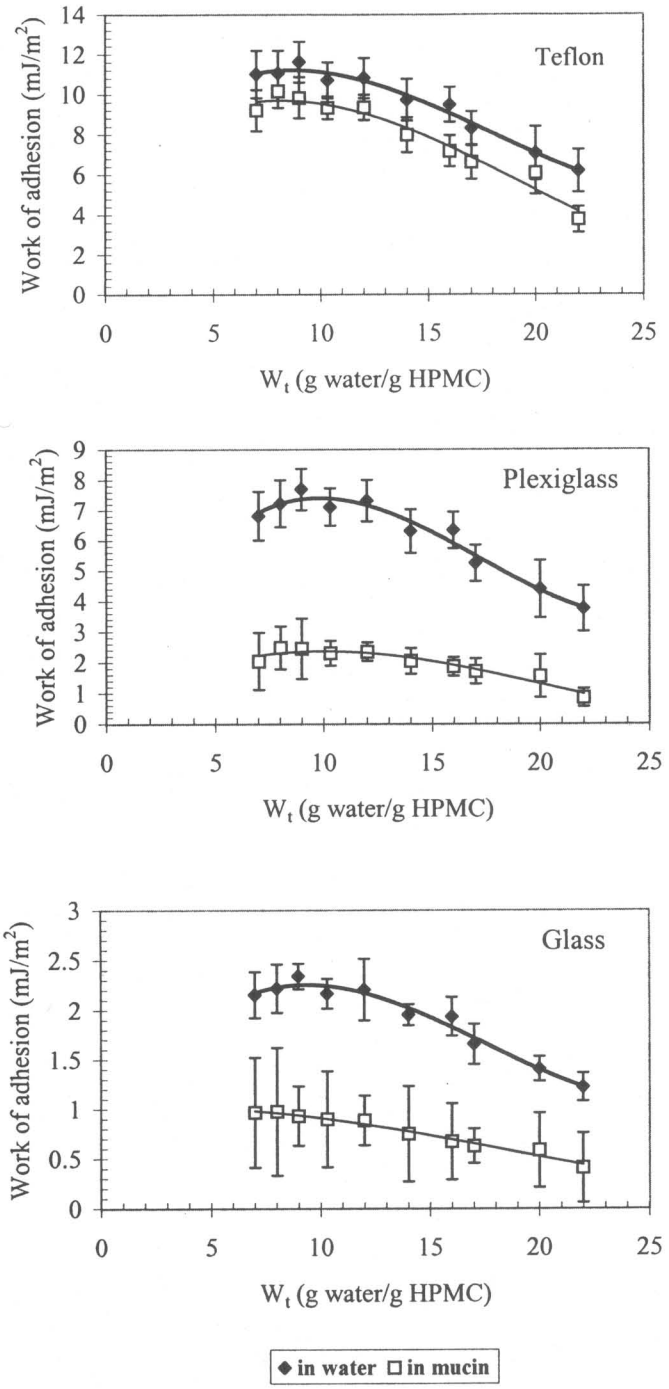

Figure 30 Effect of water content on work of adhesion between HPMC K15M gels and substrate surfaces in 2% w/w mucin solution at 25 ^{0}C

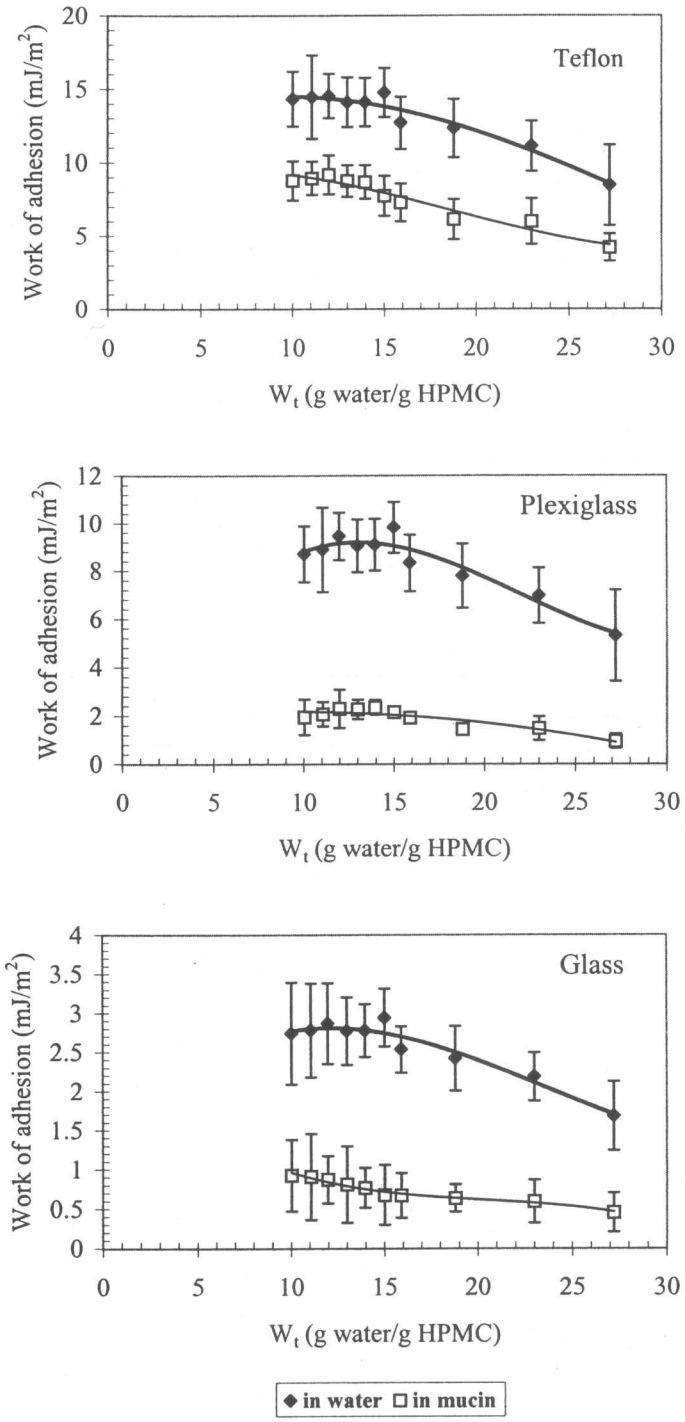

Figure 31 Effect of water content on work of adhesion between HPMC K100M gels and substrate surfaces in 2% w/w mucin solution at 25 ^{0}C

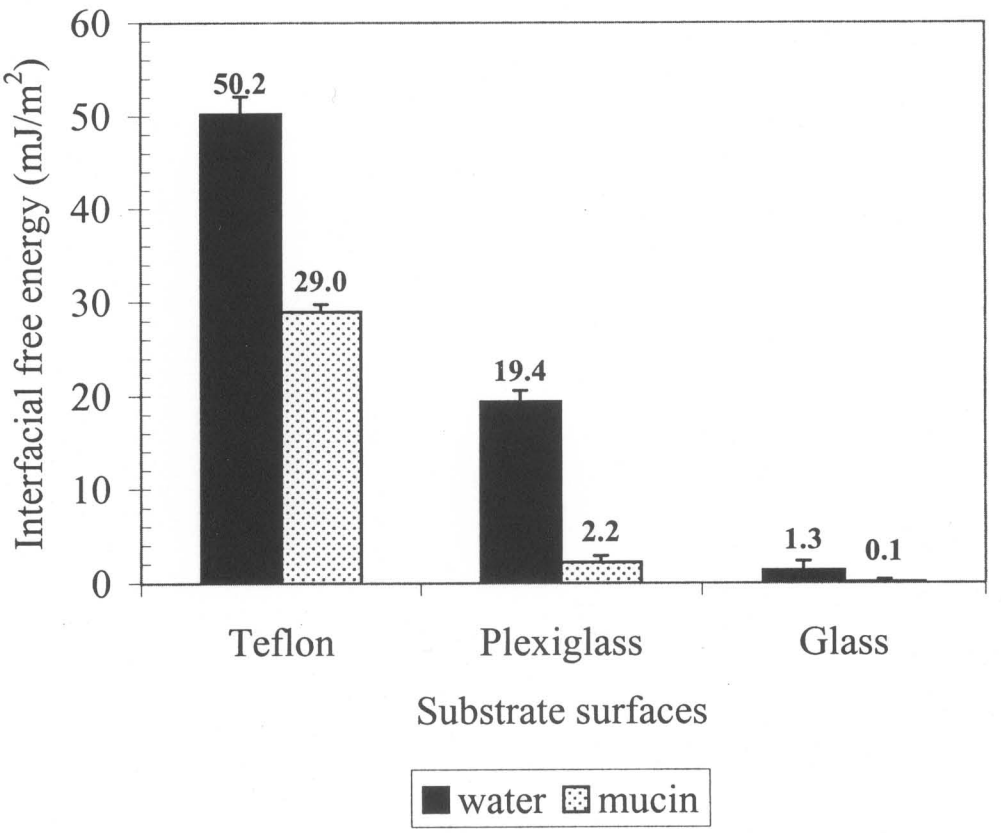

Figure 32 Interfacial free energy between substrate surfaces and medium at 25 ^{0}C

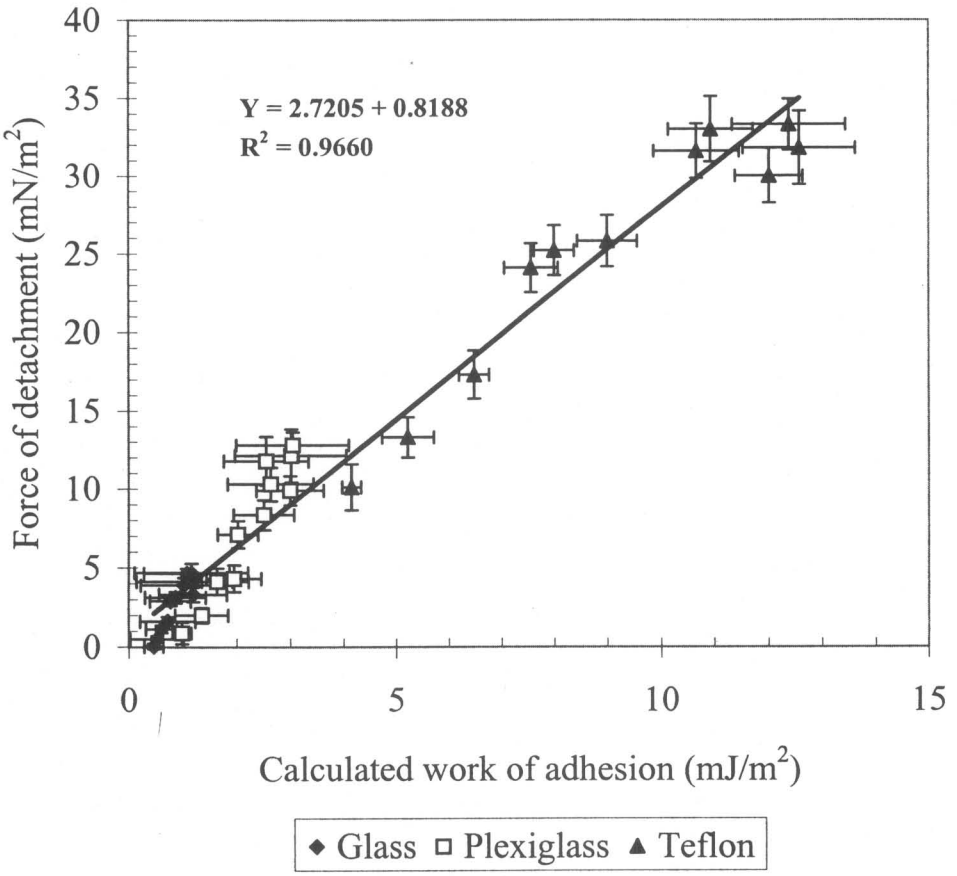

Figure 33 Correlation between calculated work of adhesion and force of detachment between HPC (300,000 g/mol) gels and substrate surfaces in 2% w/w solution at 25 ^{0}C

C. Solubility, solubility parameters and surface free energy parameters

In order to determine the correlation between solubility and solubility parameters, the solubility parameters and molar volume of methyl paraben were calculated by using the group contribution method (Table 8). The solubility parameters and the molar volume of solvents were taken from the literature (Table 9). The ideal solubilities of solid solutes were calculated from the heat of fusion and melting point data using Eq. 18. Solubility data from the literature (Table 10) was used to calculate $(\ln {}^{i}X_2/X_2)/A$ values. They were then regressed against the two dimensional radius of interaction using Eq. 31 as a model. The result from this multiple regression analysis is the following equation:

$$(\ln {}^{i}X_2/X_2)/A = -22.07 + 3.129(R_{12}^{d})^2 + 0.547(R_{12}^{s})^2 \qquad \text{Eq. 41}$$

$n = 25$, $R^2 = 0.902$, $F = 100.86$, $F(2, 22, 0.01) = 5.72$

This regression gives acceptable predicted values of $(\ln {}^{i}X_2/X_2)/A$ as shown in Figure 34. Therefore, Eq. 41 will be used to predict the solubilities of methyl paraben in several solvents used in this study.

Table 8 Calculation of solubility parameter and molar volume of methyl paraben at 25 ^{0}C

Group	V_i (cm^3/mol)	F_{di} ($J^{1/2}cm^{3/2}/mol$)	F_{pi} ($J^{1/2}cm^2/mol$)	F_{hi} (J/mol)
-OH	10.0	210	500	20,000
Phenylene	52.4	1,270	110	0
-COO	18.0	390	490	7,000
$-CH_3$	33.5	420	0	0

$V_m = \Sigma V_i = 10.0+52.4+18.0+33.5 = 113.9\ cm^3/mol$

$\delta_d = \Sigma F_{di}/V_m = (210+1,270+390+420)/113.9$

$= 20.1\ (MPa)^{1/2} = 9.8\ (cal/cm^3)^{1/2}$

$\delta_p = (\Sigma F_{pi}^2)^{1/2}/V_m = [(500)^2 + (110)^2 + (490)^2]^{1/2}/113.9$

$= 6.2\ (MPa)^{1/2} = 3.0\ (cal/cm^3)^{1/2}$

$\delta_h = (\Sigma F_{hi}/V_m)^{1/2} = [(20,000 + 7,000)/113.9]^{1/2}$

$= 15.4\ (MPa)^{1/2} = 7.5\ (cal/cm^3)^{1/2}$

$\delta_s = (\delta_p^2 + \delta_h^2)^{1/2} = [(3.0)^2 + (7.5)^2]^{1/2} = 8.1\ (cal/cm^3)^{1/2}$

$\delta_T = (\delta_d^2 + \delta_s^2)^{1/2} = [(9.8)^2 + (8.1)^2]^{1/2} = 12.7\ (cal/cm^3)^{1/2}$

Table 9 Solubility parameters and molar volumes of solvents at 25 ^{0}C [81-83]

Solvent	V_m (cm^3/mol)	δ (cal/cm^3)$^{0.5}$	δ_d (cal/cm^3)$^{0.5}$	δ_s [A] (cal/cm^3)$^{0.5}$
Ethanol	58.7	13.0	7.7	10.4
1-Propanol	75.1	12.0	7.8	9.1
1-Butanol	92.0	11.3	7.8	8.2
1-Pentanol	108.6	10.6	7.8	7.1
1-Hexanol	125.2	10.4	8.0	6.6
1-Decanol	191.8	10.0	7.5	6.6
Ethylene glycol	55.8	16.2	8.3	13.9
Propylene glycol	73.6	14.8	8.2	12.3
Glycerol	73.3	17.7	8.5	15.5
1,2 Propanediol	73.7	14.8	8.2	12.3
1,3 Propanediol	72.5	16.0	8.1	13.8
Acetic acid	57.6	10.4	7.1	7.7
Propionic acid	75.0	10.1	7.2	7.1
Pyridine	80.9	10.7	9.3	5.2
Dipropyl ether	139.4	7.6	7.3	2.3
Dibutyl ether	170.4	7.8	7.6	1.7
Ethyl acetate	98.5	9.0	7.4	5.2
Propyl acetate	115.7	8.6	7.7	3.9
Butyl acetate	132.6	8.5	7.7	3.6
Hexyl acetate	164.5	8.5	7.8	3.3
Pentane	116.2	7.1	7.1	0.0
Hexane	161.6	7.3	7.3	0.0
Heptane	147.4	7.5	7.5	0.0
n-Octane	163.5	7.6	7.6	0.0
Nonane	179.7	7.7	7.7	0.0
Decane	195.9	7.7	7.7	0.0

A = Calculated from $\delta_s^2 = \delta_p^2 + \delta_h^2$

Table 10 Solubilities of methyl paraben in individual solvents at 25 ^{0}C [97]

Solvents	X_2	Φ_1 [A]	A-values [B]	ln ($^{i}X_2/X_2$) [C]
Ethanol	0.1495	0.7450	0.1067	-0.6653
1-Propanol	0.1486	0.7909	0.1203	-0.6593
1-Butanol	0.1484	0.8217	0.1299	-0.6580
1-Pentanol	0.1528	0.8409	0.1360	-0.6872
1-Hexanol	0.1477	0.8638	0.1435	-0.6532
1-Decanol	0.0880	0.9458	0.1721	-0.1354
Ethylene glycol	0.0480	0.9067	0.1581	0.4708
Propylene glycol	0.0944	0.8611	0.1426	-0.2056
Glycerol	0.0064	0.9901	0.1886	2.4857
1,2 Propanediol	0.0941	0.8617	0.1428	-0.2024
1,3 Propanediol	0.0766	0.8847	0.1506	0.0034
Acetic acid	0.0532	0.9000	0.1558	0.3679
Propionic acid	0.0386	0.9425	0.1709	0.6887
Pyridine	0.3243	0.5968	0.0685	-1.4397
Dipropyl ether	0.0314	0.9742	0.1826	0.8952
Dibutyl ether	0.0268	0.9819	0.1855	1.0536
Ethyl acetate	0.1270	0.8560	0.1409	-0.5022
Propyl acetate	0.1366	0.8652	0.1440	-0.5751
Butyl acetate	0.1326	0.8839	0.1503	-0.5454
Hexyl acetate	0.1164	0.9164	0.1615	-0.4151
Pentane	0.000063	0.9999	0.1923	7.1066
Hexane	0.000077	0.9999	0.1923	6.9059
Heptane	0.000083	0.9999	0.1923	6.8309
Nonane	0.000106	0.9999	0.1923	6.5863
Decane	0.000121	0.9999	0.1923	6.4539

A = Calculated from Eq. 21

B = Calculated from Eq. 20

C = $^{i}X_2$ = 0.0769 (Calculated from the DSC data of methyl paraben)

T_m = 398.9 K; $\Delta^{f}H_m$ = 25,150.26 J/mol; V_m = 113.9 cm^3/mol

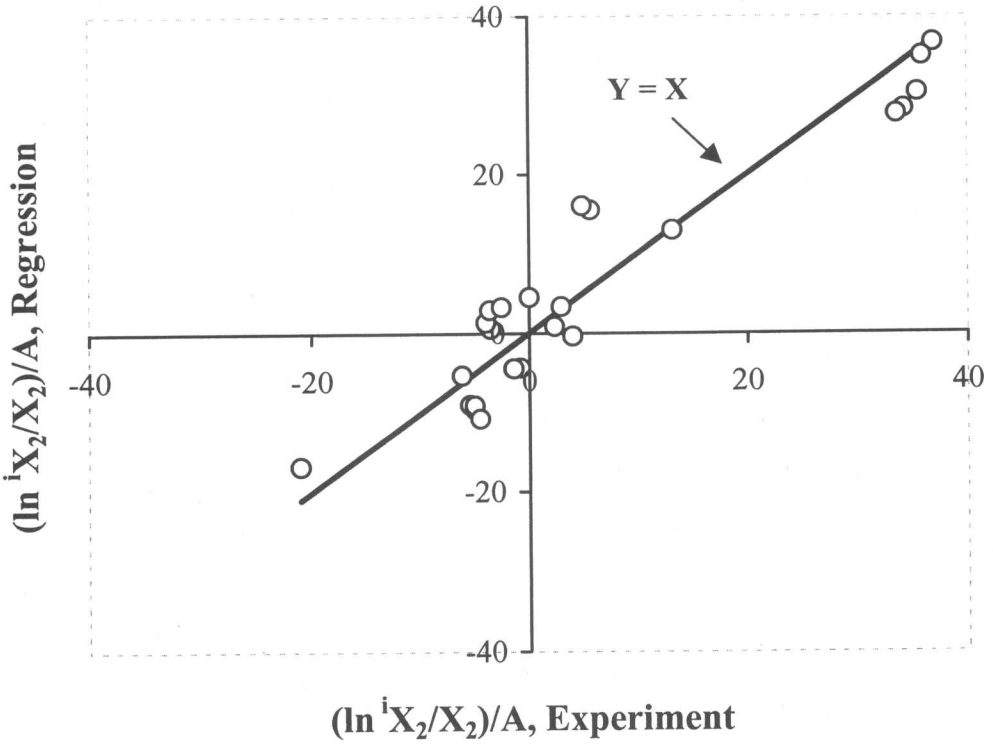

Figure 34 The plot of experimental and prediction data from solubility of methyl paraben in different solvents using multiple regression analysis

According to Beerbower et al. [96], the value of volume fraction (Φ_1) is unknown because it depends on the value of X_2. This means that the A value is also unknown. They proposed two procedures for estimating the volume fraction and A value. The first one is an iteration procedure, which begins with a value of one for the volume fraction and iterating until the volume fraction is unchanged [75, 96]. The second procedure is a root-finder method, which is more satisfactory than simple iteration. This method is used for the calculation of the mole fraction solubility of methyl paraben when the iteration procedure is not practical. The mole fraction solubility value from this method can be found by trial and error. However, the iteration procedure has mainly been used in this study because of its convenience. The example of iteration steps for the prediction of the solubility of methyl paraben in glycerol is shown in Table 11. This procedure gives an acceptable prediction as shown in Table 12.

The attempt to use solubility parameter as a tool to predict the solubility of a solute in different solvents is not a new idea; however, there is no universal approach that can be used to predict all kinds of solutes by using only a single equation. We; therefore, do not expect to use Eq. 41 as a universal equation for all solutes. However, it demonstrates that the multiple regression can be done for each solute by using the solubility data of a solute in different solvents. It is important

Table 11 The iteration procedure for calculating the mole fraction solubility of methyl paraben in glycerol at 25 ^{0}C

Step	Volume fraction of solvent [A]	A-value [B]	ln ($^iX_2/X_2$) [C]	X_2
1	1	0.192358	2,533684	0.006103
2	0.990548	0.188739	2.486014	0.006401
3	0.990088	0.188563	2.483707	0.006416
4	0.990066	0.188555	2.483592	0.006417
5	0.990064	0.188554	2.483586	0.006417
6	0.990064	0.188554	2.483586	0.006417
7	0.990064	0.188554	2.483586	0.006417
8	0.990064	0.188554	2.483586	0.006417
9	0.990064	0.188554	2.483586	0.006417
10	0.990064	0.188554	2.483586	0.006417

A = Calculated from Eq. 21

B = Calculated from Eq. 20

C = Calculated from Eq. 41

Table 12 Examples of calculated mole fraction solubility of methyl paraben in different solvents at 25 ^{0}C

Solvents	X_2 (Experiment)[A]	X_2 (Reference)[B]	X_2 (Calculation)[C]
n-Octane	0.000100 (0.000025)[D]	-	0.000293
Ethanol	0.1452 (0.0230)	0.1495	0.1397
Glycerol	0.0070 (0.0005)	0.0064	0.0064
Propylene glycol	0.1041 (0.0212)	0.0944	0.1336

A = Data from this experiment

B = Data from reference 97

C = Calculated from Eq. 41

D = Standard deviation

to note that solvents used for the solubility study should provide broad properties, i.e., strong, intermediate and non-hydrogen bonding. Therefore, the attempt of this study is to show that an expanded solubility parameter with two dimensional approach can be used to predict the solubility of a solute in a certain kind of solvent if the solubility parameters and polarity of the solvent and solute are known. In fact, this parameter is easy to calculate using the group contribution method. Since our purpose is to combine this approach with the prediction of adhesion, the correlation as Eq. 32 and 33 can be used to simulate the possibility of this combination between the knowledge of solubility parameter and surface free energy parameters.

D. The application of surface free energy analysis to bioadhesive design

❖ Computer simulation

Since a three-phase system approach has been shown to be an appropriate approach to explain adhesion behavior, all the simulations presented here are using this approach to predict the properties of a good bioadhesive system. According to Eq. 40, work of adhesion between a substrate surface and different adhesive systems in different

environments can be estimated as shown in Figures 35-37. These figures show the effect of polarity and total surface free energy of polymer system on the change of work of adhesion as the surface tension of the medium and the surface free energy of a substrate surface is fixed. The summation of these simulations is shown in Table 13. These simulations demonstrate that the matching of polarity between a substrate surface and a polymer system is the important criteria for a good adhesive system. This finding was pointed out by Lehr et al. [33] where they showed that a better adhesion occurred when a bioadhesive system had a similar polarity to a mucosal surface. In addition to the polarity, the total surface free energy of a polymer system also plays a role in adhesive capacity; however, it is not as significant when the different between polarity of a medium and a substrate surface is high. It is interesting to note that a difficult task is obvious when the polarities of a medium and a substrate surface are the same ($x^p_L = x^p_S$). The worst case is when both surface free energy and polarity of a medium and a substrate surface are the same. In this condition, the work of adhesion is always zero (Figure 37), which means that no adhesion occurs. This, unfortunately, may be the case for the GI-tract because the surface free energies of the GI fluid and mucosal surface are similar. However, there is no current data available related to the polarity. Another possibility for GI-tract condition is $\gamma_L > \gamma_S$; therefore, a low surface free energy system is supposed to be a

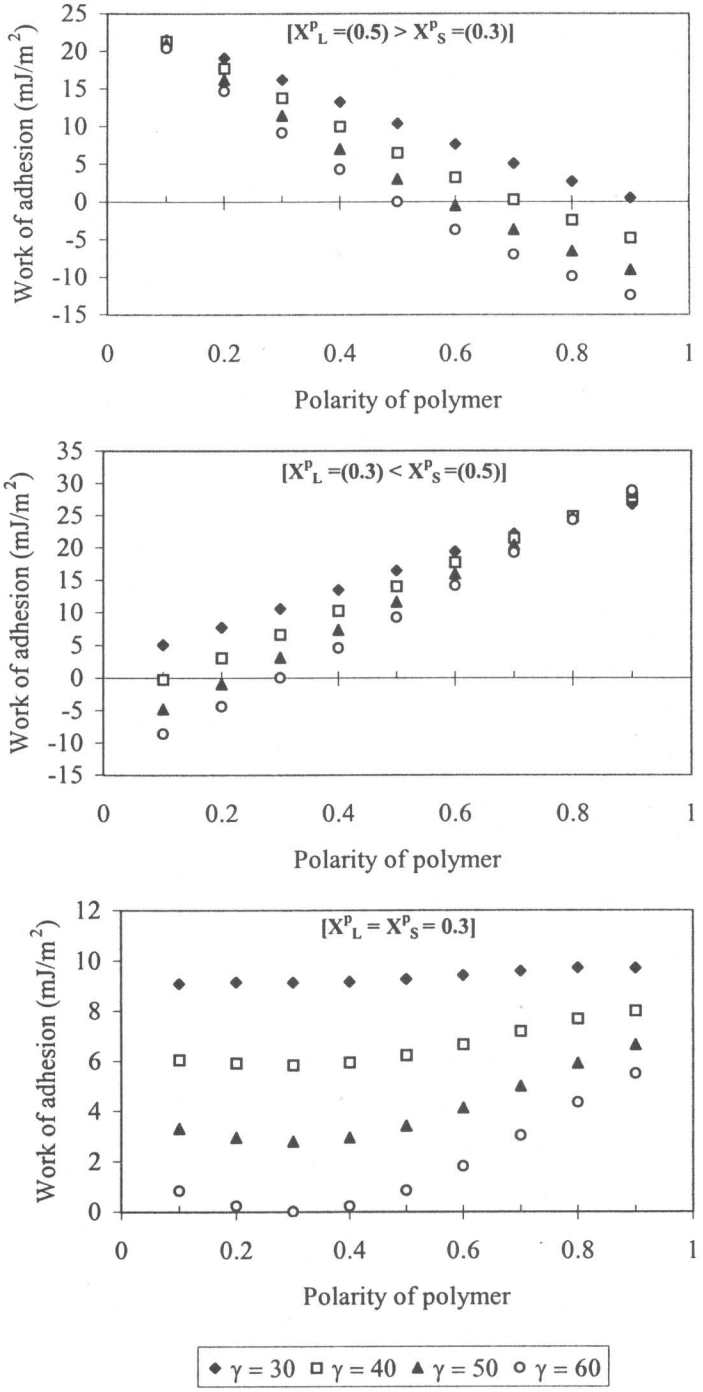

Figure 35 The effect of polarity and total surface free energy of polymer system on the change of work of adhesion when the surface tension of the medium (60 mN/m) is higher than the surface free energy of the substrate surface (45 mJ/m^2)

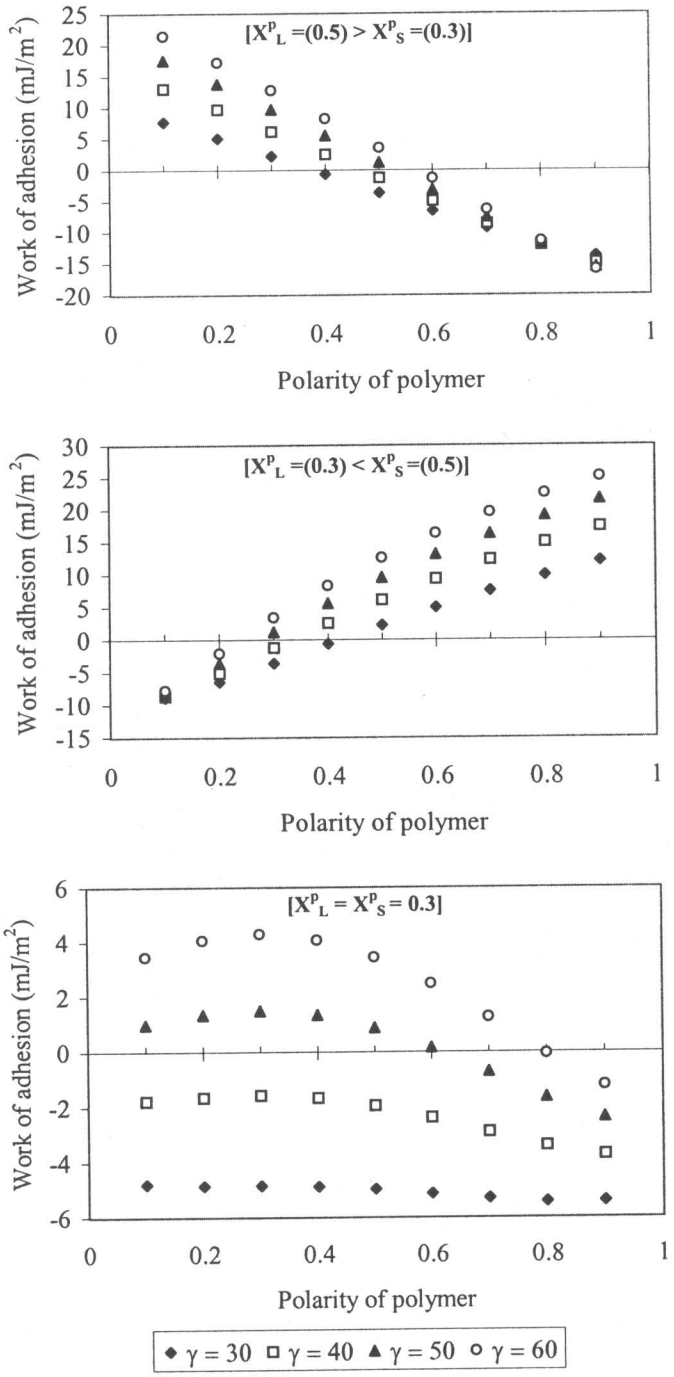

Figure 36 The effect of polarity and total surface free energy of polymer system on the change of work of adhesion when the surface tension of the medium (45 mN/m) is less than the surface free energy of the substrate surface (60 mJ/m^2)

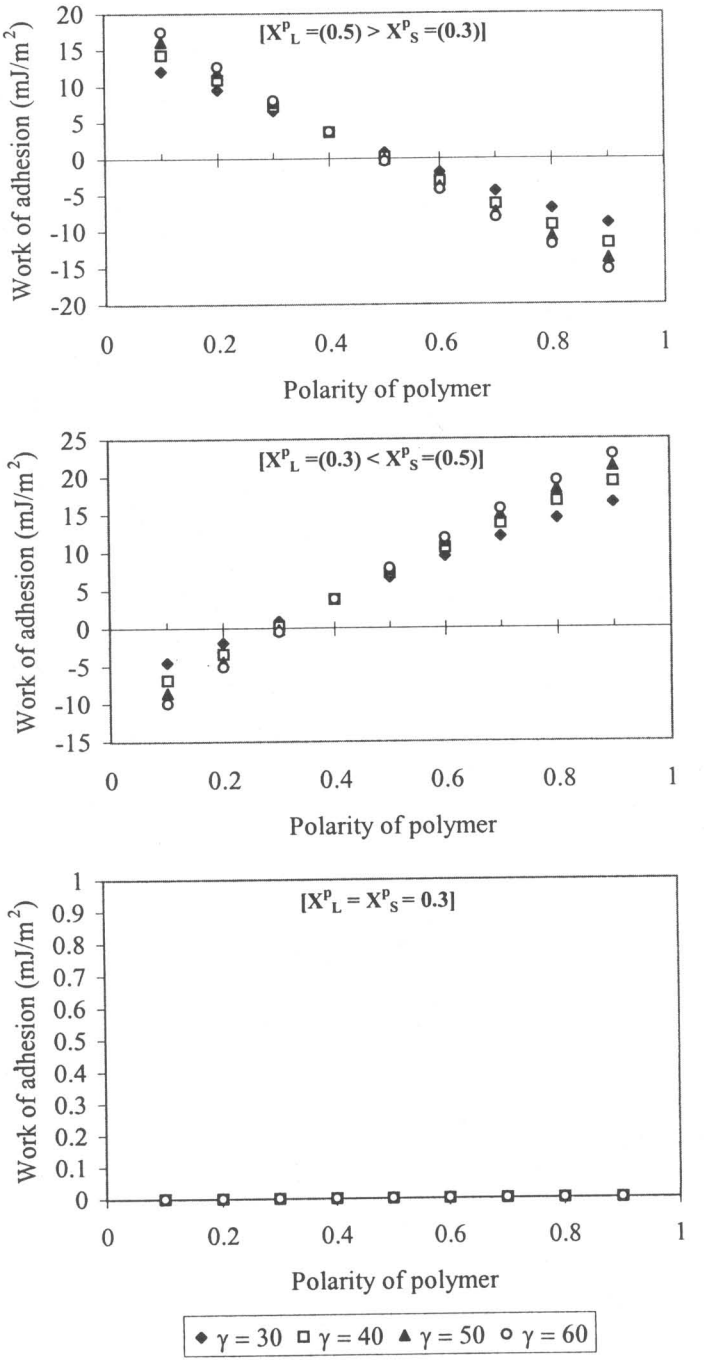

Figure 37 The effect of polarity and total surface free energy of polymer system on the change of work of adhesion when the surface tension of the medium (45 mN/m) is the same as than the surface free energy of the substrate surface (45 mJ/m^2)

Table 13 Different approaches to get good adhesion

Surface free energy	Polarity ($x^p = \gamma^p/\gamma$)	Approaches
$\gamma_L > \gamma_S$	$x^p_L > x^p_S$	Lower x^p_p ; Lower γ_P
	$x^p_L < x^p_S$	Higher x^p_p ; Lower γ_P
	$x^p_L = x^p_S$	Difficult ; Lower γ_P
$\gamma_L < \gamma_S$	$x^p_L > x^p_S$	Lower x^p_p ; Higher γ_P
	$x^p_L < x^p_S$	Higher x^p_p ; Higher γ_P
	$x^p_L = x^p_S$	Difficult ; Higher γ_P
$\gamma_L = \gamma_S$	$x^p_L > x^p_S$	Lower x^p_p ; Higher γ_P
	$x^p_L < x^p_S$	Higher x^p_p ; Higher γ_P
	$x^p_L = x^p_S$	Very Difficult

good candidate. However, there are some problems regarding the lack of wetting and the chance of aggregation if a small particle is used.In the practical situation; however, other factors, such as rheology and surface area, need to be considered. For example, adhesion can be increased by increasing the surface area of contact between an adhesive system and a substrate surface. This can be done by applying a microparticulate system or using a phase-change system in which the liquid can change to a higher viscous gel after it spreads on the surface. It is important to note that there are several uncontrollable factors involved in the GI-tract, i.e., the movement of the GI-tract, the possibility of contact between a bioadhesive system and a mucosal surface, and mucus turnover. Movement of the GI-tract will provide a certain force to overcome a bioadhesive system, which adheres to a mucosal surface. The possibility of contact between a bioadhesive system and a mucosal surface is reduced because of the wetting problem or because of a reduction of surface area from aggregation. The latter problem can be overcome in other targets, i.e., buccal and vaginal, by applying a certain force during application but this is not the case in the GI-tract.

In order to predict both adhesion behavior and solubilizing capacity at the same time, the relation between solubility parameter and surface free energy as shown in Eq. 32 and 33 is used. Figure 38 shows the effect of molar volume and polarity of solvent on the mole fraction

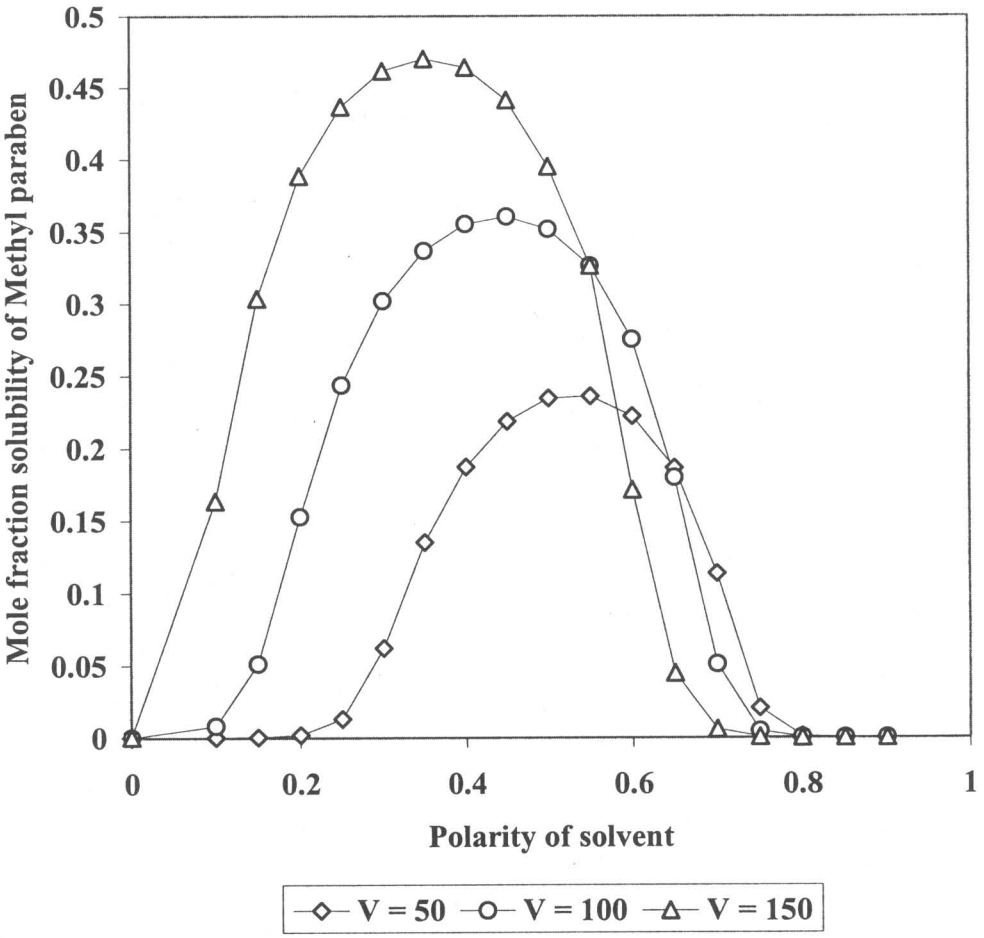

Figure 38 Prediction of mole fraction solubility of methyl paraben as a function of polarity and molar volume of solvent; total surface free energy of solvent is 60 mJ/m^2

solubility of methyl paraben when the surface tension of the solvent system is fixed at 60 mN/m. It demonstrates that the peak of the methyl paraben solubility curve is related to the polarity of methyl paraben (x^p = 0.41). In addition, the molar volume of a solvent system is also affected by the solubility of a solute. For example, the polarity of a solvent system, which gives a maximum solubility of methyl paraben differs from the polarity of methyl paraben, as the molar volume of the solvent is different from methyl paraben. This plot, therefore, provides information, which can be used to choose the appropriate solvent system. Since we know the surface free energy and polarity of the solvent, the adhesion property of this system can also be predicted by using a three- phase system equation (Eq. 6). The example of this estimation is shown in Figure 39, where the combination of data from Figures 36 and 38 are combined. In this figure, the assumptions have been made that the surface free energies of a substrate surface and the environment are 60 and 45 mJ/m^2, respectively. The polarity of these two systems on the other hand are the same, with a value of 0.3.

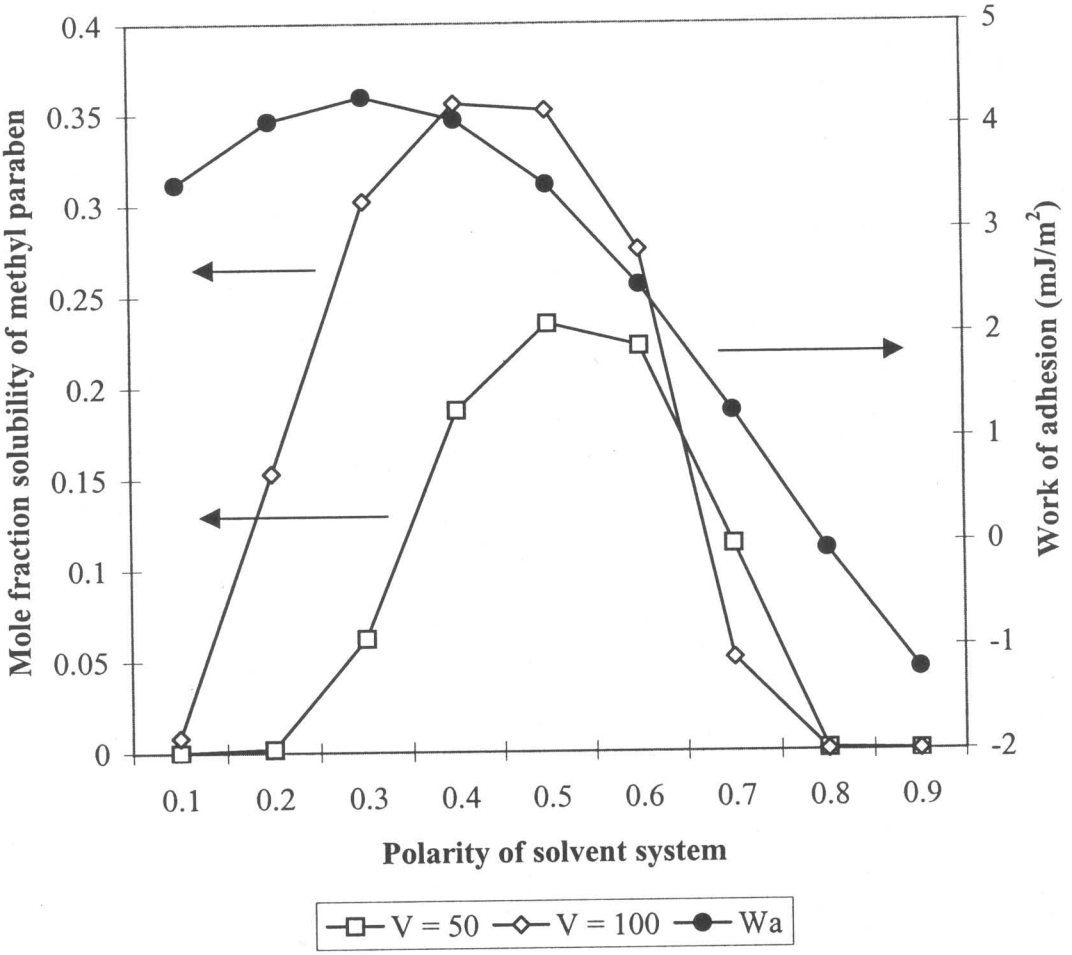

Figure 39 Prediction of mole fraction solubility of methyl paraben and work of adhesion between a substrate surface and a polymer system as a function of polarity; the conditions are explained in the context

Chapter 4: Conclusions

The conclusions from this study can be summarized as follows:

1. The surface free energy parameters have been demonstrated to be useful in that they can be used to predict adhesion behavior in a three-phase system (adhesive-medium-substrate).

2. In an aqueous environment, the hydrophilicity of the gel surface increases as the water content of polymer gel increases, which results in a decrease in interfacial free energy between the polymer gel surface and water.

3. In an aqueous environment, analysis of polar and dispersive components of surface free energy shows that a polar contribution is more important to the work of adhesion, while dispersive contribution produce a negative effect. This polar contribution is more significant when the substrate surface is more hydrophobic. The explanation of this behavior is not related to a higher polar interaction between the polymer gel and the substrate surface, but rather it is mainly related to the higher polar interfacial free energy between the hydrophobic surface and water.

4. The parabolic nature of adhesion behavior of a hydrophilic polymer as a function of water contents can be explained by assessing the state of water in polymer gels. The initially absorbed water is non-freezable water or bound water, which is important in controlling the

initial flexibility of the polymer chains needed for the beginning of the adhesion process. The excess water is the freezable water in polymer gels that accumulates at the interface and interferes with the interaction between polymer gels and the substrate surface. This results in the reduction of adhesion.

5. The molecular weight of the polymer plays a role in the adhesion process by changing the holding capacity of water molecules in polymer chains. The higher molecular weight polymer needs more water to initiate the flexibility of the polymer chain, giving it the capability of holding more water inside the polymer chains. In other words, a higher molecular weight polymer needs more absorbed water to start adhesion and will lose adhesion at higher water contents. However, this study shows that there is no specific rule to explain the relationship between the molecular weight and the maximum work of adhesion.

6. The presence of mucin in the aqueous medium reduces the adhesion by changing the surface free energy parameters of the system. The main reason for this reduction is the surface-active property of mucin, which reduces the surface tension of the medium, as well as the surface free energy of polymer gels and the substrate surface, and the interfacial free energy between the substrate surface and medium.

7. An expanded solubility parameter system with a two-dimensional approach shows an acceptable prediction for the solubility

of solute in different solvents. This can be done by using a multiple regression analysis. However, there are still some areas of uncertainty in the understanding of solubility parameter and its applications. Since this approach has not been proved yet to be a precise approach for quantitative solubility prediction, more work has to be done.

8. Simulations of methyl paraben solubility in solvents with fixed surface free energy demonstrate that the solubilizing capacity of solvents is affected by the polarity and molar volume of the solvents.

9. Simulations of the various situations demonstrate that the adhesion behavior in a three-phase system is influenced by both the polarity and the total surface free energy of a bioadhesive.

10. A combination of the surface free energy parameters and solubility parameter can be used to predict the property of a polymer system with desired bioadhesive properties and solubilizing capacity.

On the basis of this study, future work should aim directly to the use of solubility parameter to predict the bioadhesion process. This will hopefully allow one to develop a unified approach which can be used to predict both bioadhesive behavior and solubilizing capacity of a bioadhesive system by knowing only a single parameter, i.e., solubility parameter. An understanding of the properties of the GI-fluid, mucosal surface and the movement of the GI-tract is also important to explore. Parameters required include the surface free energy and polarity of the

GI-fluid and mucosal surface, and the critical force involved in the GI-tract movement. In addition, the effect of ionic interactions and the interpenetration process, which were ignored in this study should also be evaluated, so that a precise design of bioadhesive systems for drug delivery in the GI-tract can be accomplished.

Chapter V: References

1. Longer, M.A., and Robinson, J.R., Fundamental aspects of bioadhesion., *Pharm.Int.*, 114-117(May 1986)
2. Peppas, N.A., and Buri, P.A., Surface, interfacial and molecular aspects of polymer bioadhesion on soft tissues., *J.Cont.Rel.*, 2: 257-275(1985)
3. Gu, J-M., Robinson, J.R., and Leung, S-H., Binding of acrylic polymers to mucin/epithelial surfaces: Structure-property relationships, *CRC Crit.Rev.Ther.Drug Carrier syst.*, 5(1): 21-67(1988)
4. Woodley, J., Bioadhesion: New possibilities for drug administration?, *Clin.Pharmacokinet.*, 40(2): 77-84(2001)
5. Park, K., and Robinson, J.R., Bioadhesive polymers as platforms for oral-controlled drug delivery: method to study bioadhesion, *Int.J.Pharm.,* 19: 107-127(1984)
6. Nakamura, F., Ohta, R., Machida, Y., and Nagai, T., *In vitro* and *in vivo* nasal mucoadhesion of some water-soluble polymers, *Int.J.Pharm.,* 134: 173-181(1996)
7. Illum, L., Jorgensen, H., Bisgaard, H., Krogsgaard, O., and Rossing, N., Bioadhesive microspheres as a potential nasal drug delivery system, *Int.J.Pharm.,* 39: 189-199(1987)

8. Nagai, T., Adhesive topical drug delivery system, *J.Cont.Rel.,* 2: 121-134(1985)

9. Ishida, M., Machida, Y., Nambu, N., and Nagai, T., New mucosal dosage form of insulin, *Chem.Pharm.Bull.,* 29: 810-816(1981)

10. Gandhi, R.B., and Robinson, J.R., Oral cavity as a site for bioadhesive drug delivery, *Adv.Drug Del.Rev.,* 13(1&2): 43-74(1994)

11. Merkle, H.P., and Wolany, G.J.M., Mucoadhesive patches for buccal peptide administration, In: *Buccal and nasal administration as an alternative to parenteral administration,* Duchene, D. (Ed.), Editionds de Sante, Paris, France, 1992, 110-124

12. Robinson, J.R., and Mlynek, G.M., Bioadhesive and phase-change polymers for ocular drug delivery, *Adv.Drug Del.Rev.,* 16: 45-50(1995)

13. Yang, X., and Robinson, J.R., Bioadhesion in mucosal drug delivery, In: *Biorelated polymers and gels: controlled release and applications in biomedical engineering,* Okano, T. (Ed.), Academic Press, USA., 1998, 135-192

14. Yahagi, R., Onishi, H., and Machida, Y., Preparation and evaluation of double-phase mucoadhesive suppositories of lidocaine utilizing Carbopol and white beeswax, *J.Cont.Rel.,* 61: 1-8(1999)

15. Knuth, K., Amiji, M., and Robinson, J.R., Hydrogel delivery systems for vaginal and oral applications: Formulation and biological considerations, *Adv.Drug Del.Rev.,* 11: 137-167(1993)

16. Lee, C-H, and Chien, Y.W., Development and evaluation of a mucoadhesive drug delivery system for dual-controlled delivery of Nonoxynol-9, *J.Cont.Rel.,* 39: 93-103(1996)

17. Duchene, D., Touchard, F., and Peppas, N.A., Pharmaceutical and medical aspects of bioadhesive systems for drug administration, *Drug Del.Ind.Pharm.,* 14(2&3): 283-318(1988)

18. Duchene, D., and Ponchel, G., Bioadhesion of solid oral dosage forms, Why and how?, *Eur.J.Pharm.Biopharm.*, 44: 15-23(1997)

19. Ponchel, G., and Irache, J-M., Specific and non-specific bioadhesive paticulate systems for oral delivery to gastrointestinal tract, *Adv.Drug Del.Rev.,* 34: 191-219(1998)

20. Lehr, C-M., From sticky stuff to sweet receptors: Achievements, limits, and novel approaches to bioadhesion, *Eur.J.Drug Metab. Pharmacokinet.,* 21: 139-148(1996)

21. Naisbett, B., and Woodley, J., The potential use of tomato lectin for oral drug delivery 3: Bioadhesion *in vivo, Int.J.Pharm.,* 114: 227-236(1995)

22. Hassain, N., Jani, P.V., and Florence, A.T., Enhanced oral uptake of tomato lectin-conjugated nanoparticles in the rat, *Pharm.Res.*, 14(5): 613-618(1997)

23. Forter, S.N.E., Pearson, J.P., Hutton, D.A., Allen, A., and Dettmar, P.W., Interaction of polyacrylates with porcine pepsin and the gastric mucus barrier: A mechanism for mucosal protection, *Clin.Sci.*, 87: 719-726(1994)

24. Lowe, P.J., and Temple, C.S., Calcitonin and insulin in isobutylcyanate nanocapsules: Protection against proteases and effect on intestinal absorption in rats, *J.Pharm.Pharmacol.*, 46: 547-552(1994)

25. Akiyama, Y., LueBen, H.L., de Boer, A.G., Verhoef, J.C., and Junginger, H.E., Novel peroral dosage forms with protease inhibitory activities II: Design of fast dissolving poly(acrylate) and controlled drug-releasing capsule formulations with trypsin inhibiting properties, *Int.J.Pharm.*, 138: 13-23(1996)

26. Haltner, E., Easson, J.H., and Lehr, C-M., Lectins and bacterial invasion factors for controlling endo- and trancytosis of bioadhesive drug carrier systems, *Eur.J.Pharm.Biopharm.*, 44: 3-13(1997)

27. Harris, D., Fell, J.T., Sherma, H.L., and Taylor, D.C., GI transit of potential bioadhesive formulations in man: a scintigraphic study., *J.Cont.Rel.*, 12: 45-53(1990)

28. Kinloch, A.J., The science of adhesion: Part 1 Surface and interfacial aspects., *J.Mat.Sci.*, 15: 2141-2166(1980)

29. Mittal, K.L., The role of the interface in adhesion phenomena, *Polym.Eng.Eci.*, 17(7): 467-473(1977)

30. Gutowski, W., Physico-chemical criteria for maximum adhesion Part I: Theoretical concepts and experimental evidence, *J.Adhesion*, 19: 29-49(1985)

31. Baier, R.E., Shafrin, E.G., and Zisman, W.A., Adhesion: mechanisms that assist or impede it, *Science*, 162: 1360-1368(1968)

32. Lehr, C-M., Bouwstra, J.A., Spies, F., Onderwater, J., van Het Noordeinde, J., Vermeij-Keers, C., van Munsteren, C.J., and Junginger, H.E., Visualization studies of the mucoadhesive interface., *J.Cont.Rel.*, 18: 249-260(1992)

33. Lehr, C-M., Bouwstra, J.A., Bodde, H.E., and Junginger, H.E., A surface energy analysis of mucoadhesion: contact angle measurements on Polycarbophil and pig intestinal mucosa in physiologically relevant fluids., *Pharm.Res.*, 9(1): 70-75(1992)

34. Lehr, C-M., Bodde, H.E., Bouwstra, and Junginger, H.E., A surface energy analysis of mucoadhesion II: Prediction of mucoadhesive performance by spreading coefficients., *Eur.J.Pharm.Sci.*, 1: 19-30(1993)

35. Rillosi, M., and Buckton, G., Modelling mucoadhesion by use of surface energy terms obtained by the Lewis acid-Lewis base approach., *Int.J.Pharm.*, 117: 75-84(1995)

36. Peppas, N.A., and Sahlin, J.J., Hydrogels as mucoadhesive and bioadhesive materials: A review, *Biomaterials*, 17: 1553-1561(1996)

37. Bodde, H.E., Principle of bioadhesion, In: *Bioadhesion possibilities and future trends,* Gurny, R., and Junginger, H.E.(Eds.), Wissenschaftliche Verlagsgesllschaft mbH., Stuttgart, Germany, 1990, 44-64

38. Iyengar, Y., and Erickson, D.E., Role of adhesive-substrate compatibility in adhesion, *J.Appl.Polym.Sci.*, 11: 2311-2324(1967)

39. Jackson, L.C., A scienctific technique for adhesive development, *Adhesive age*, 30-31(March 1975)

40. Leung, S-H.S., and Robinson, J.R., The contribution of anionic polymer structural features to mucoadhesion., *J.Cont.Rel.*, 5: 223-231(1988)

41. Jabbari, E., Wisniewski, N., and Peppas, N.A., Evidence of mucoadhesion by chain interpenetration at a poly(acrylic acid) mucin interface using ATR-FTIR spectroscopy, *J.Cont.Rel.*, 26: 99-108(1993)

42. Mortazavi, S.A., Carpenter, B.G., and Smart, J.D., An investigation of the rheological behaviour of the mucoadhesive/mucosal interface., *Int.J.Pharm.*, 83: 221-225(1992)

43. Mortazavi, S.A., and Smart, J.D., Factors influencing gel-strengthening at the mucoadhesive-mucus interface., *J.Pharm.Pharmacol.*, 46: 86-90(1994)

44. Mortazavi, S.A., An in vitro assessment of mucus/mucoadhesive interactions, *Int.J.Pharm.*, 124: 173-182(1995)

45. Mortazavi, S.A., and Smart, J.D., An investigation into the role of water movement and mucus gel dehydration in mucoadhesion., *J.Cont.Rel.*, 25: 197-203(1993)

46. Chen, J.L., and Cyr, G.N., Compositions producing adhesion through hydration, In: *Adhesion in biological systems.*, Manly, R.S.(Ed.), Academic Press, New York, USA., 1970, 163-181

47. Zografi, G., Interfacial Phenomena, In: *Remington: The science and practice of pharmacy*, Gennaro, A.R.(Ed.), Mack Publishing Company, Easton, Pennsylvania, USA., 1995, 241-251

48. Hiemenz, P.C., and Rajagopalan, R.(Eds.), Surface tension and contact angle: Application to pure substrance, In: *Principles of colloid and surface chemistry: Revised and expanded* (3rd ed.), Marcel Dekker, Inc., New York, USA., 1997, 248-296

49. van Oss, C.J., Chaudhury, M.K., and Good, R.J., Interfacial Lifshitz-van der Waals and polar interactions in macroscopic systems, *Chem.Rev.*, 88: 927-941(1988)

50. Israelachvili, J.N.(Ed.), van der Waals forces, In: *Intermolecular and surface forces* (2nd ed.), Academic Press Inc., San Diego, USA., 1992, 83-108

51. Fowkes, F.M., Attractive forces at interfaces., *Ind.Eng.Chem.*, 56(12): 40-52(1964)

52. Owen, D.K., and Wendt, R.C., Estimation of the surface free energy of polymers., *J.Appl.Polym.Sci.*, 13: 1741-1747(1969)

53. Wu, S., Surface and interfacial tensions of polymers, oligomers, plasticizers, and organic pigments, In: *Polymer handbook* (3rd ed.), Brandrup, J., and Immergut, E.H. (Eds.), John Wiley and Sons, New York, USA., 1989, 411-434

54. Wu, S., Calculation of interfacial tension in polymer systems, *J.Polym.Sci. C.*, 34: 19-30(1971)

55. Wu, S., Polar and nonpolar interactions in adhesion., *J.Adhesion.*, 5: 39-55(1973)

56. Israelachvili, J.N.(Ed.), Adhesion, In: *Intermolecular and surface forces* (2nd ed.), Academic Press Inc., San Diego, USA., 1992, 312-330

57. Newmann, A.W., Absolom, D.R., Francis, D.W., Omenyi, S.N., Spelt, J.K., Policova, Z., Thomson, C., Zingg, W., and van Oss, C.J., Measurement of surface tensions of blood cells and proteins, *Ann.N.Y.Acad.Sci.,* 276-298(1983)

58. Van Oss, C.J., Good, R.J., and Chaudhury, M.K., The role of van der Waals forces and hydrogen bonds in "hydrophobic interactions" between biopolymers and low energy surfaces, *JCIS.*, 111(2): 378-390(1986)

59. Vogler, E.A., Interfacial chemistry in biomaterials science, In: *Wettability*, Berg, J.C. (Ed.), Marcel Dekker, Inc., New York, USA., 1993, 183-250

60. Absolom, D.R., Lamberti, F.V., Policova, Z., Zingg, W., van Oss, C.J., and Newmann, A.W., Surface thermodynamics of bacterial adhesion, *Appl.Env.Microbiol.*, 46: 90-97(1983)

61. Morra, M., and Cassinelli, C., Bacterial adhesion to polymer surfaces: A critical review of surface thermodynamic approaches, *J.Biomater.Sci. Polymer Edn.,* 9(1): 55-74(1997)

62. Pringle, J.H., and Fletcher, M., Influence of substratum wettability on attachment of freshwater bacteria to solid surfaces, *Appl.Env.Microbiol.*, 45(3): 811-817(1983)

63. Bos, R., van der Mei, H.C., and Busscher, H.J., Physico-chemistry of initial microbial adhesive interactions: its mechanisms and methods for study, *FEMS Microb.Rev.*, 23: 179-230(1999)

64. Busscher, H.J., Weerkamp, A.H., van der Mei, H.C., van Pelt, A.W.J., de Jong, H.P., and Arends, J., Measurement of the surface free energy of bacterial cell surfaces and its relevance for adhesion, *Appl.Env.Microbiol.*, 48: 980-983(1984)

65. Wang, I-W., Anderson, J.M., Jacobs, M.R., and Marchant, R.E., Adhesion of *Staphylococcus epidermidis* to biomedical polymers: contributions of surface thermodynamics and hemodynamic shear conditions, *JBMS.*, 29: 485-493(1995)

66. Esposito, P., Colombo, I., and Lovrecich, M., Investigation of surface properties of some polymers by a thermodynamic and mechanical approach: possibility of predicting mucoadhesion and biocompatibility, *Biomaterials*, 15(3): 177-182(1994)

67. Kaelble, D.H., and Moacanin, J., A surface energy analysis of bioadhesion, *Polymer*, 18(May): 475-482(1977)

68. Holly, F.J., and Refojo, M.J., Wettability of hydrogels I : Poly(2-hydroxyethyl methacrylate)., *JBMS.*, 9: 315-326(1975)

69. Ko, Y.C., Ratner, B.D., and Hoffman, A.S., Characterization of hydrophilic-hydrophobic polymeric surfaces by contact angle measurement, *JCIS.*, 82(1): 25-37(1981)

70. Andrade, J.D., Ma, S.M., King, R.N., and Gregonis, D.E., Contact angles at the solid-water interface., *JCIS.*, 72(3): 488-494(1979)

71. Andrade, J.D., King, R.N., Gregonis, D.E., and Coleman, D.L., Surface characterization of poly(hydroxyethyl methacrylate) and related polymers. I: contact angle methods in water., *J.Polym.Sci:Polym.Symp.*, 66: 313-336(1979)

72. King, R.N., Andrade, J.D., Ma, S.M., Gregonis, D.E., and Brostrom, L.R., Interfacial tensions at acrylic hydrogel-water interfaces, *JCIS.*, 103(1): 62-75(1985)

73. Hamilton, W.C., A technique for the characterization of hydrophilic solid surfaces., *JCIS.*, 40(2): 219-222(1972)

74. Hildebrand, J.H., and Scott, R.L. (Eds.), Solutions of nonelectrolytes, In: *The solubility of nonelectrolytes* (3rd ed.), Reinhold Publishing Corporation, New York, USA., 1950, 449-468

75. Martin, A. (Ed.), Solubility and related phenomena, In: *Physical pharmacy: Physical chemical principles in pharmaceuticl science,* Lea & Febiger, Philadelphia, USA., 1960, 339-394

76. Grulke, E.A., Solubility parameter values, In: *Polymer handbook* (3rd ed.), Brandrup, J., and Immergut, E.H. (Eds.), John Wiley and Sons, New York, USA., 1989, 519-559

77. Yalkowsky, S.H. (Ed.), Characterization of solutions, In: *Solubility and solubilization in aqueous media*, Oxford University Press, New York, USA., 1999, 20-48

78. Amidon, G.L., Yalkowsky, S.H., and Leung, S., Solubility of nonelectrolytes in polar solvents II: solubility of aliphartic alcohols in water, *J.Ph.Sci.*, 63(12): 1858-1866(1974)

79. Martin, A., and Mauger, J., The curious solubility of phenobarbital: how to use solubility parameters, *Am.J.Pharm.Educ.*, 52(Spring): 68-75(1988)

80. Martin, A., Newburger, J., and Adjei, A., Extended Hidebrand solubility approach: solubility of theophylline in polar binary solvents, *J.Ph.Sci.*, 69(5): 487-491(1980)

81. van Krevelen, D.W., and Hoftyzer, P.J. (Eds.), Cohesive properties and solubility, In: *Prperties of polymers: Their estimation and correlation with chemical structure* (2nd ed.), Elsevier Scientific Publishing Company, Amsterdam, Netherlands, 1977, 129-159

82. Fedors, R.F., A method for estimating both the solubility parameters and molar volumes of liquids, *Polym.Eng.Sci.*, 14(2): 147-154(1974)

83. Barton, A.F.M. (Ed.), Homologous series and homophorphs, In: *CRC Handbook of solubility parameters and other cohesion parameters*, CRC Press, Inc., Florida, USA., 1983, 61-89

84. Barton, A.F.M., Solubility parameters, *Chem.Rev.*, 75(6): 731-753(1975)

85. Steven, M.P. (Ed.), Molecular weight and polymer solutions, In: *Polymer chemistry: an introduction* (2nd ed.), Oxford University Press, Inc., New York, USA., 1990, 40-69

86. Hildebrand, J.H., and Scott, R.L. (Eds.), Evaluation of solubility parameters, In: *The solubility of nonelectrolytes* (3rd ed.), Reinhold Publishing Corporation, New York, USA., 1950, 424-434

87. Scatchard, G., Equilibria in nonelectrolyte solutions in relation to the vapor pressures and densities of the components, *Chem.Rev.*, 8(2): 321-333(1931)

88. Hansen, C.M., The universality of the solubility parameter, *I&EC Product Res.Del.*, 8(1): 2-11(1969)

89. Blanks, R.F., and Prausnitz, J.M., Thermodynamics of polymer solubility in polar and nonpolar systems, *I&EC Fundamentals*, 3(1): 1-8(1964)

90. Chen, S-A., Polymer miscibility in organic solvents and in plasticizers: a two-dimensional approach, *J.Appl.Polym.Sci.*, 15: 1247-1266(1971)

91. Shaw, M.T., Studies of polymer-polymer solubility using a two-dimensional solubility parameter approach, *J.Appl.Polym.Sci.*, 18: 449-472(1974)

92. Archer, W.L., Hansen solubility parameters for selected cellulose ether derivatives and their use in the pharmaceutical industry, *Drug Del.Ind.Pharm.*, 18(5): 599-616(1992)

93. Luciani, A., Champagne, M.F., and Utracki, L.A., Interfacial tension in polymer blends: Part 1: Theory, *Polym.Networks Blends*, 6(1): 41-50(1996)

94. Martin, A., Wu, P.L., Adjei, A., Lindstrom, R.E., and Elworthy, P.H., Extended Hildebrand solubility approach and the log linear solubility equation, *J.Ph.Sci.*, 71(8): 849-856(1982)

95. Wu, P.L., Beerbower, A., and Martin, A., Extended Hansen approach: calculating partial solubility parameters of solid solutes, *J.Ph.Sci.*, 71(11): 1285-1287(1982)

96. Beerbower, A., Wu, P.L., and Martin, A., Expanded solubility parameter approach I: napthalene and benzoic acid in individual solvents, *J.Ph.Sci.*, 73(2): 179-188(1984)

97. Martin, A., Wu, P.L., and Beerbower, A., Expanded solubility parameter approach II: p-hydroxybenzoic acid and methyl p-hydroxybenzoic acid in individual solvents, *J.Ph.Sci.*, 73(2): 188-194(1984)

98. Bustamante, P., Escalera, B., Martin, A., and Selles, E., Predicting the solubility of sulfamethoxypyridazine in individual solvents I: calculating partial solubility parameters, *J.Ph.Sci.*, 78(7): 567-573(1989)

99. Bustamante, P., Pena, M.A., and Barra, J., The modified extended Hansen method to determine partial solubility parameters of drugs containing a single hydrogen bonding group and their sodium derivatives: benzoic acid/Na and ibuprofen/Na, *Int.J.Pharm.*, 194: 117-124(2000)

100. Koenhen, D.M., and Smolders, C.A., The determination of solubility parameters of solvents and polymers by means of correlations with other physical quantities, *J.Appl.Polym.Sci.*, 19:1163-1179(1975)

101. Samaha, M.W., and Naggar, V.F., Relationship between the solubility parameter and the surface free energy of some solids, *Drug Del.Ind.Pharm.*, 16(7): 1135-1151(1990)

102. Wu, S., Estimate of the critical surface tension for polymers from molecular constitution by a modified Hildebrand-Scott equation, *J.Phys.Chem.*, 72(9): 3332-3334(1968)

103. Beerbower, A., Surface free energy: A new relationship to bulk energies, *JCIS.*, 35: 126-132(1971)

104. Panzer, J., Components of solid surface free energy from wetting measurements, *JCIS.*, 44(1): 142-161(1973)

105. Gardon, J.L., Critical review of concepts common to cohesive energy density, surface tension, tensile strength, heat of mixing, interfacial tension, and Butt joint strength, *JCIS.*, 59(3): 582-596(1977)

106. Rowe, R.C., Adhesion of film coating to tablet surfaces: A theoretical approach based on solubility parameters, *Int.J.Pharm.*, 41: 219-222(1988)

107. Rowe, R.C., Binder-substrate interactions in tablets: A theoretical approach based on solubility parameters, *Acta.Pharm.Technol.*, 34(3): 144-146(1988)

108. Rowe, R.C., Polar/non-polar interactions in the granulation of organic substrates with polymer binding agents, *Int.J.Pharm.*, 56: 117-124(1989)

109. Hancock, B.C., York, P., and Rowe, R.C., The use of solubility parameters in pharmaceutical dosage form design, *Int.J.Pharm.*, 148: 1-21(1997)

110. Barra, J., Bustamante, P., and Doelker, E., Use of the solubility parameter and surface energy concepts in the formulation of solid dosage forms, *S.T.P.Pharm.Sci.*, 9(4): 293-305(1999)

111. Johnson, B.A., and Zografi, G., Adhesion of hydroxypropyl cellulose films to low surface solid substrates, *J.Ph.Sci.*, 75(6): 529-533(1986)

112. Lee, H.B., Jhon, M.S., and Andrade, J.D., Nature of water in synthetic hydrogels I: dialatometry, specific conductivity, and differential scanning calorimetry of Polyhydroxyethyl methacrylate., *JCIS.*, 51(2): 225-231(1975)

113. Davies, M.L., and Tighe, B.J., The potential of hydrogen polymers in sensor applications., *Selective Electrode Rev.*, 13:159-226(1991)

114. Hatakeyama, H., and Hatakeyama, T., Interaction between water and hydrophilic polymers., *Thermochimica Acta.*, 308: 3-22(1998)

115. Hatakeyama, T., Nakamura, K., and Hatakeyama, H., Determination of bound water content in polymers by DTA, DSC and TG., *Thermochimica Acta.*, 123: 153-161(1988)

116. Nakamura, K., Hatakeyama, T., and Hatakeyama, H., Studies on bound water of cellulose by differential scanning calorimetry., *Text.Res.J.*, 607-613(Sept 1981)

117. Sung, Y.K., et.al., Thermal and pulse NMR analysis of water in Poly(2-hydroxyethyl methacrylate)., *J.Appl.Polym.Sci.*, 26: 3719-3728(1981)

118. Yoshida, H., Hatakeyama, T., and Hatakeyama, H., Characterization of water in polysaccharide hydrogels by DSC., *J.Thermal Anal.*, 40: 483-489(1992)

119. Tait, M.J., Ablett, S., and Franks, F., An NMR investigation of water in carbohydrate systems., In: *Water structure at the water-polymer interface.*, Jellinek., H.H.G.(Ed.)., Plenum Press, New York, USA., 1972, 29-38

120. Aoki, S., Ando, H., Ishii, M., Watanabe, S., and Ozawa, H., Water behavior during drug release from a matrix as observed using differential scanning calorimetry, *J.Cont.Rel.*, 33: 365-374(1995)

121. van Oss, C.J., Absolom, D.R., and Neumann, A.W., Applications of net repulsive van der Waals forces between different particles, macromolecules or biological cells in liquids, *Colloids and Surfaces*, 1: 45-56(1980)

122. Visser, J., On Hamaker constants: a comparison between Hamaker constants and Lifshitz-van der Waals constants, *Adv.Colloids Interface Sci.*, 3: 331-363(1972)

123. Mortazavi, S.A., and Smart, J.D., An investigation of some factors influencing the in vitro assessment of mucoadhesion, *Int.J.Pharm.*, 116: 223-230(1995)

124. Nokhodchi, A., Ford, J.L., and Rubinstein, M.H., Studies on the interaction between water and hydroxypropylmethylcellulose, *J.Ph.Sci.*, 86(5): 608-615(1997)

125. Ford, J.L., Thermal analysis of hydroxypropylcellulose and methylcellulose: powders, gels and matrix tablets, *Int.J.Pharm.*, 179: 209-228(1999)

126. McCrystal, C.B., Ford, J.L., and Rajabi-Siahboomi, A.R., Water distribution studies within cellulose ethers using differential scanning calorimetry 1: effect of polymer molecular weight and drug addition, *J.Ph.Sci.*, 88(8): 792-796(1999)

127. McCrystal, C.B., Ford, J.L., and Rajabi-Siahboomi, A.R., Water distribution studies within cellulose ethers using differential scanning calorimetry 2: effect of polymer substitution type and drug addition, *J.Ph.Sci.*, 88(8): 797-801(1999)

128. Mitchell, K., Ford, J.L., Armstrong, D., Elliott, P., Rostron, C., and Hogan, J., The influence of substitution type on the performance of methylcellulose and hydroxypropylmethylcellulose in gels and matrices, *Int.J.Pharm.*, 100: 143-154(1993)

129. Zografi, G., States of water associated with solid, *Drug Del.Ind. Pharm.*, 14(14): 1905-1926(1988)

130. Mikos, A.G., and Peppas, N.A., Measurement of the surface tension of mucin solutions, *Int.J.Pharm.*, 53: 1-5(1989

131. Finholt, P., and Solvang, S., Dissolution kinetics of drugs in human gastric juice: the role of surface tension, *J.Ph.Sci.*, 57(8): 1322-1326(1968)

132. Efentakis, M., and Dressman, J.B., Gastric juice as a dissolution medium: surface tension and pH, *Eur.J. Drug Met.Pharmacokinet.*, 23(2): 97-102(1998)

133. Spychal, R.T., Savalgi, R.S., Marrero, J.M., Saverymuttu, S.H., Kirkham, J.S., and Northfield, T.C., Thermodynamic effects of bile acids in the stomach, *Gastroenterology*, 99: 305-310(1990)

134. Spychal, R.T., Marrero, J.M., Saverymuttu, S.H., and Northfield, T.C., Measurement of the surface hydrophobicity of human gastrointestinal mucosa, *Gastroenterology*, 97: 104-111(1989)

135. Hills, B.A., Butler, B.D., and Lichtenberger, L.M., Gastric mucosal barrier: hydrophobic lining to the lumen of the stomach, *Am.J.Physiol.*, 244: G561-G568(1983)

136. Goggin, P.M., Northfield, T.C., and Spychal, R.T., Factors affecting gastric mucosal hydrophobicity in man, *Scan.J.Gastroenterol.*, 26(suppl 181): 65-73(1991)

137. Mack, D.R., Neumann, W., Policova, Z., and Sherman, P.M., Surface hydrophobicity properties of rabbit stomach in vitro, *Pediatr. Res.*, 35(2): 209-213(1994)

138. Larsson, K., On phospholipids and hydrophobicity of the gastric wall, *J.Disp.Sci.Technol.*, 15(3): 353-357(1994)

139. Lichtenberger, L.M., The hydrophobic barrier properties of gastrointestinal mucus, *Annu.Rev.Physiol.*, 57: 565-583(1995)